The NUMEN experiment

Manuela Cavallaro

INFN – Laboratori Nazionali del Sud

(Italy)

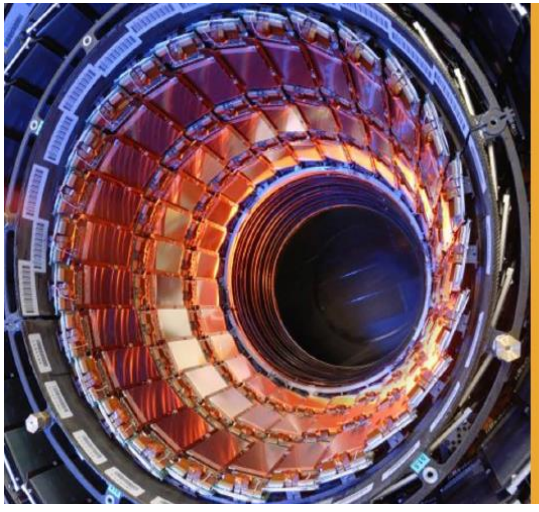

XXVI GIORNATE DI STUDIO SUI RIVELATORI

Scuola F. Bonaudi

Cogne, 13 – 17 February 2017

NUMEN

NUclear **M**atrix **E**lements for **N**eutrinoless double beta decay

Physics case: use of **nuclear reactions** to extract information of the **Nuclear Matrix Elements** entering in the expression relating the 0νββ decay half life to the neutrino absolute mass scale

$$\left(T_{1/2}^{0\nu\beta\beta}(0^+ \rightarrow 0^+)\right)^{-1} = G_{0\nu\beta}\left|M^{0\nu\beta}\right|^2 \left|f(m_i, U_{ei})\right|^2$$

Pilot experiment (DOCET) performed at INFN-Laboratori Nazionali del Sud in 2012 to test the feasibility

NUMEN proposed within the INFN «What Next» initiative in 2014

NURE project was approved for funding by ERC-Starting Grant in 2016

NUMEN

NUclear **M**atrix **E**lements for **N**eutrinoless double beta decay

TeBe

Theory

NUMEN_gr3
(R&D and experiments)
INFN CSN-III

NUMEN

NURE

CS-upgrade

SiCILIA INFN call

SiCILIA

NUMEN

NUclear **M**atrix **E**lements for **N**eutrinoless double beta decay

The collaboration

Spokespersons: F. Cappuzzello and C. Agodi

E. Aciksoz, L. Acosta, C. Agodi, X. Aslanouglou, N. Auerbach, J. Bellone, R. Bijker, S. Bianco, D. Bonanno, D. Bongiovanni, T. Borello, I. Boztosun, V. Branchina, M.P. Bussa, L. Busso, S. Calabrese, L. Calabretta, A. Calanna, D. Calvo, F. Cappuzzello, D. Carbone, M. Cavallaro, E.R. Chávez Lomelí, M. Colonna, G. D'Agostino, N. Deshmuk, P.N. de Faria, C. Ferraresi, J.L. Ferreira, P. Finocchiaro, A. Foti, G. Gallo, U. Garcia, G. Giraudo, V. Greco, A. Hacisalihoglu, J. Kotila, F. Iazzi, R. Introzzi, G. Lanzalone, A. Lavagno, F. La Via, J.A. Lay, H. Lenske, R. Linares, G. Litrico, F. Longhitano, D. Lo Presti, J. Lubian, N. Medina, D. R. Mendes, A. Muoio, J. R. B. Oliveira, A. Pakou, L. Pandola, H. Petrascu, F. Pinna, F. Pirri, S. Reito, D. Rifuggiato, M.R.D. Rodrigues, A. Russo, G. Russo, G. Santagati, E. Santopinto, O. Sgouros, S.O. Solakcı, G. Souliotis, V. Soukeras, S. Tudisco, R.I.M. Vsevolodovna, R. Wheadon, V. Zagatto

Italy, Brazil, Greece, México, Germany, Turkey, Israel, Romania, Spain

73 members, 9 countries

In Italy: LNS, Catania, Torino, Genova

NUMEN is a challenging program

Experiments with the MAGNEX spectrometer

Upgrade of the LNS accelerator and beam lines

Nuclear reaction theory

LNS, Genova, Germany, Spain, Israel

R&D on new technologies

- Detectors
- Reaction target
- Mechanics

INFN-Torino and Politecnico Romania, Mexico

Outlook

- Large acceptance magnetic spectrometry
- The MAGNEX spectrometer at INFN-LNS

- The physics case
- The NUMEN program

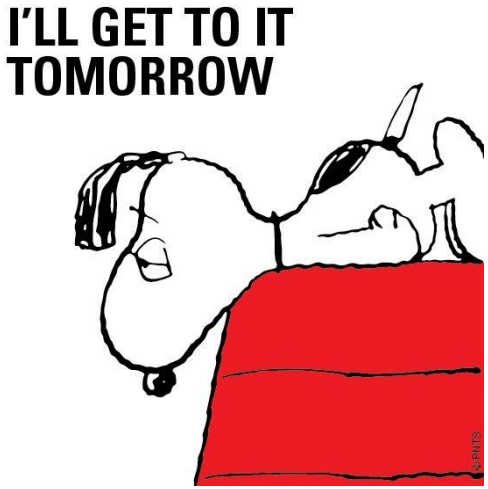

Magnetic spectrometry

Main Concepts

The study of the **motion of charged particles** through a **magnetic field** is a well established technique to explore the **microscopic structure** of the matter.

- Average motion and the concept of **beam**
- Analogy between **beam** and **light ray**
- Optics of charged particle beams and **aberrations**

Magnetic spectrometry: Using static magnetic fields to learn about microscopic world

Lorentz force $\vec{F} = q\vec{v} \wedge \vec{B}$

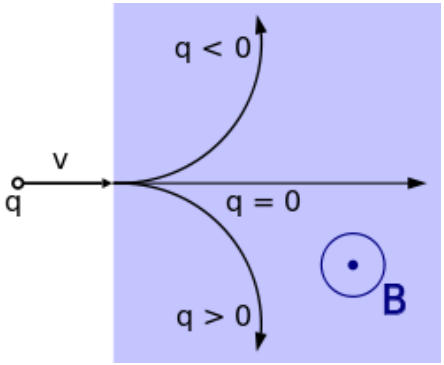

If $\vec{v} \perp \vec{B}$ and $\vec{B}$ is uniform

$$F = qvB = m\frac{v^2}{\rho}$$

curvature radius

$$B\rho = \frac{p}{q}$$

Macroscopic world

Microscopic world

- If **B** is known, a measurement of ρ corresponds to a measurement of **p/q**
- If also **q** is known (by supplementary detectors) one gets information about **p** (momentum spectrometry)
- If also the **velocity** of the particle is known, one directly accesses its **mass** (mass spectrometry)

Some historical background

At least 6 Nobel prizes in physics and chemistry have been awarded to now for studies connected to magnetic spectrometry

1903 - Marie Skłodowska Curie and Pierre Curie

for their joint researches on the radiation phenomena

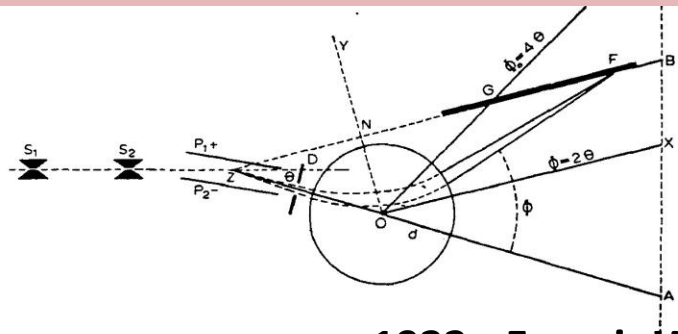

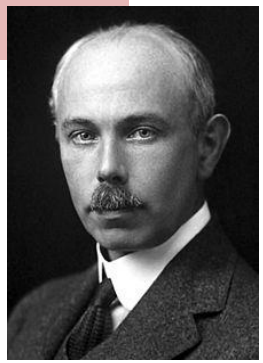

1922 - Francis William Aston

for his discovery, by means of his mass spectrograph, of isotopes

1906 - Joseph John Thomson

investigations on the conduction of electricity by gases

2002 - JOHN B. FENN and KOICHI TANAKA

for their development of soft desorption ionisation methods for mass spectrometric analyses of biological macromolecules

1989 - Wolfgang Paul

for the development of the ion trap technique

Magnetic spectrometry and nuclear reactions

Nuclear physics has taken profit by the use of magnets to select and detect the charged particles emitted in a nuclear reaction

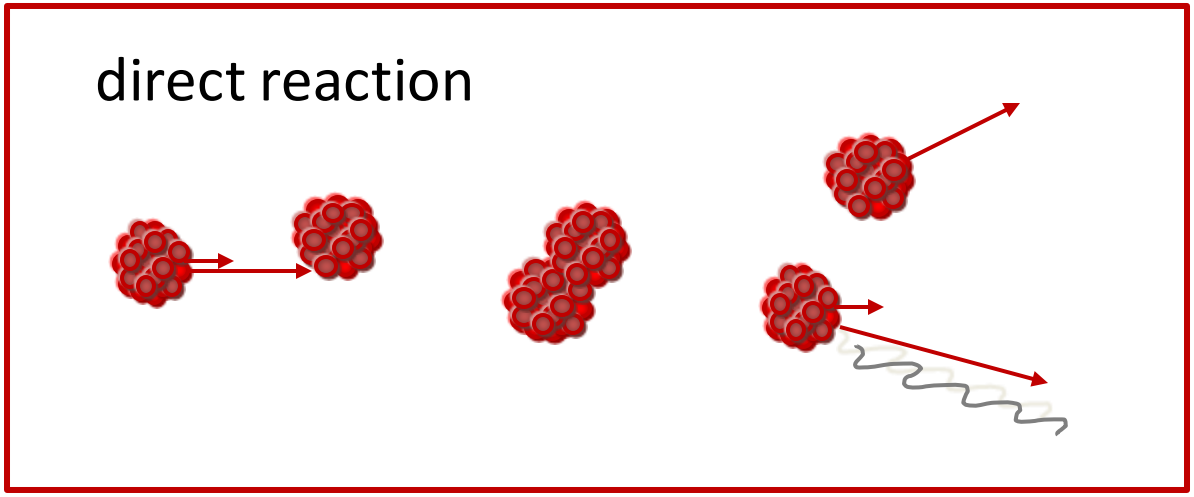

- Nuclear reactions produce fragments (charged particles) and radiation (γ-rays)

- Fragments carry the elementary information of the structure of colliding nuclei and of the reaction mechanism

Looking for fragments

what, at **what angle** and at **what energy**?

Magnetic spectrometers can provide extremely clean information about fragments thanks to their properties:

Selectivity:

- Typically $10^{9\div11}$ nuclei/sec (beam intensity) colliding against $10^{16\div18}$ nuclei/cm^2 (target thickness)
- Studying a particular reaction is how to look for a needle in a haystack
- Effective suppression of unwanted background

$$B\rho = \frac{p}{q}$$

- Possibility to measure at very forward angles (zero-degree) where clearest spectroscopic information

Resolution:

- Both in mass and momentum
  (measuring positions instead of energies)

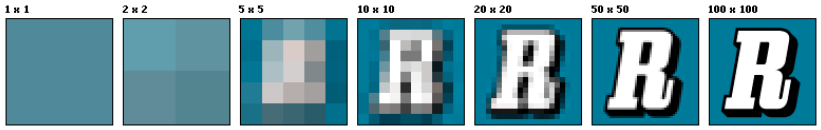

Some analogy

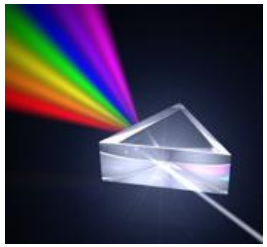

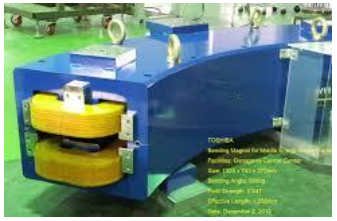

Prism

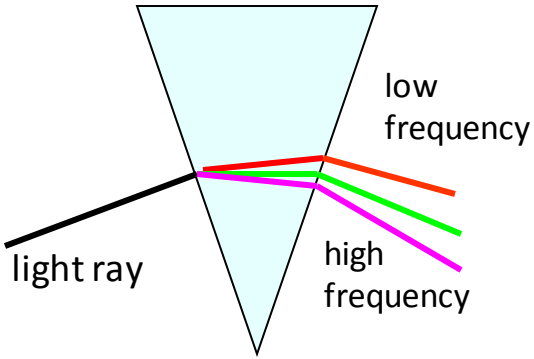

Magnetic dipole

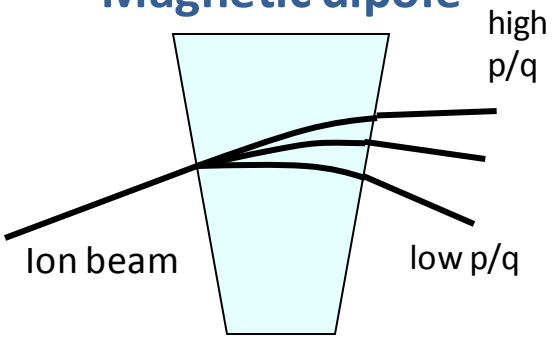

Deflection depending
on the frequency

Deflection depending on p/q
(magnetic rigidity)

Transform frequency or
p/q intervals in positions

Dispersive elements

used as analizers

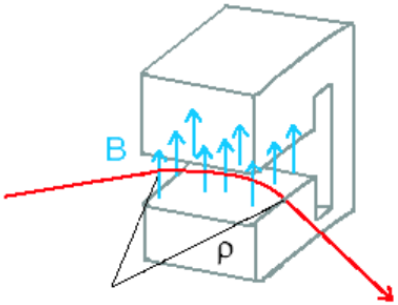

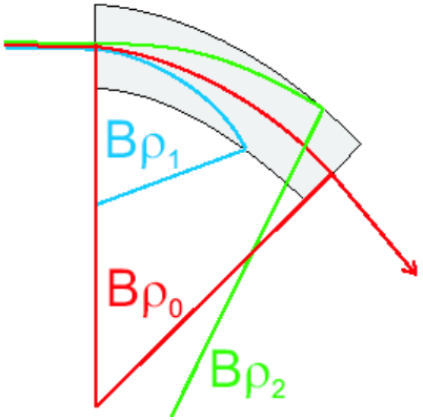

Some analogy

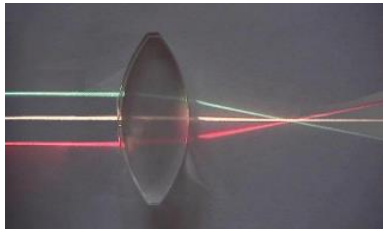

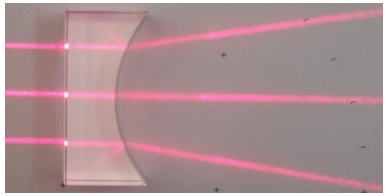

Convergent and divergent lens

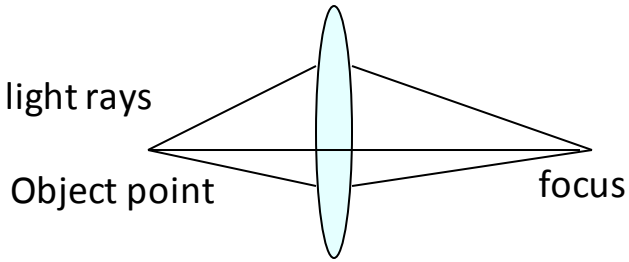

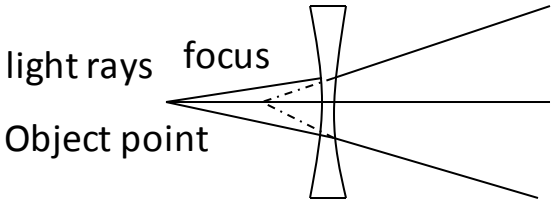

Magnetic quadrupole

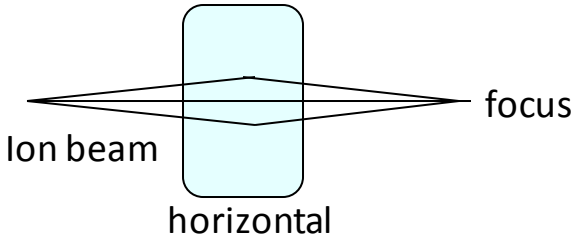

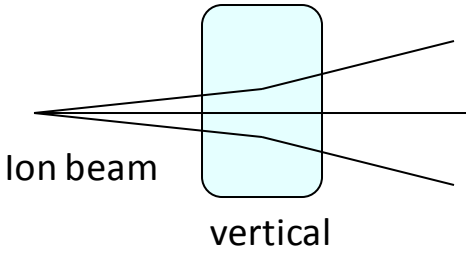

Focusing elements

used to concentrate intensity

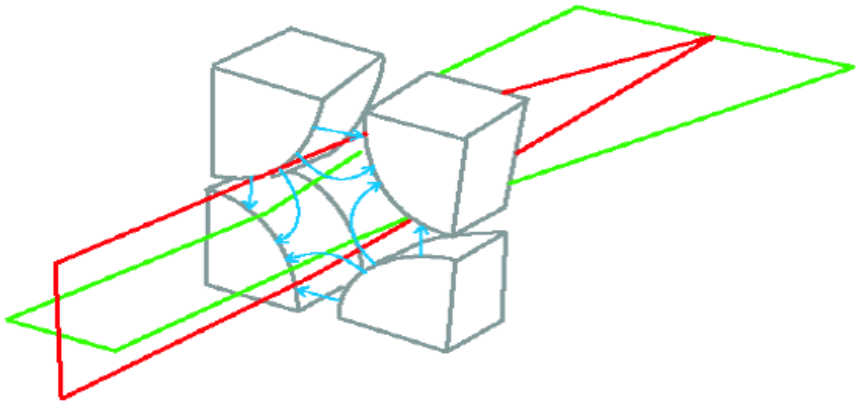

Light spectrometer

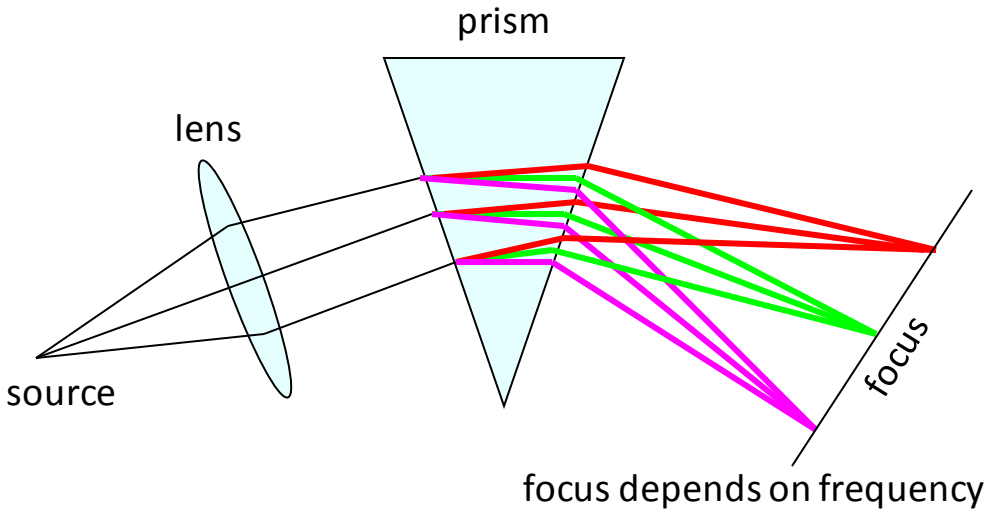

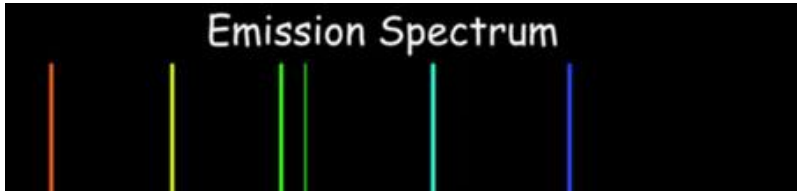

Magnetic spectrometer

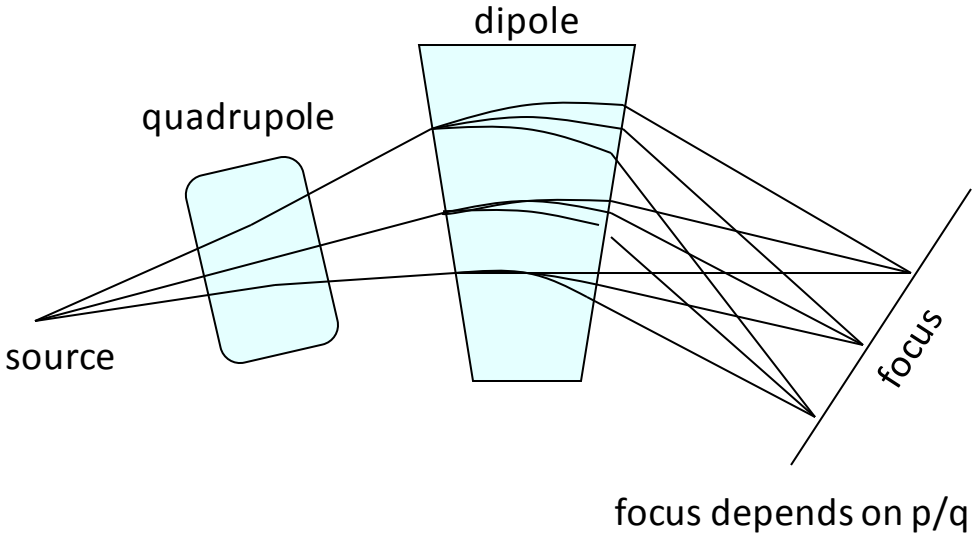

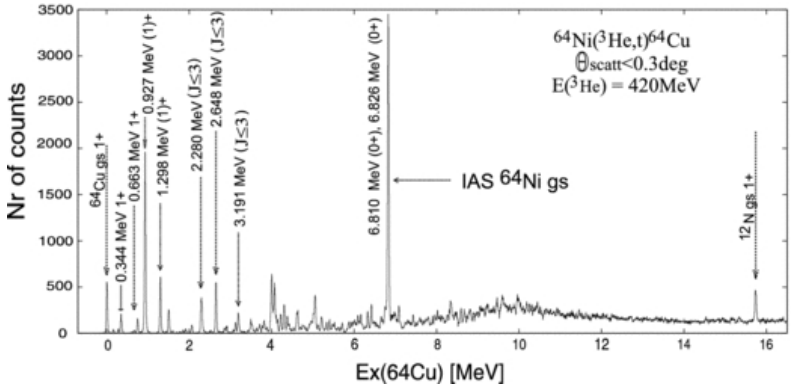

Advantages of conventional magnetic spectrometry

- Good selection of reaction products
- Possibility to measure near 0°
- High momentum and mass resolution

Magnetic spectrometers quickly became essential tools in nuclear physics laboratories. Different layouts have been established, depending on the optimization of one of these functions.

Examples of magnetic spectrometers

High resolution Δp/p=1/10000, Δp/p=1/38000

Low acceptance <10 msr

Light ions (p, d, 3He)

Q3D

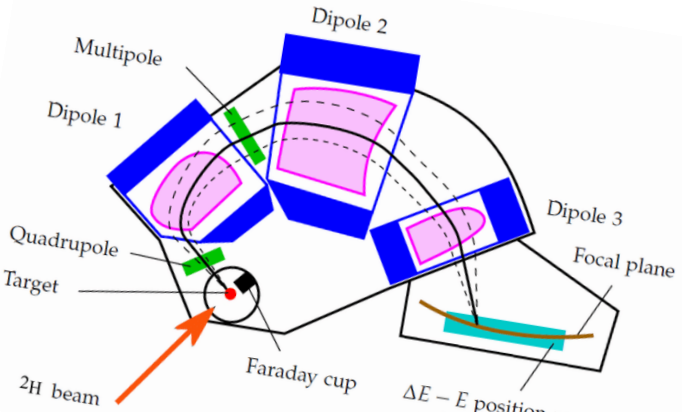

K600@i-Themba

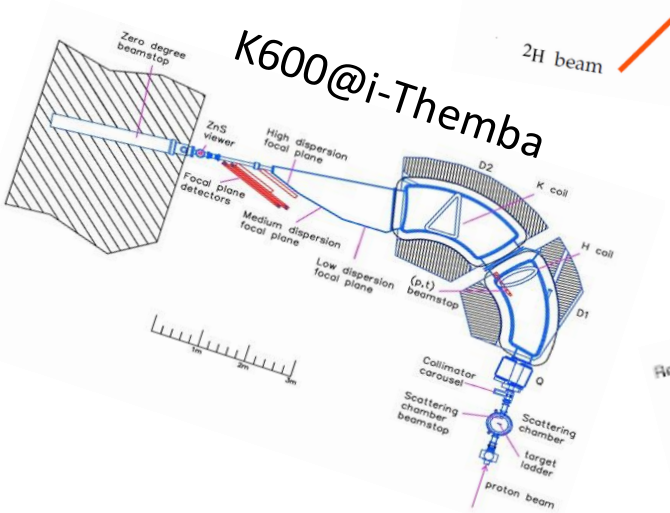

Grand-Raiden@RCNP

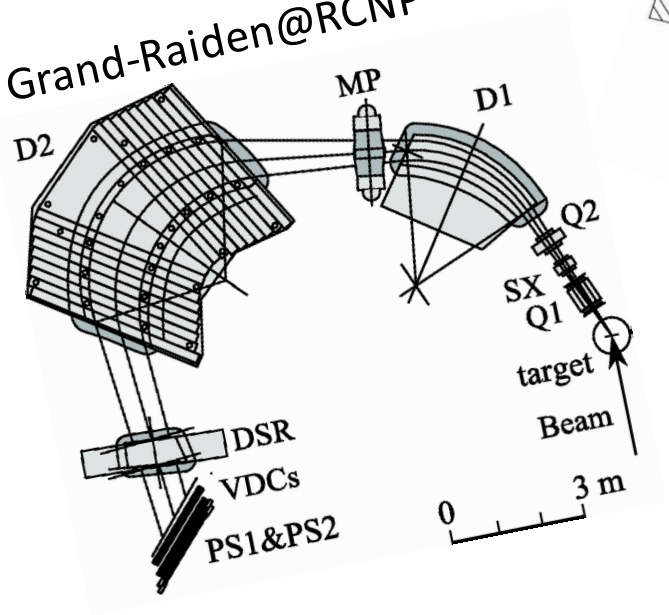

Split Poles

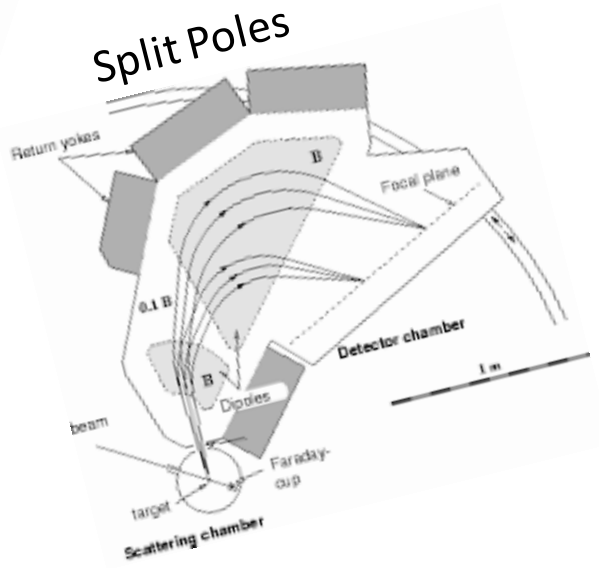

Necessity to go towards large acceptance

- To detect **rare processes** (products of reactions induced by radioactive ion beams or characterized by low cross-sections)

- Large momentum phase space in a unique setting

Examples of large acceptance magnetic spectrometers

VAMOS@GANIL

Large acceptance 50 msr
Heavier ions
Resolution??

MAGNEX@LNS

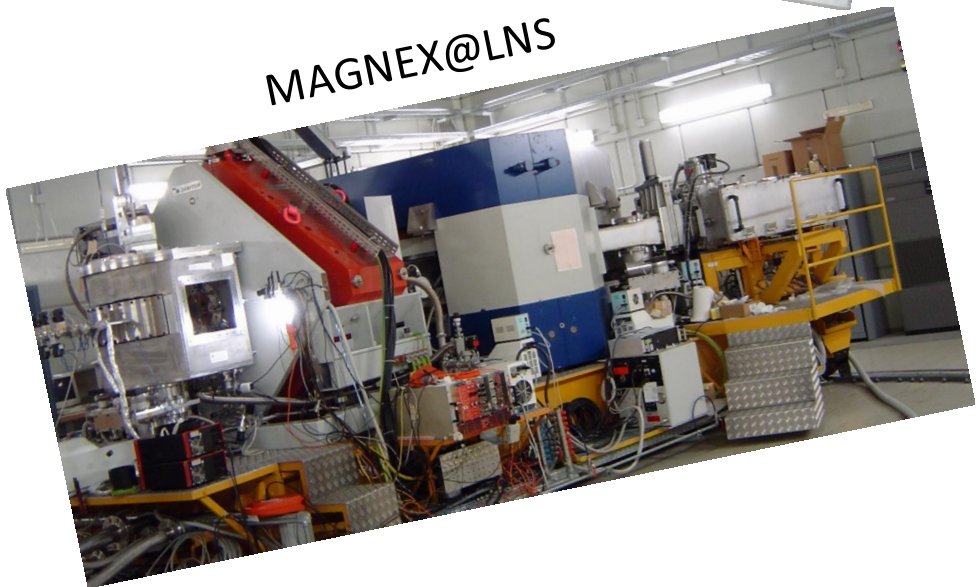

PRISMA@LNL

Large acceptance and aberrations

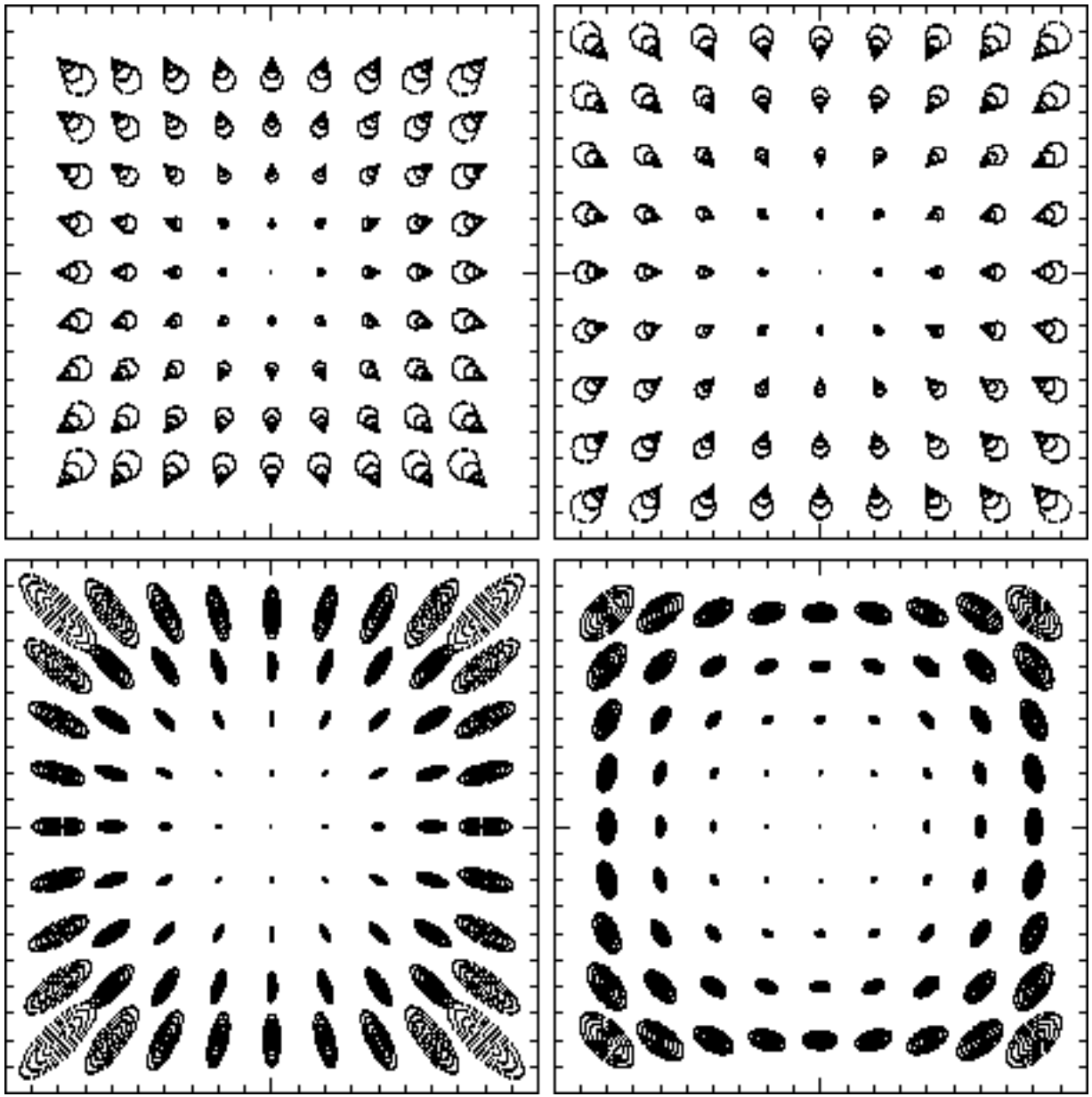

The large acceptance problem

Small acceptance → High resolution

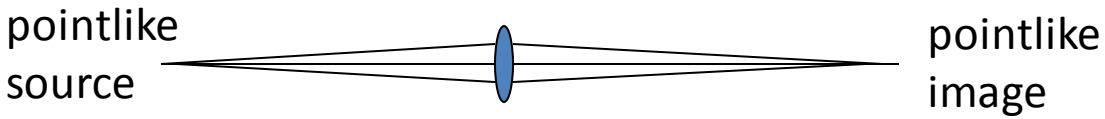

All the rays have a common focus

Large acceptance → aberrations

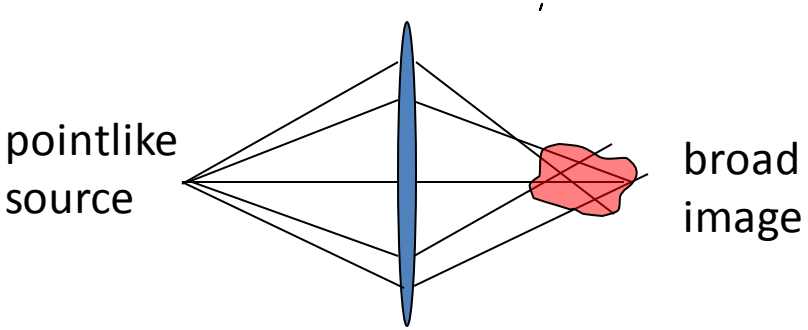

Each ray has its own trajectory: focus not anymore a useful concept

The large acceptance problem

The motion of a charged particle beam, under the action of magnetic fields, can be described as the dynamical evolution of the representative hyper-volume

$$F: \vec{X}_i \rightarrow \vec{X}_f$$

Taylor expansion

$$x_i(f) = \sum_j R_{ij} x_j(i) + \sum_{j,k} T_{ijk} x_j(i) x_k(i) + ...$$

Aberrations

F transport matrix

$$\mathbf{X}_i = (x_i, \theta_i, y_i, \varphi_i, l_i, \delta_i)$$

$$\mathbf{X}_f = (x_f, \theta_f, y_f, \varphi_f, l_f, \delta_f)$$

x, θ, y, ϕ horizontal and vertical coordinates and angles at the impact point of the ion trajectory with a plane normal to the central trajectory,

l trajectory length

$\delta = (p - p_0)/p_0$, is the fractional momentum, where p_0 is the reference momentum and p is the actual one.

The large acceptance problem

$$x_i(f) = \sum_j R_{ij}\, x_j(i) + \sum_{j,k} T_{ijk}\, x_j(i)\, x_k(i) + \ldots..$$

Aberrations

First order matrix elements:

$$(a|b) = \frac{\partial a_f}{\partial b_i}$$

$$R = \begin{pmatrix} (x|x) & (x|\theta) & (x|y) & (x|\varphi) & (x|\ell) & (x|\delta) \\ (\theta|x) & (\theta|\theta) & (\theta|y) & (\theta|\varphi) & (\theta|\ell) & (\theta|\delta) \\ (y|x) & (y|\theta) & (y|y) & (y|\varphi) & (y|\ell) & (y|\delta) \\ (\varphi|x) & (\varphi|\theta) & (\varphi|y) & (\varphi|\varphi) & (\varphi|\ell) & (\varphi|\delta) \\ (\ell|x) & (\ell|\theta) & (\ell|y) & (\ell|\varphi) & (\ell|\ell) & (\ell|\delta) \\ (\delta|x) & (\delta|\theta) & (\delta|y) & (\delta|\varphi) & (\delta|\ell) & (\delta|\delta) \end{pmatrix}.$$

Natural recipes for large acceptance: Human versus fly eyes

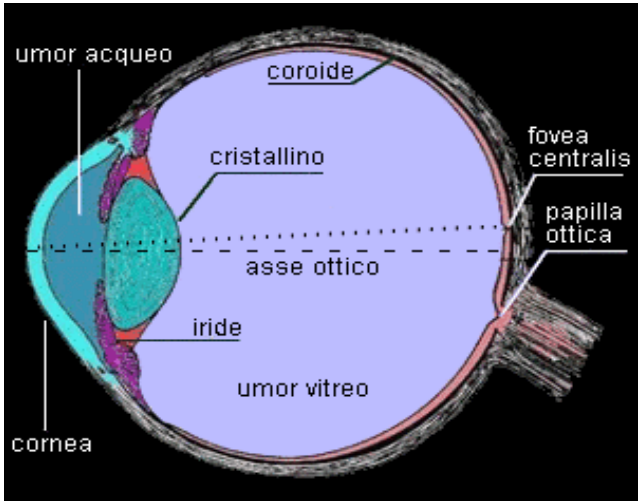

Large acceptance optical devices:

- Many small lenses in the fly versus a unique large one for man.
- Strong aberrations for us.
- Aberrations greatly compensated by brain reconstruction of the image
- Reconstruction based on neural networks and a long learning step
- What about a ***"clever"*** spectrometer?

Clever Spectrometers

Tracking instead of focusing

Spectrometer reconstructing a net image by an optically aberrated one

The MAGNEX spectrometer

Catania
INFN
Laboratori Nazionali del Sud

The LNS laboratory in Catania

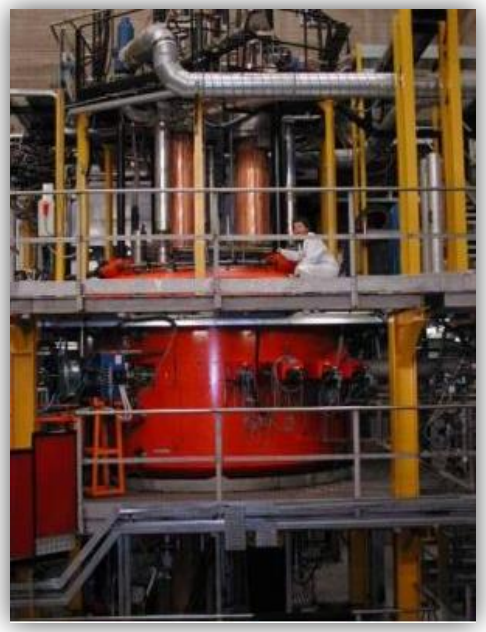

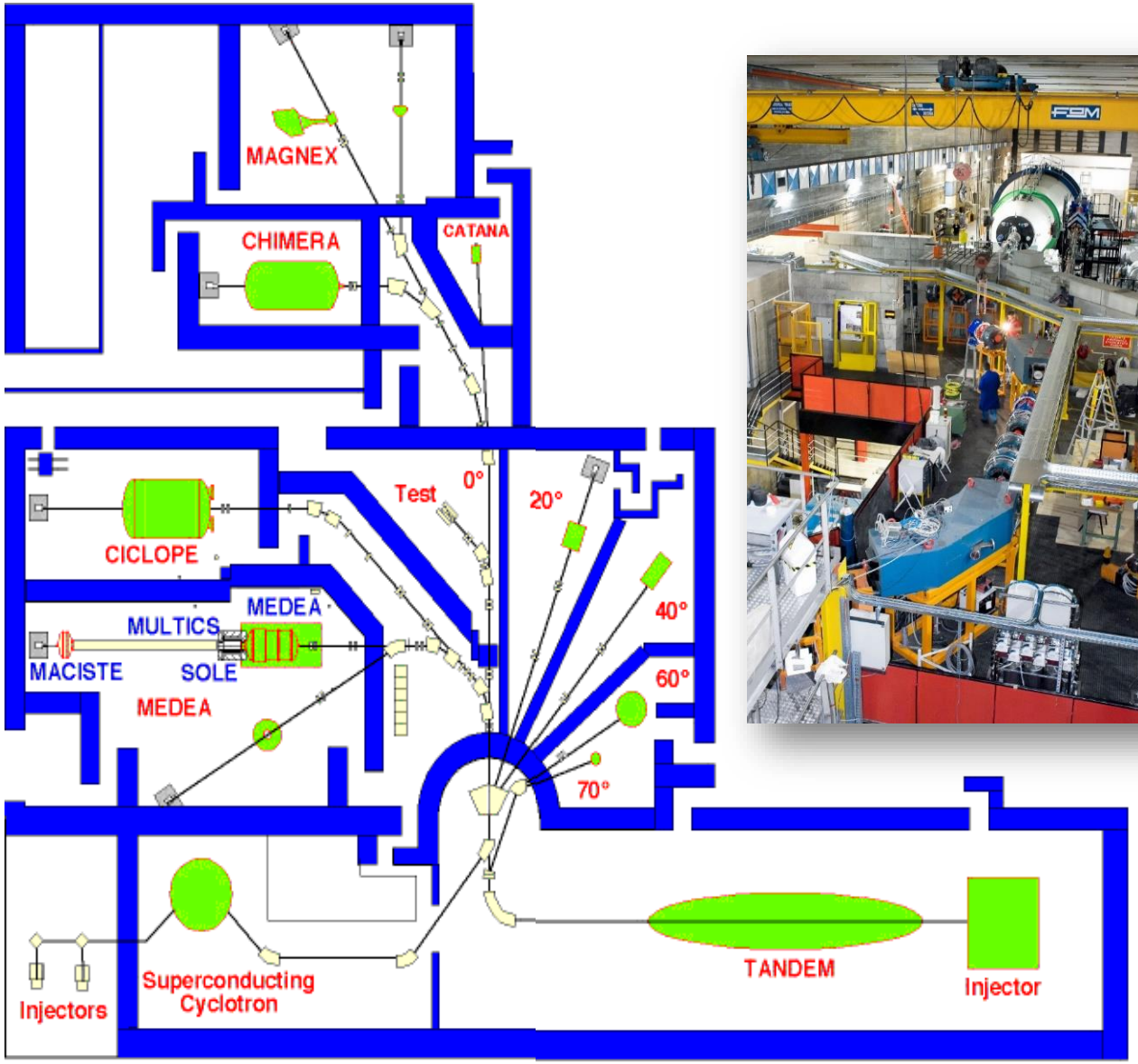

Superconducting cyclotron K800

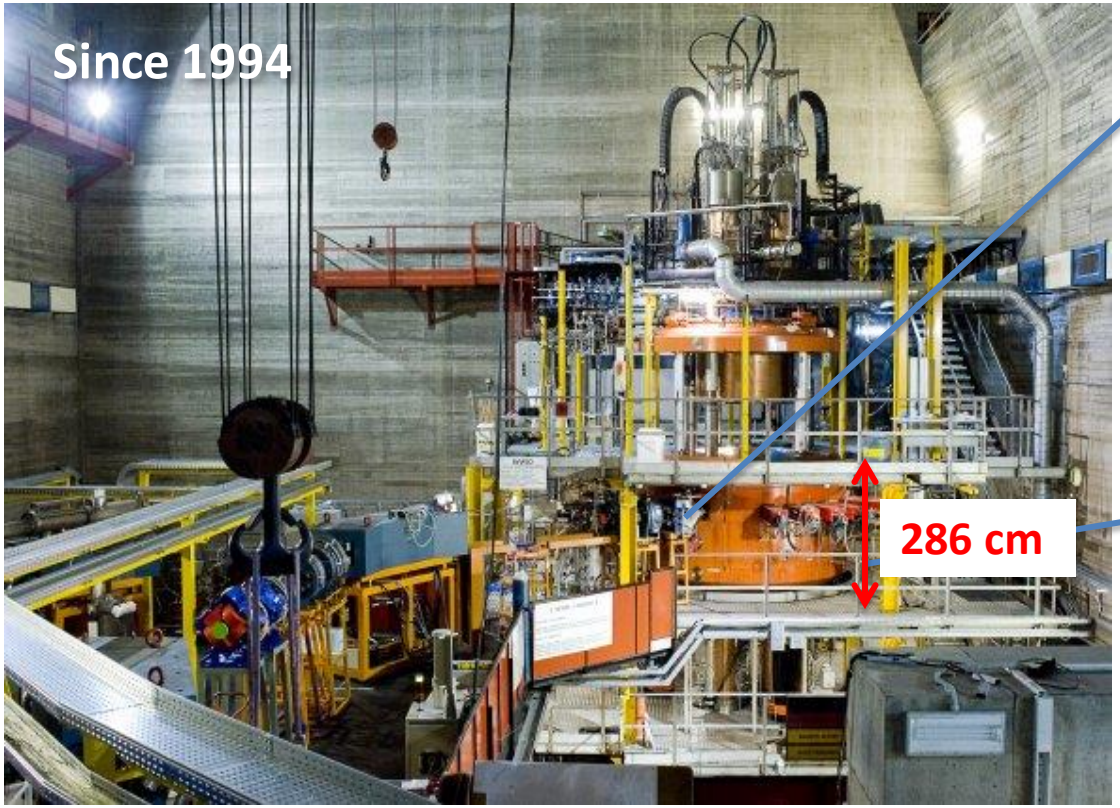

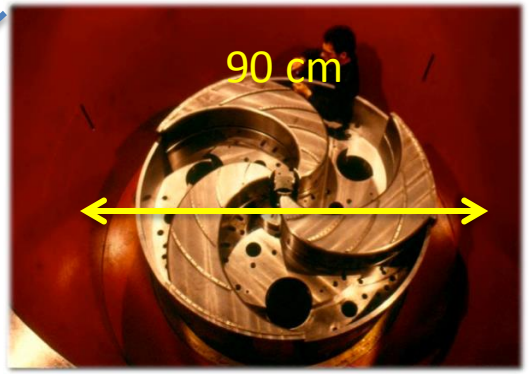

- **176 Tons**
- **Max magnetic field: 4.8 T**

- Accelerating ion beams from proton to Uranium at energy up to 80 MeV/A
- Superconducting magnets with Niobium-Titanium coils in liquid Helium at 4.2 K

MAGNEX: a large acceptance QD spectrometer

- **The Quadrupole**: vertically focusing
  (Aperture radius 20 cm, effective length 58 cm. Maximum field strength 5 T/m)

- **The Dipole**: momentum dispersion (and horizontal focus)
  (Mean bend angle 55°, radius 1.60 m. Maximum field ~ 1.15 T)

- **The surface coils**, located between the dipole pole faces and the inner high vacuum chamber, giving tunable quadrupolar and sextupolar corrections

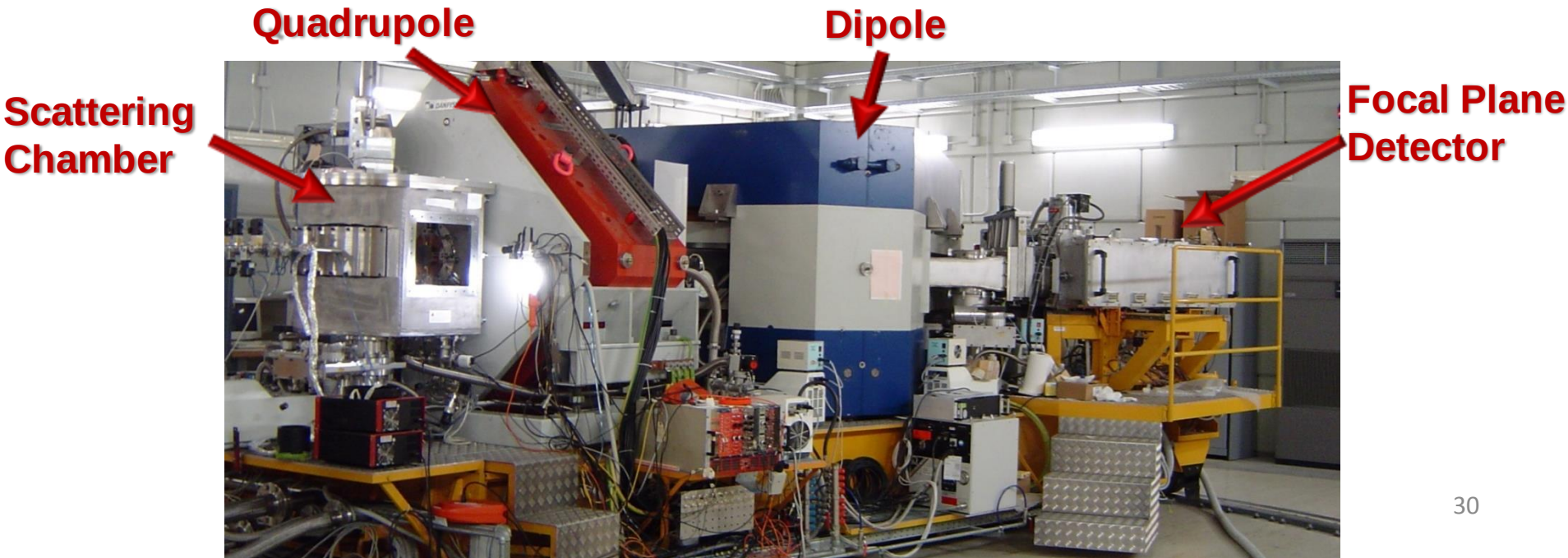

MAGNEX characteristics

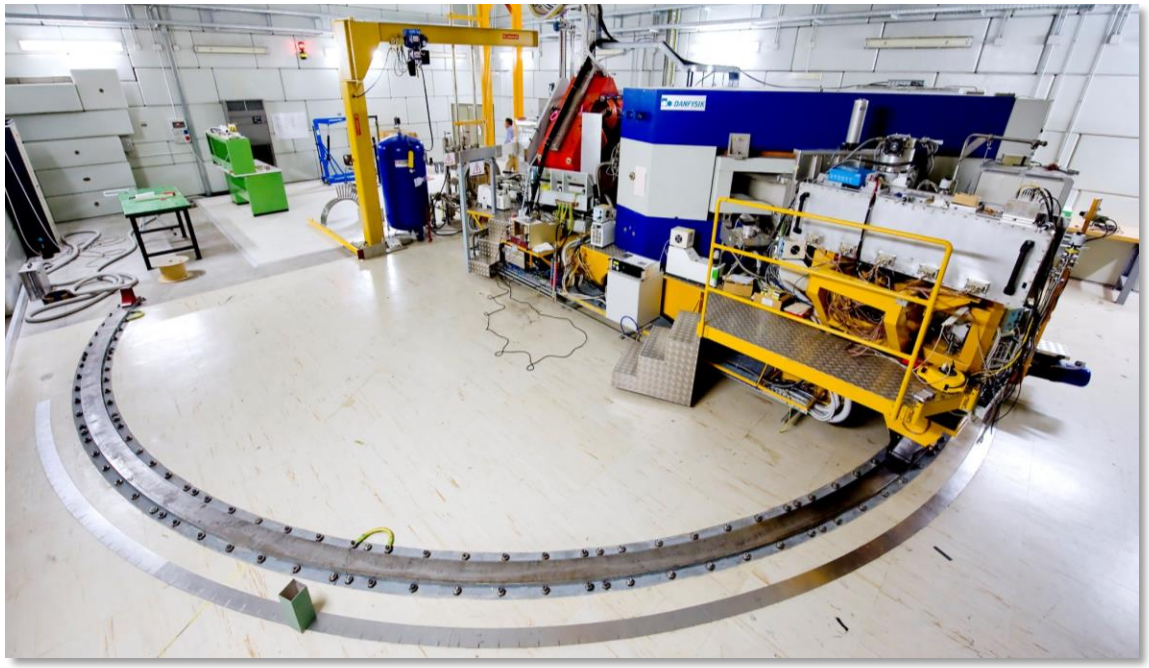

Measured resolution:
Energy $\Delta E/E \sim 1/1000$
Angle $\Delta\theta \sim 0.3^\circ$
Mass $\Delta m/m \sim 1/160$

We have measured in a **wide mass range** (from protons to medium-mass nuclei)

Optical characteristics	Measured values
Angular acceptance (Solid angle)	50 msr
Angular range	–20° - +85°
Momentum (energy) acceptance	-14%, +10% (-28%,+20%)
Momentum dispersion for k= - 0.104 (cm/%)	3.68
Maximum magnetic rigidity	1.8 T m

F. Cappuzzello et al., Eur. Phys. Journ. A (2016) 52:167

The large acceptance problem

$$F: \vec{X}_i \rightarrow \vec{X}_f$$

F transport matrix

Large acceptance

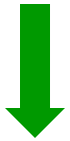

Aberrations

$$x_i(f) = \sum_j R_{ij} x_j(i) + \sum_{j,k} T_{ijk} x_j(i) x_k(i) + \ldots..$$

Up to 10° order

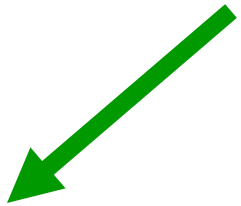

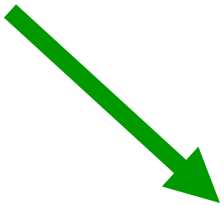

Careful hardware design
(to minimize the aberrations)

Software ray-reconstruction
(to know the aberrations)

Hardware minimisation of aberrations

- Rotation of the focal plane detector of 59°
- Shift of the focal plane detector

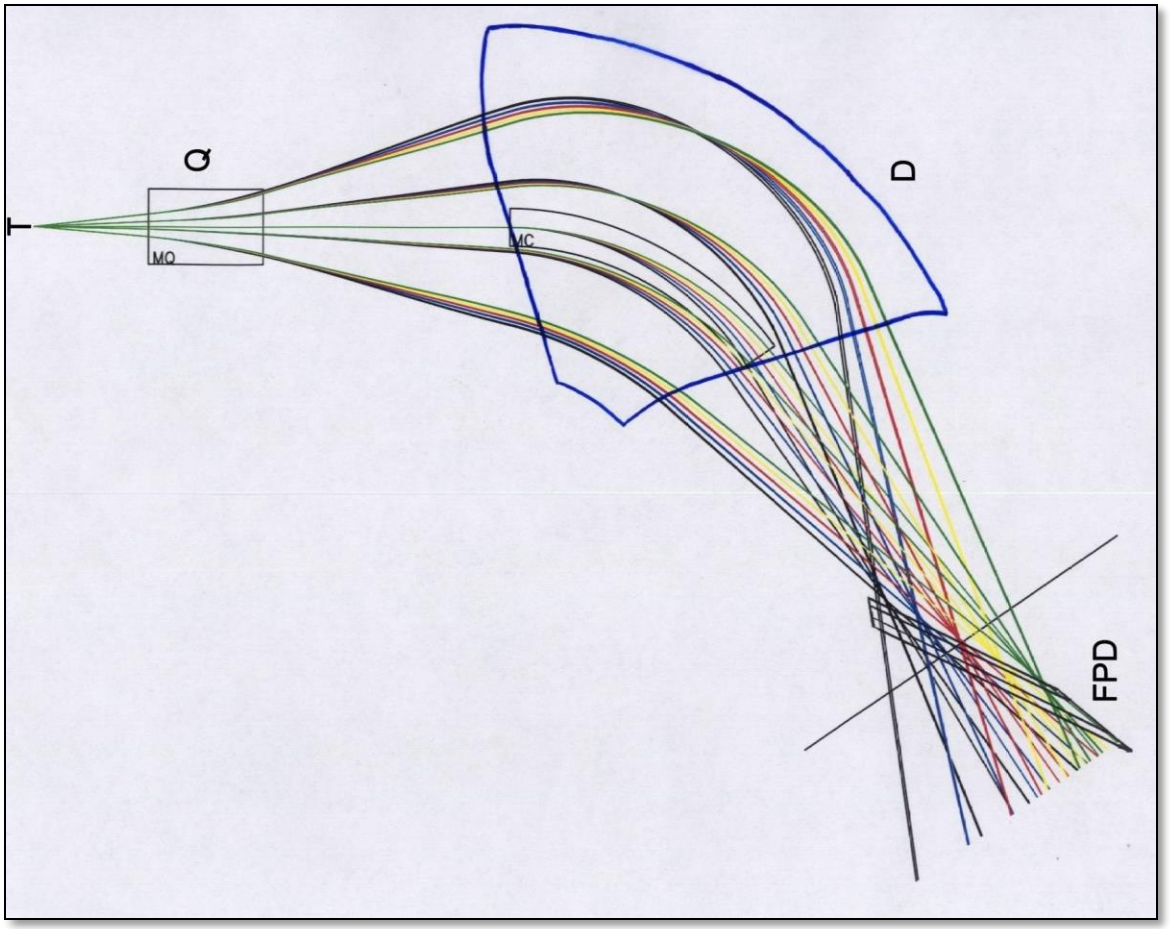

Hardware minimisation of aberrations

- Introduction of surface coils in the dipole pole tips

- Shaping of dipole entrance and exit boundaries (8th order polynomial)

Hardware minimisation of aberrations

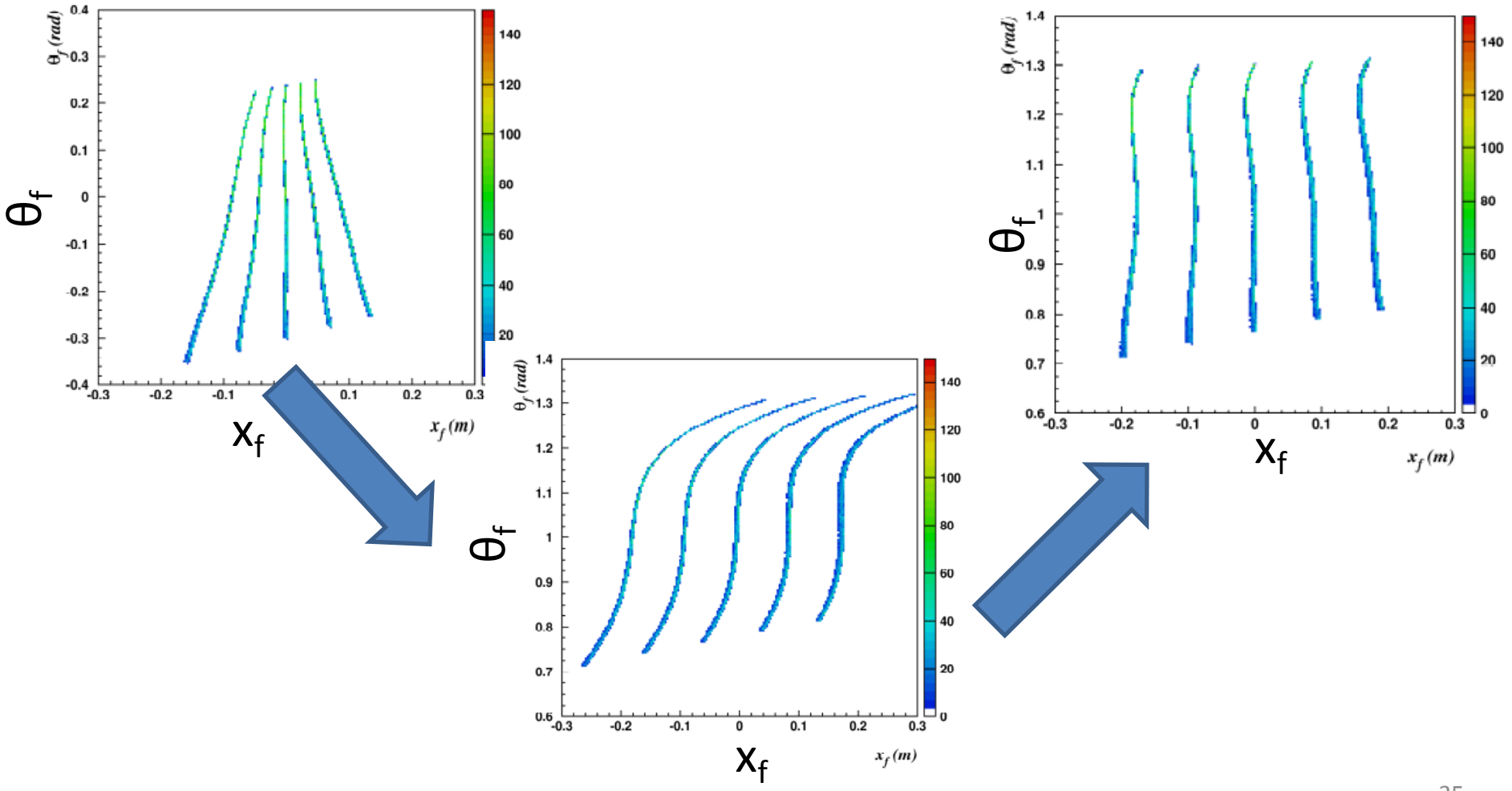

The large acceptance problem

$$F: \vec{X}_i \rightarrow \vec{X}_f$$

F transport matrix

Large acceptance

Aberrations

$$x_i(f) = \sum_j R_{ij} x_j(i) + \sum_{j,k} T_{ijk} x_j(i) x_k(i) + \ldots..$$

Up to 10° order

Careful hardware design
(to minimize the aberrations)

Software ray-reconstruction
(to know the aberrations)

Software ray-reconstruction

ALGEBRIC RAY-RECONSTRUCTION

- ✓ Solution of the equation of motion for each detected particle
- ✓ Inversion of the transport matrix
- ✓ Application to the final measured parameters

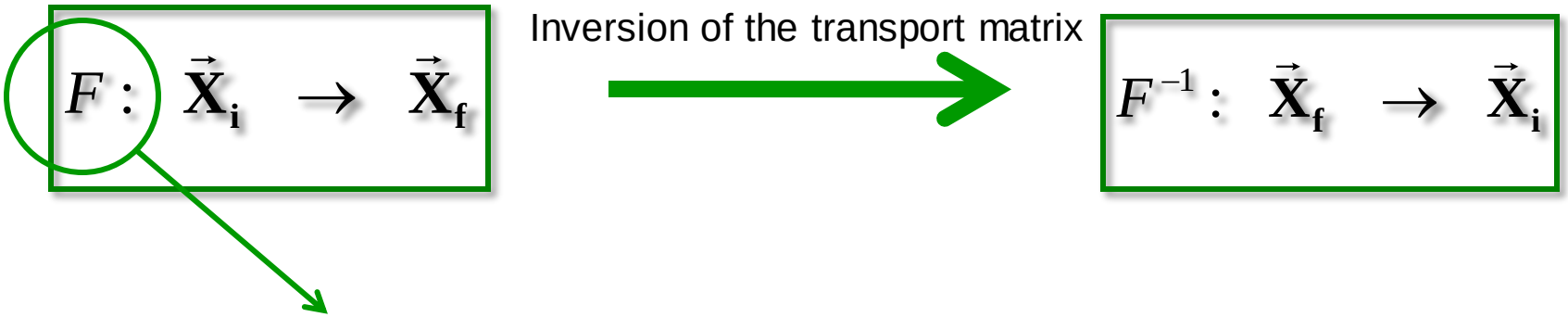

1) Detailed knowledge of the geometry and magnetic field

1) Detailed knowledge of the magnetic field

Measurement of the field (3D map)

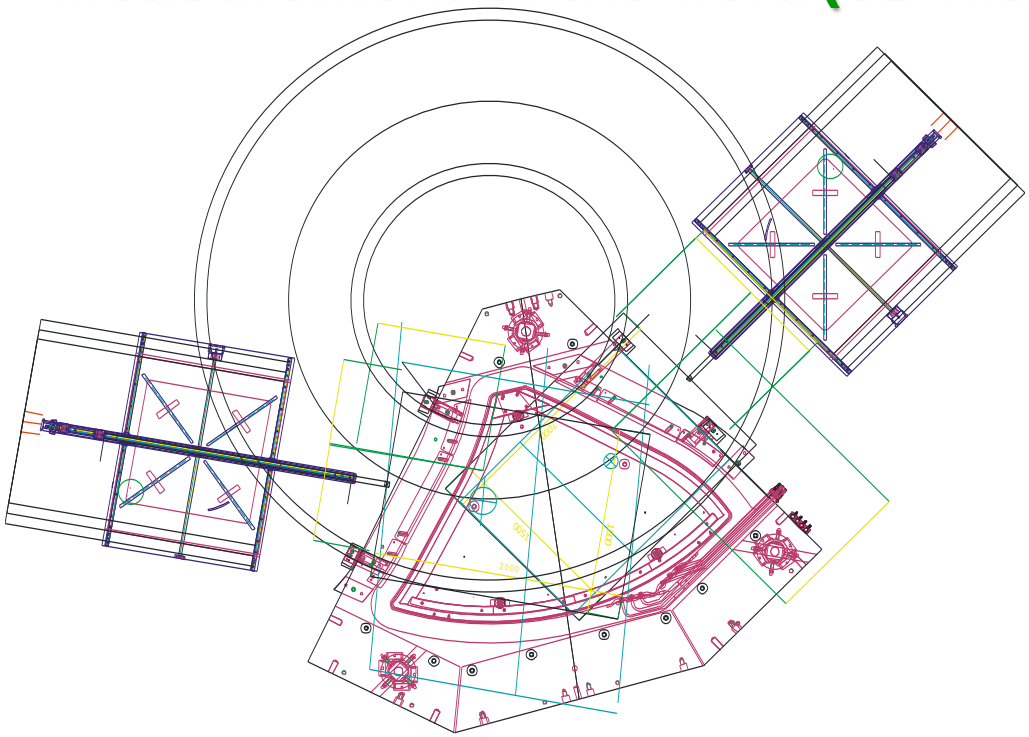

Measurements at Danfysik
240000 points
2 months (night and day)

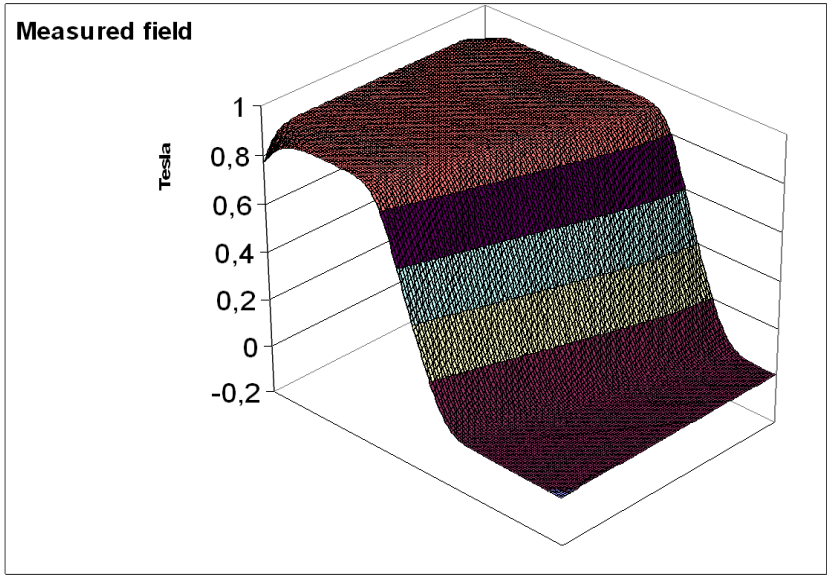

Interpolation of the field

Regular function up to 10° order

A.Lazzaro et al., NIMA 570 (2007) 192

A.Lazzaro et al., NIMA 585 (2008) 136

A.Lazzaro et al., NIMA 591 (2008) 394

A.Lazzaro et al., NIMA 602 (2009) 494

Software ray-reconstruction

ALGEBRIC RAY-RECONSTRUCTION

✓ Solution of the equation of motion for each detected particle
✓ Inversion of the transport matrix
✓ Application to the final measured parameters

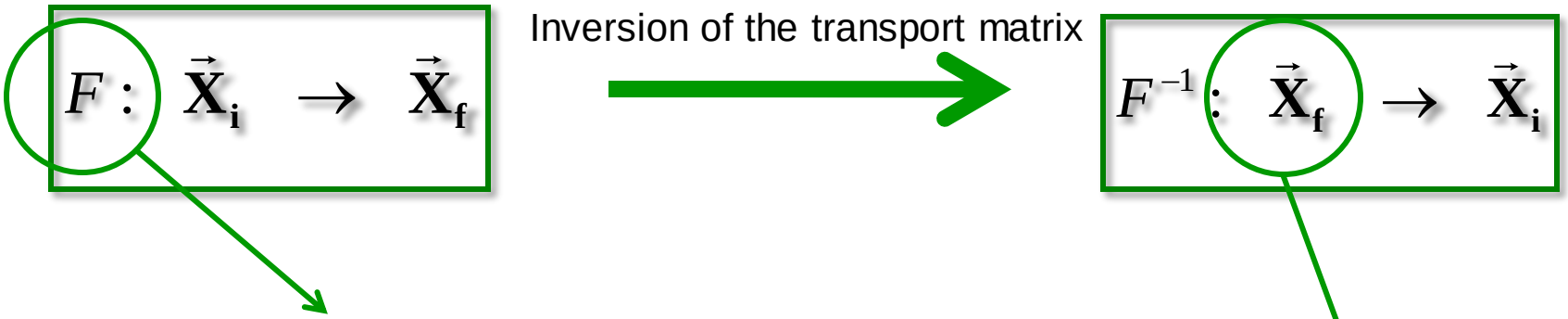

1) Detailed knowledge of the geometry and magnetic field

2) High resolution measurement at the focal plane (highly performing detectors)

2) MAGNEX Focal Plane Detector

Two tasks to accomplish:

1) High resolution measurement at the focal plane of the phase space parameters (X_{foc}, Y_{foc}, θ_{foc}, ϕ_{foc})

2) Identification of the reaction ejectiles (Z, A) - crucial aspect for heavy ions

Hybrid detector:
Gas section: proportional wires and drift chambers
+
Stopping wall of silicon detectors

2) MAGNEX Focal Plane Detector
Wire-based detector

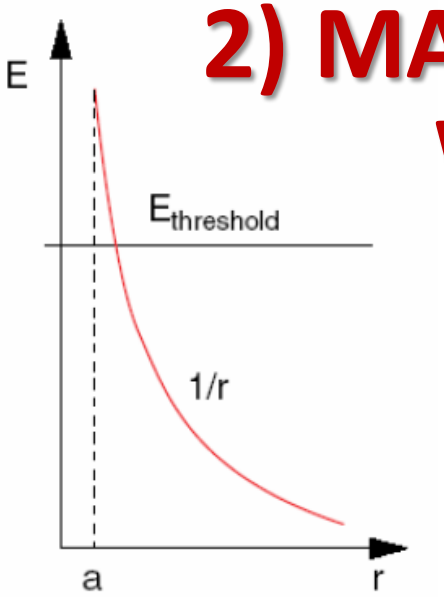

$$E(r) = \frac{CV_0}{2\pi\varepsilon_0} \cdot \frac{1}{r}$$

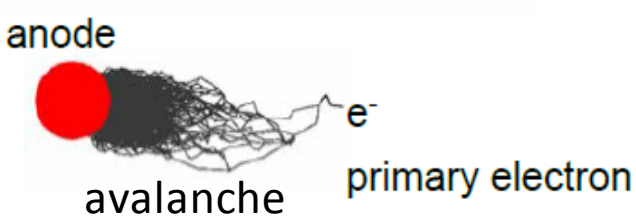

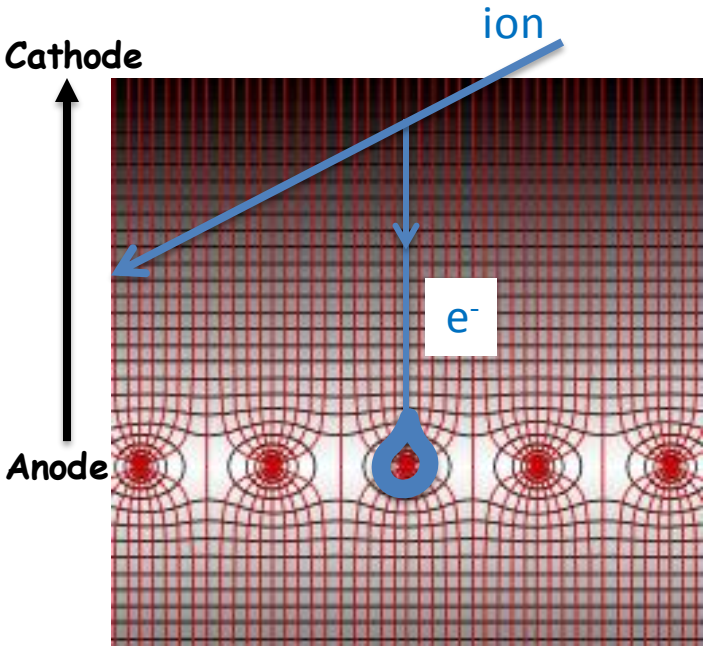

Multi-Wire Proportional Chamber -MWPC

Properties:

- Flexible geometry and large area (~m^2)
- Cheap
- Many well developed position encoding methods
- Works in magnetic field
- Electron avalanche multiplication (Gain) ≈ 10^4-10^5
- Position resolution ➔ down to 100 µm for 1 mm wire spacing (limited in size)
- Rate capability ≈ 10^4 Hz/mm^2

2) MAGNEX Focal Plane Detector

Large volume: 1360mm X 200mm X 96mm

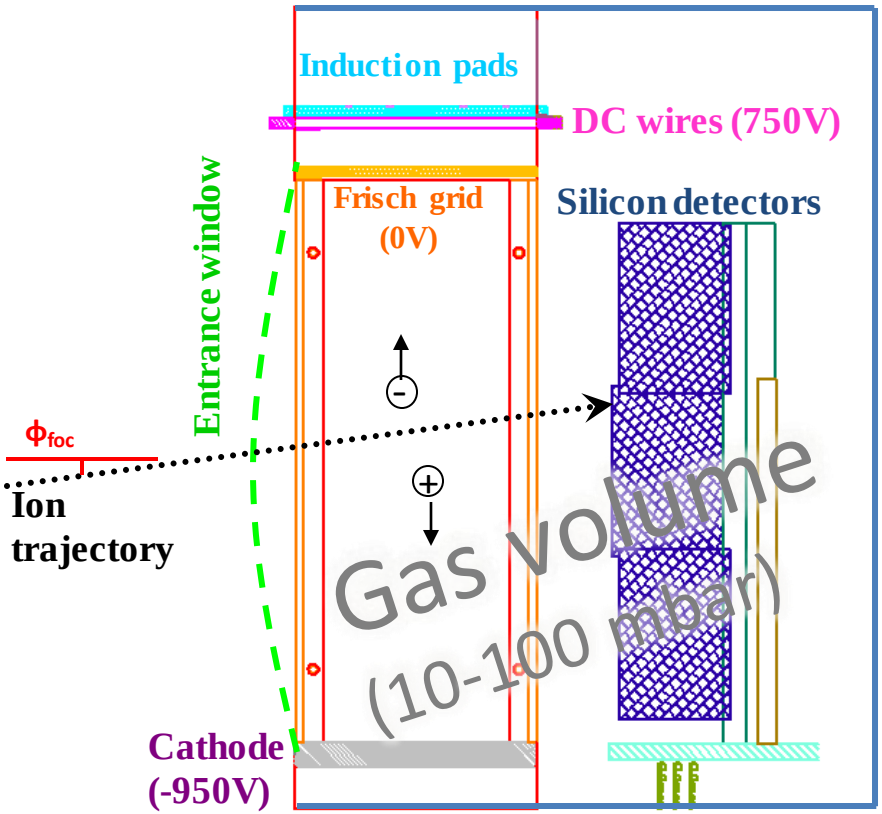

Section view

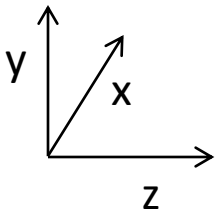

Wall of 60 stopping 7 X 5 cm^2 Silicon detectors
Covered area 100 X 20 cm^2
Thickness 500 – 1000 µm

M.Cavallaro et al. EPJA 48: 59 (2012)

D.Carbone et al. EPJA 48: 60 (2012)

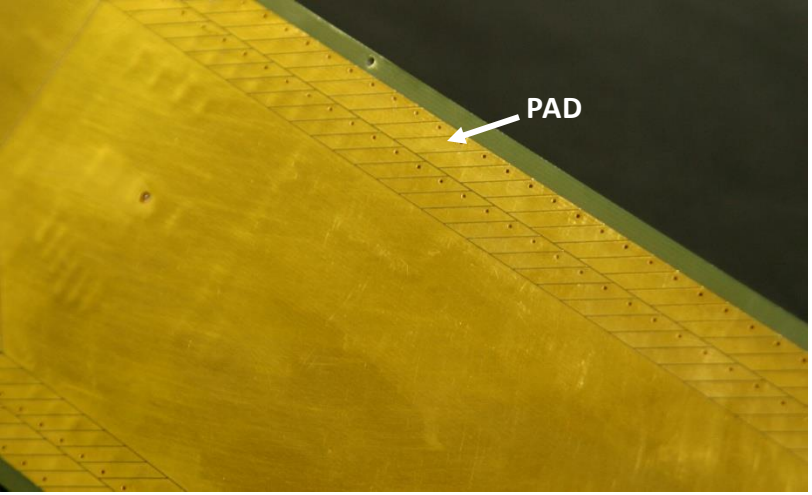
PAD

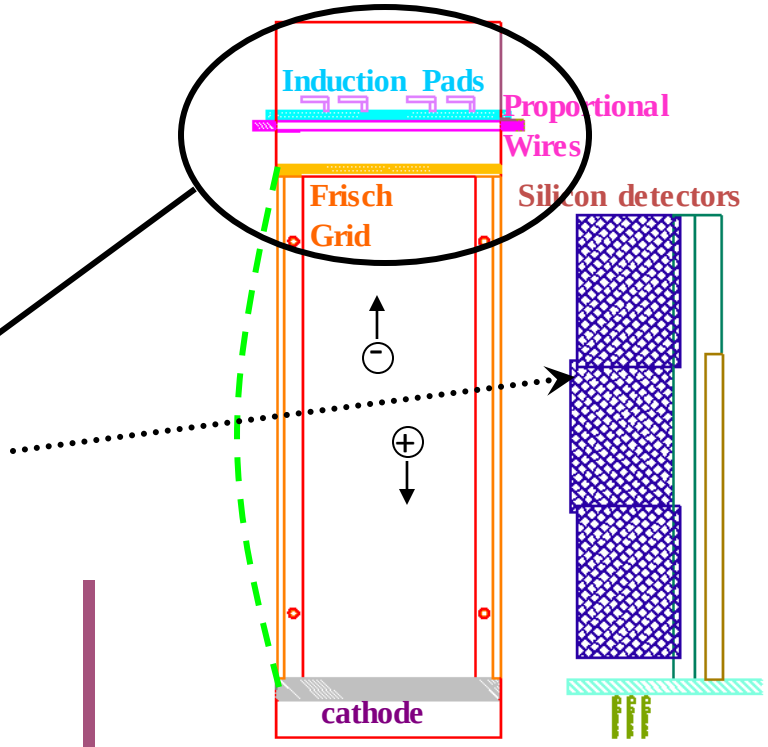
Induction Pads
Proportional Wires
Frisch Grid
Silicon detectors
cathode

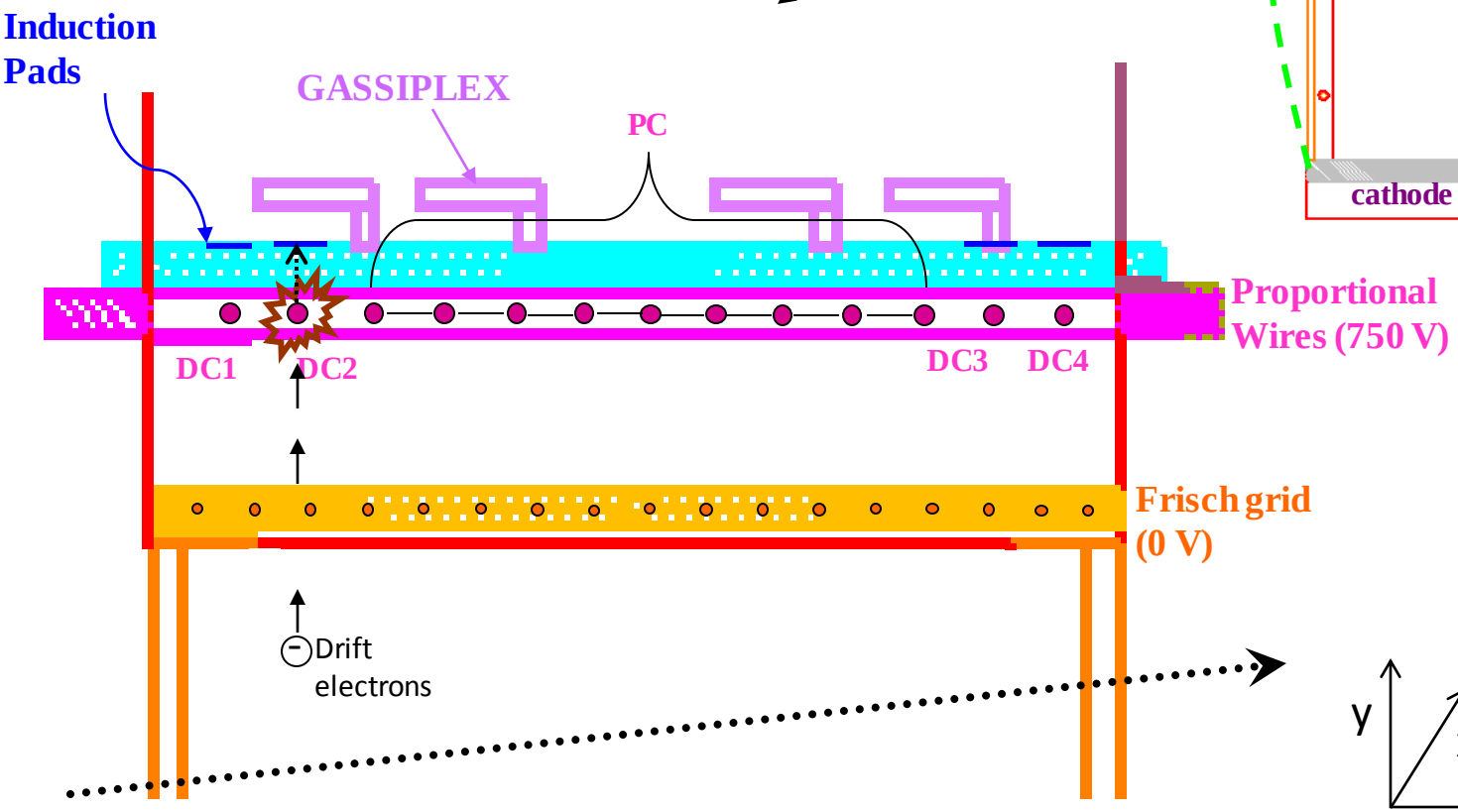
Induction Pads
GASSIPLEX
PC
Proportional Wires (750 V)
DC1
DC2
DC3
DC4
Frisch grid (0 V)
Drift electrons
y
x
z

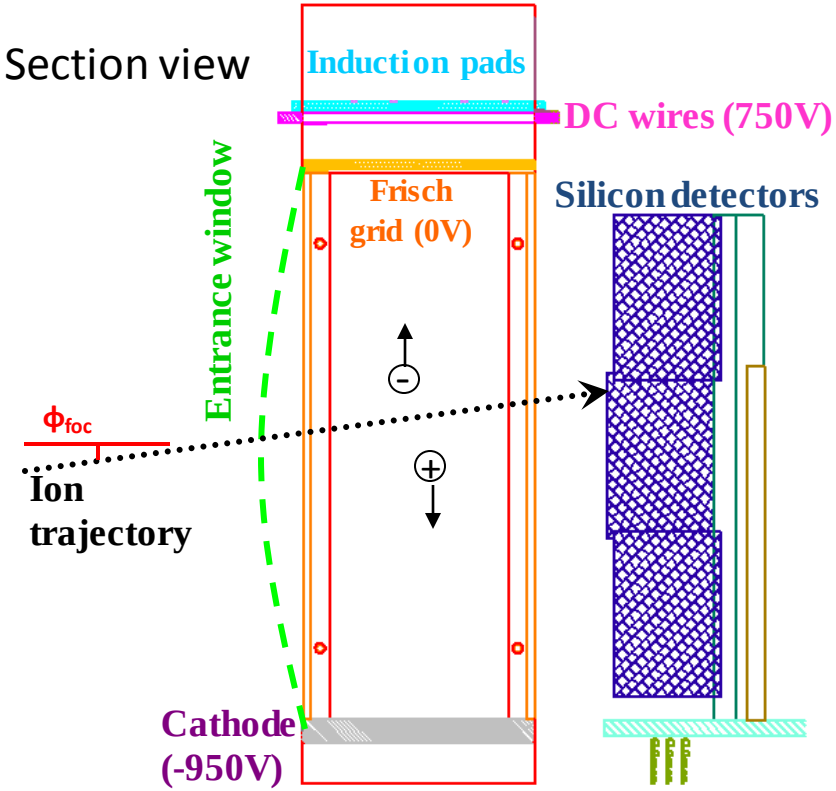

60 Silicon Detectors
→ E_{res}

5 Proportional Wires
→ ΔE

Ion identification

4 Induction Strip
→ X_1, X_2, X_3, X_4
→ X_{foc}, θ_{foc}

4 Drift Chamber (DC)
→ Y_1, Y_2, Y_3, Y_4
→ Y_{foc}, Φ_{foc}

Ray-reconstruction

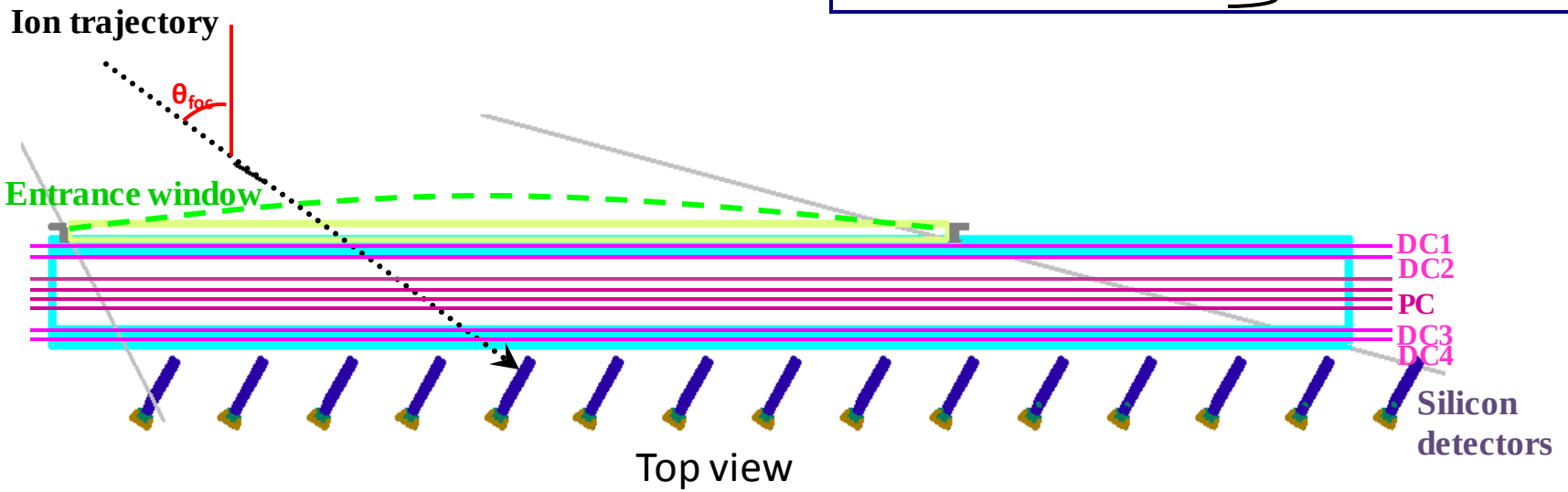

Particle Identification

F. Cappuzzello et al., NIMA 621 (2010) 419

Z identification

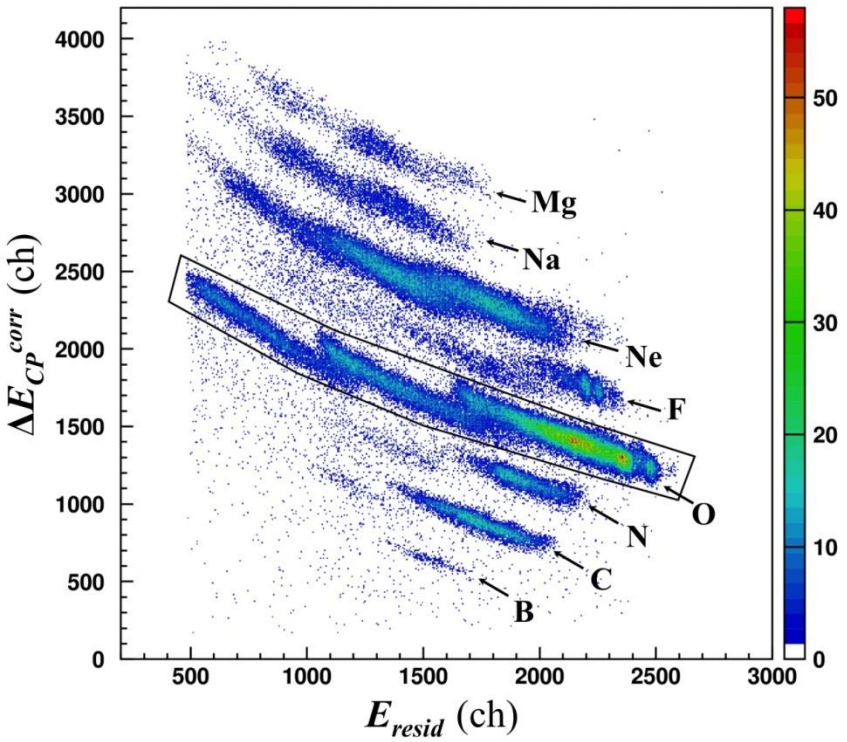

A identification

$$B\rho = \frac{p}{q} \rightarrow X_{foc}^2 \propto \frac{m}{q^2} E_{resid}$$

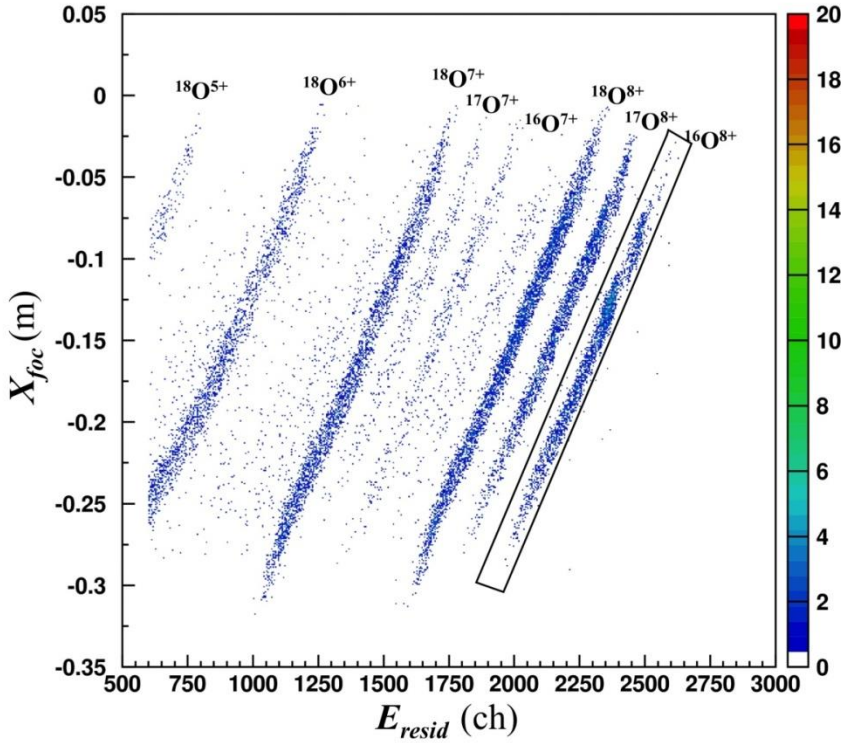

Mass resolution Δm/m ~ 1/160

MAGNEX FPD characteristics

Horizontal and vertical position resolution (FWHM)	0.6 mm
Horizontal and vertical angular resolution (FWHM)	0.3°
Mass resolution[a]	0.6%
Explored ion mass range	from $A = 1$ to $A = 48$
Energy loss resolution[b]	6.3%
Maximum incident ion rate (uniform distribution)	5 kHz
Maximum incident ion rate (localized in ~ 1 cm)	2 kHz

For O at 300 MeV
10^4 Hz/mm^2

Software ray-reconstruction

ALGEBRIC RAY-RECONSTRUCTION

✓ Solution of the equation of motion for each detected particle
✓ Inversion of the transport matrix
✓ Application to the final measured parameters

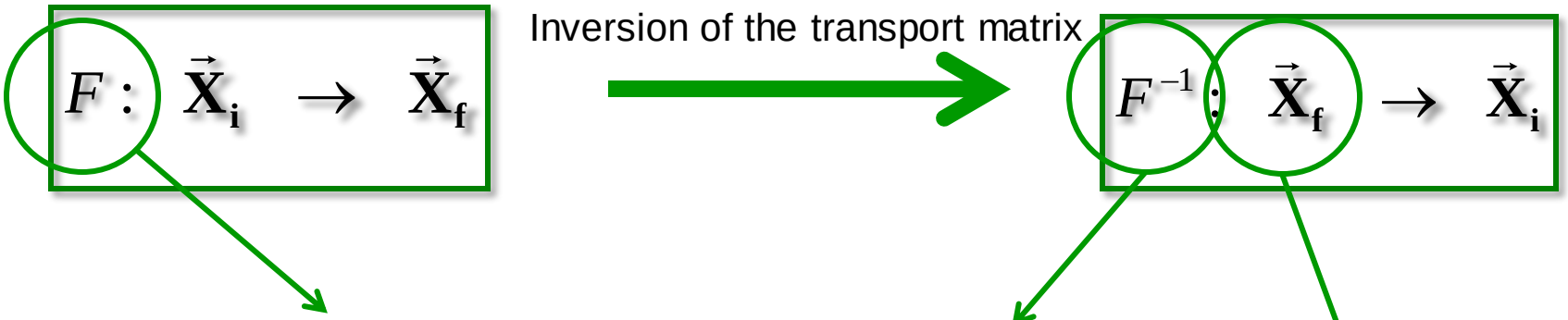

1) Detailed knowledge of the geometry and magnetic field

3) Algorithm to transport and invert

2) High resolution measurement at the focal plane (highly performing detectors)

3) Algorithm to transport and invert

ALGEBRIC
RAY-RECONSTRUCTION
(*Differential Algebras*)
COSY-INFINITY

Solution of the equation of motion for each detected particle

$$F : \vec{X}_i \rightarrow \vec{X}_f$$

Direct transport map

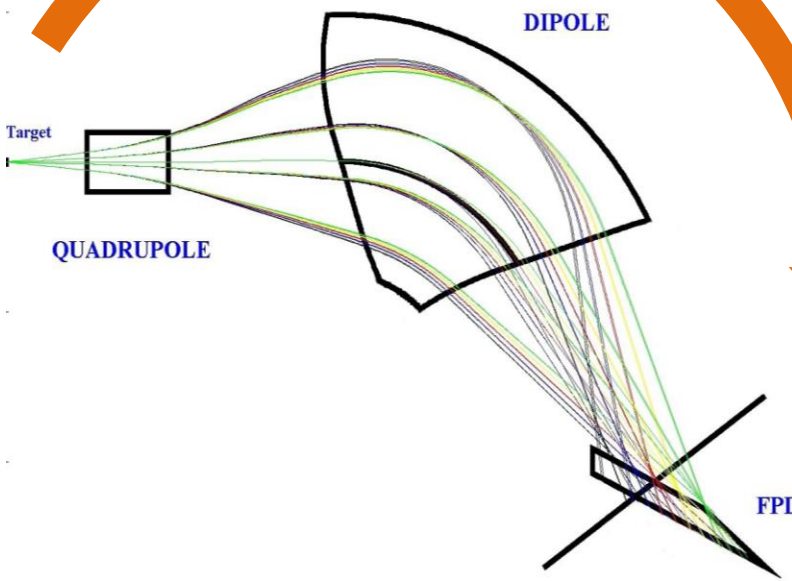

$\vec{P}_i(E^*, \theta_{lab})$

Physical Parameters at the target

$\vec{P}_f(X_{foc}, Y_{foc}, \theta_{foc}, \varphi_{foc})$

Geometrical Parameters at the FPD

F. Cappuzzello, et al., NIM A 638, (2011) 74

3) Algorithm to transport and invert

Examples of parameters at the focal plane

Black: measured parameters
Red: Simulated parameters

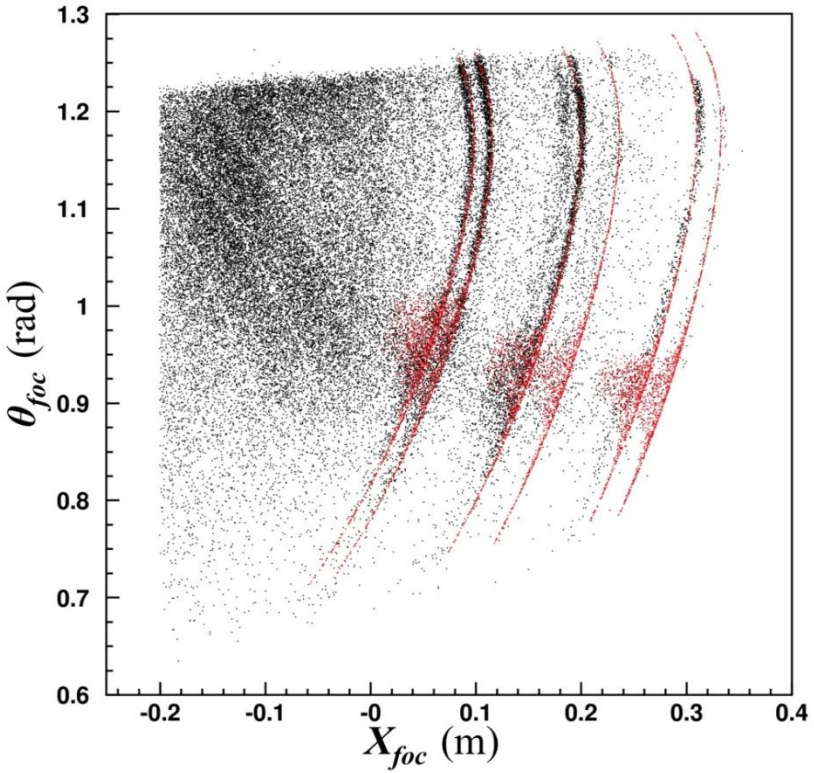

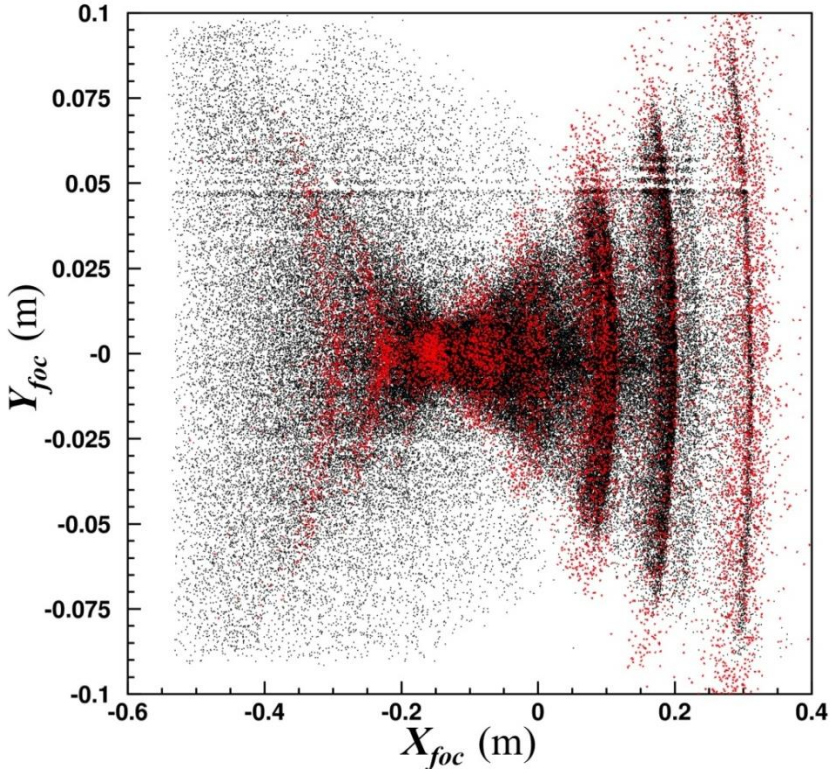

3) Algorithm to transport and invert

Effect of high order aberrations

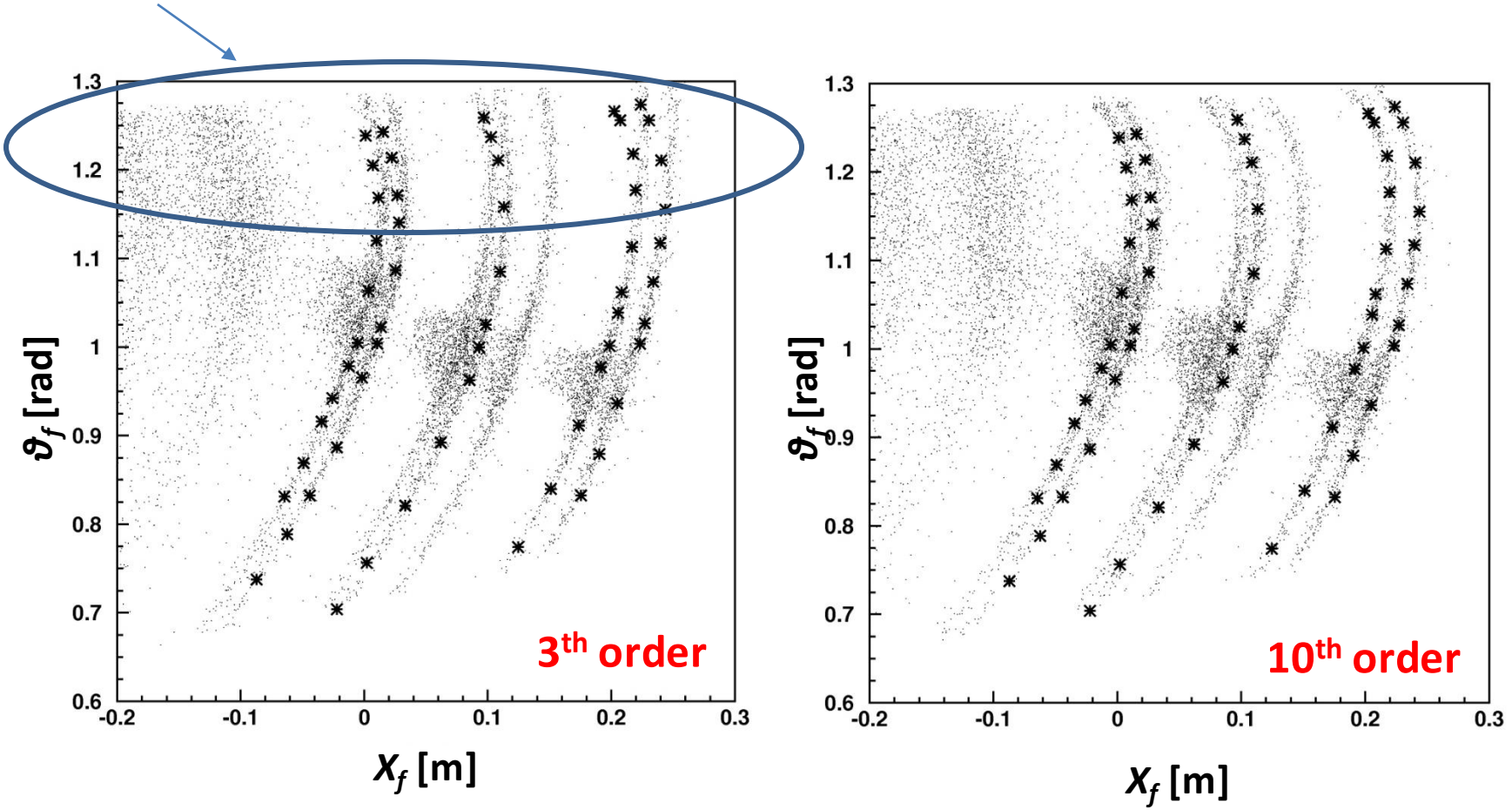

3) Algorithm to transport and invert

ALGEBRIC RAY-RECONSTRUCTION
(*Differential Algebras*)
COSY-INFINITY

Solution of the equation of motion for each detected particle

$$F^{-1} : \vec{X}_f \rightarrow \vec{X}_i$$

Inverted transport map

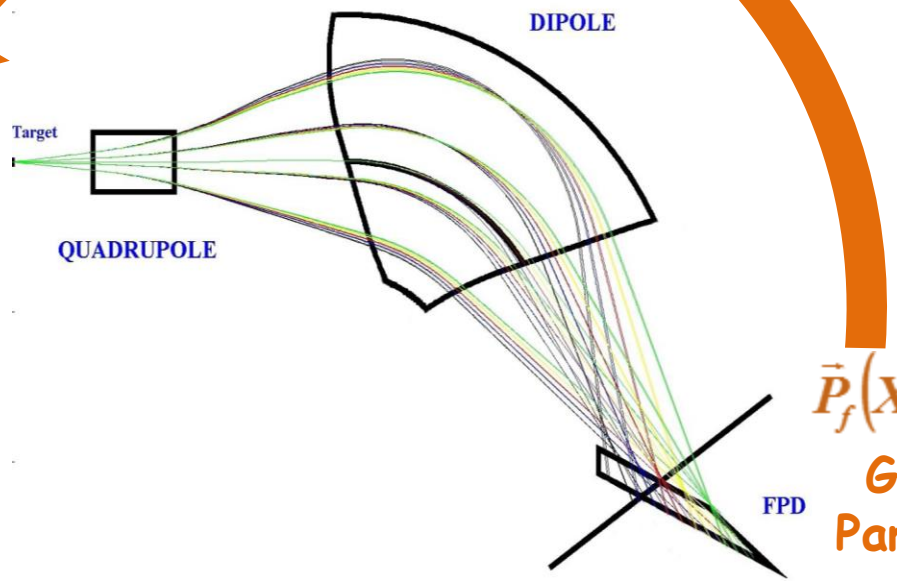

$\vec{P}_i(E^*, \theta_{lab})$
Physical Parameters at the target

$\vec{P}_f(X_{foc}, Y_{foc}, \theta_{foc}, \varphi_{foc})$
Geometrical Parameters at the FPD

F. Cappuzzello, et al., NIM A 638, (2011) 74

3) Algorithm to transport and invert

High order aberrations!

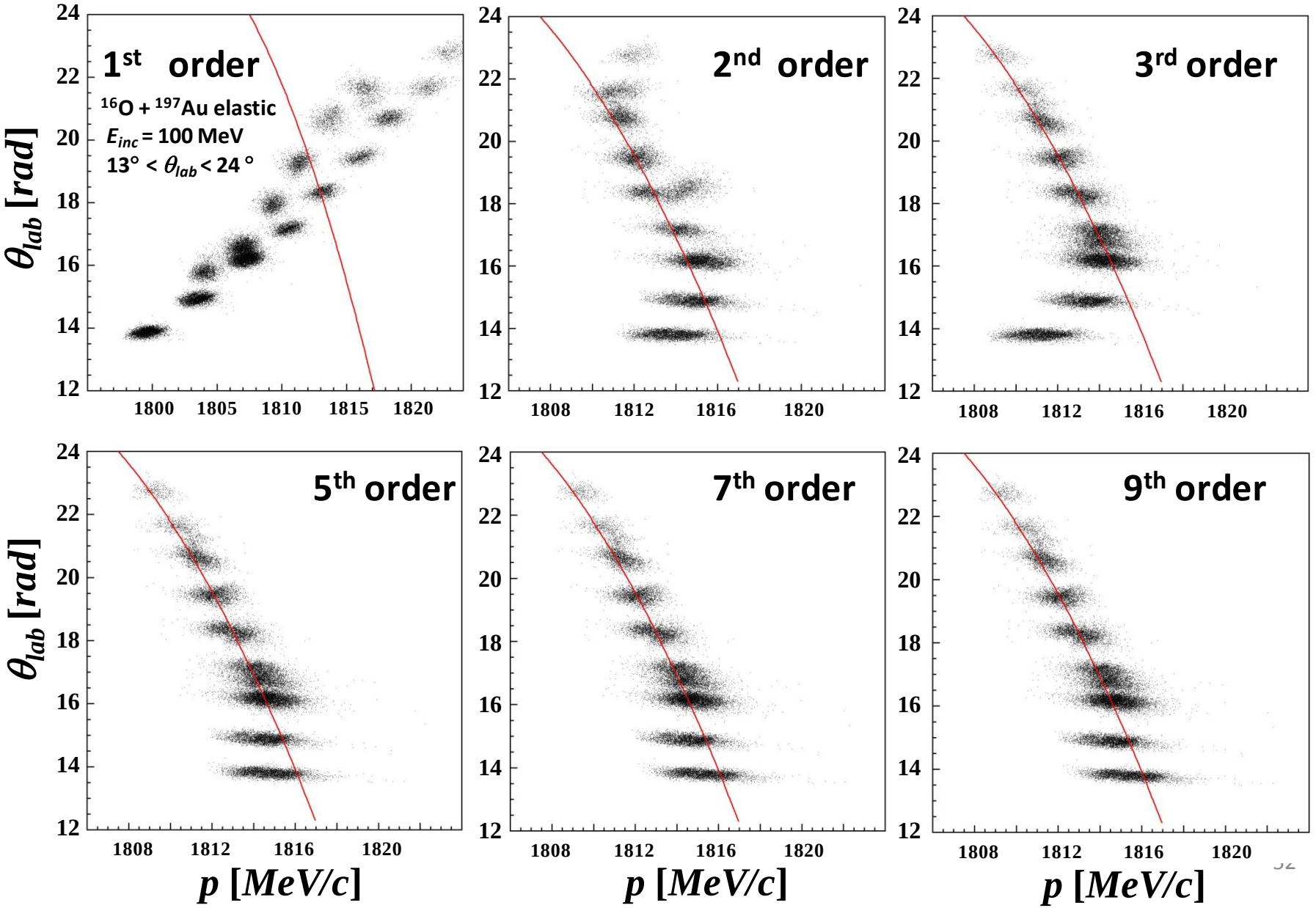

3) Algorithm to transport and invert

$^{27}Al(^{16}O,^{16}O)^{27}Al$ at 100 MeV

$13° < \theta_{lab} < 20°$

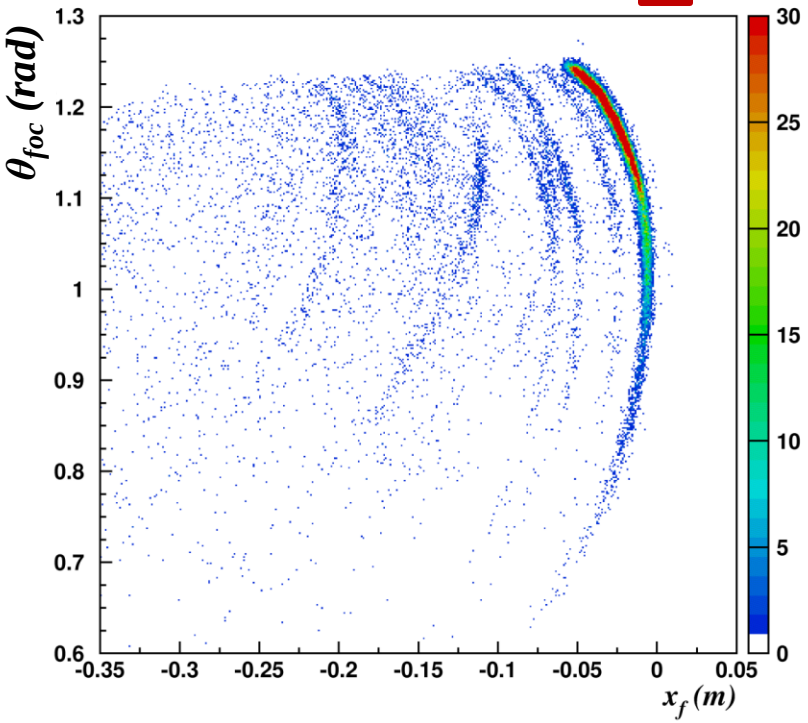

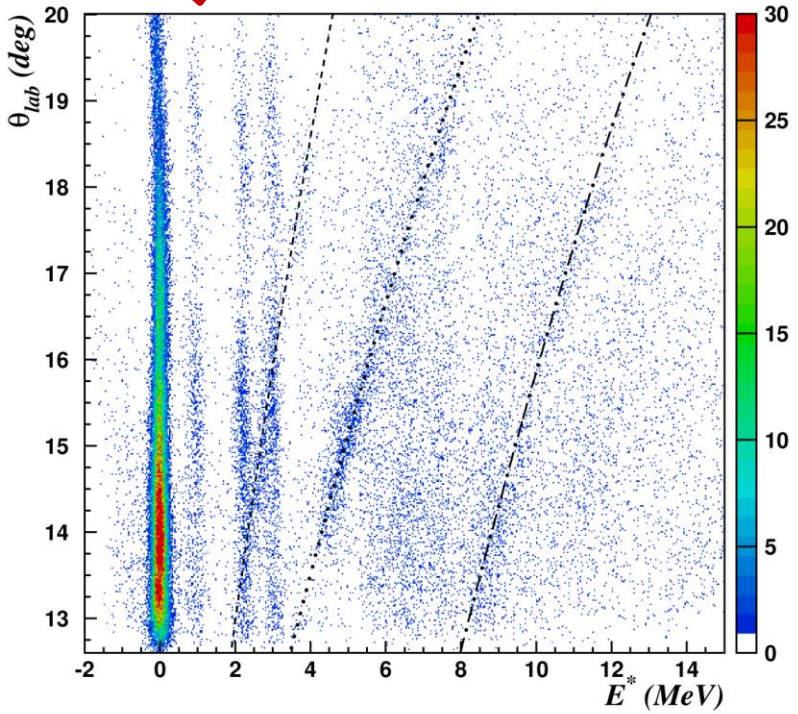

$$E^* = Q - K\left(1 + \frac{M_{ejectile}}{M_{residual}}\right) + E_{beam}\left(1 - \frac{M_{beam}}{M_{residual}}\right) + 2\frac{\sqrt{M_{beam}M_{ejectile}}}{M_{residual}}\sqrt{E_{beam}K}\cos\theta_{lab}$$

M. Cavallaro et al., NIMA 648 (2011) 46-51

F. Cappuzzello et al., NIMA 638 (2011) 74-82

Typical energy spectra

$^{12}C(^{18}O,^{16}O)^{14}C$

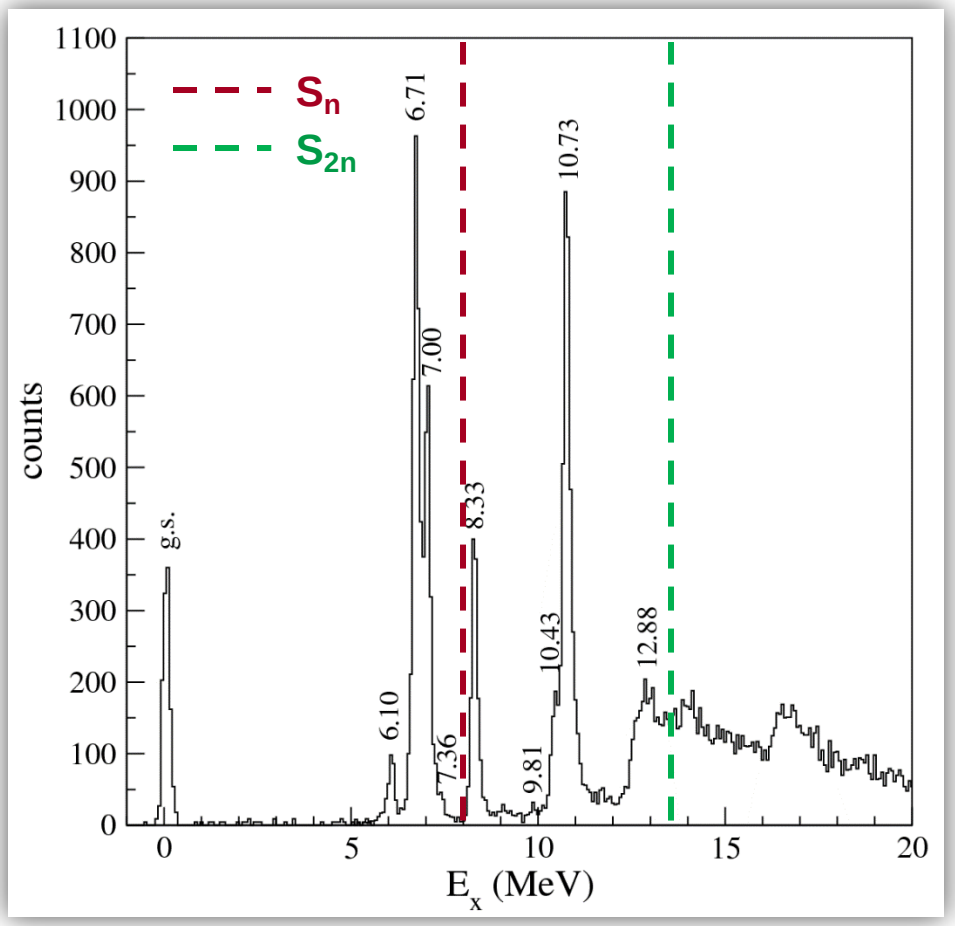

$^{13}C(^{18}O,^{16}O)^{15}C$

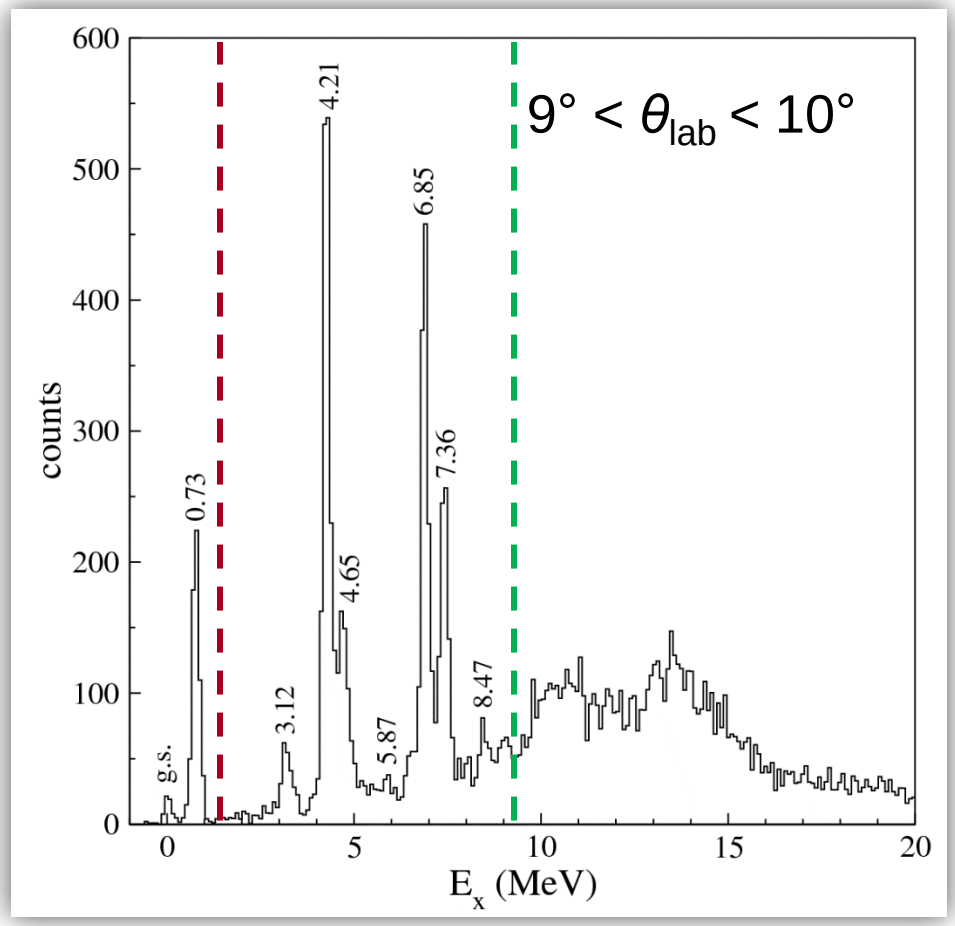

3-peaks α-source ^{241}Am + ^{239}Pu + ^{244}Cm

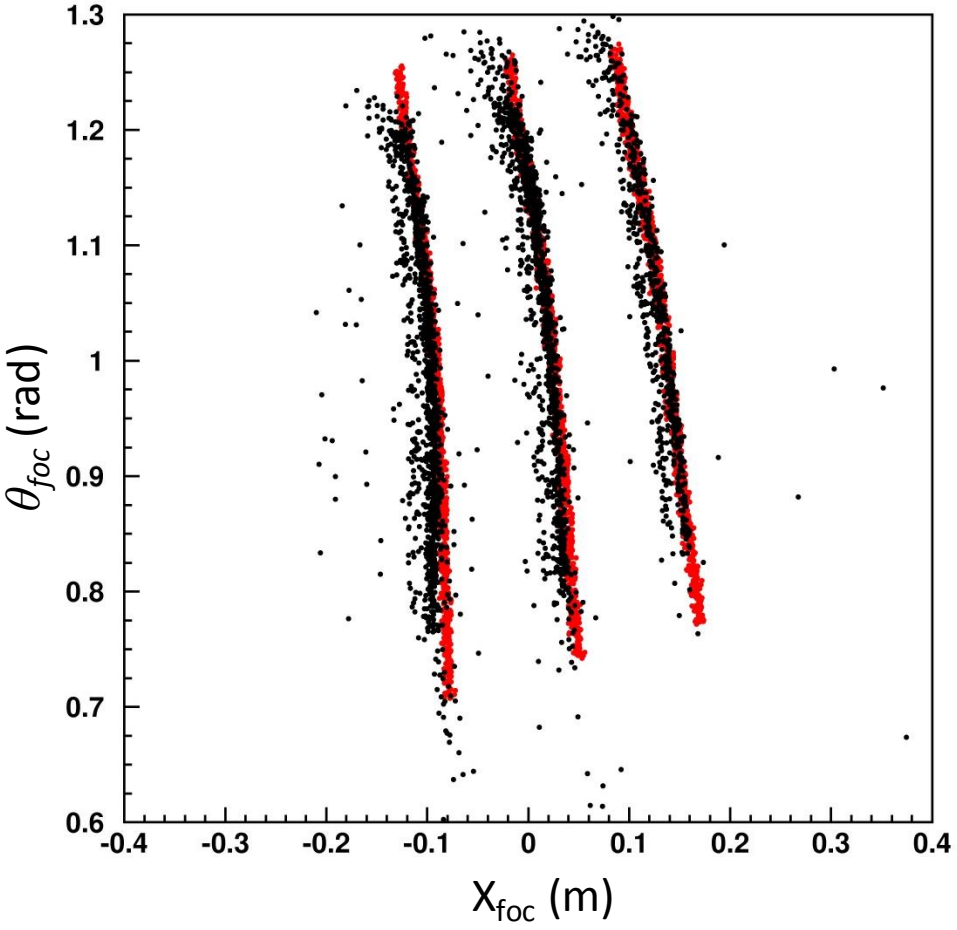

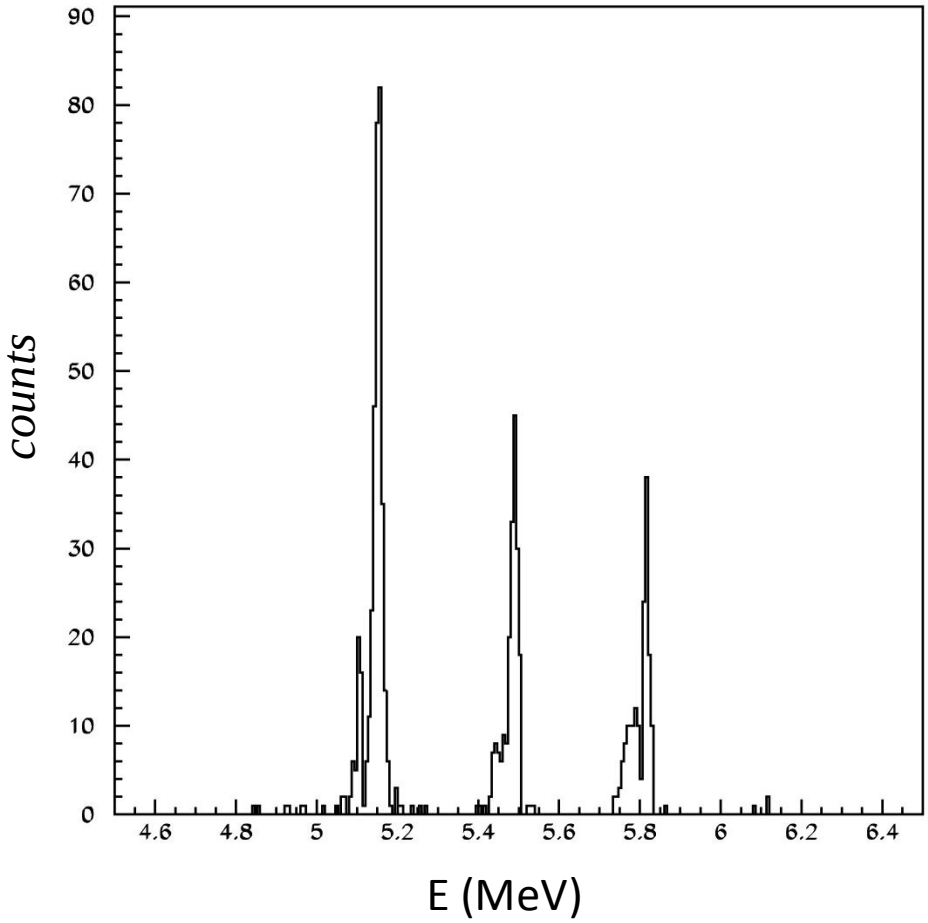

3) Algorithm to transport and invert

$^{27}Al(^{16}O,^{16}O)^{27}Al$ at 100 MeV

$13° < \theta_{lab} < 20°$

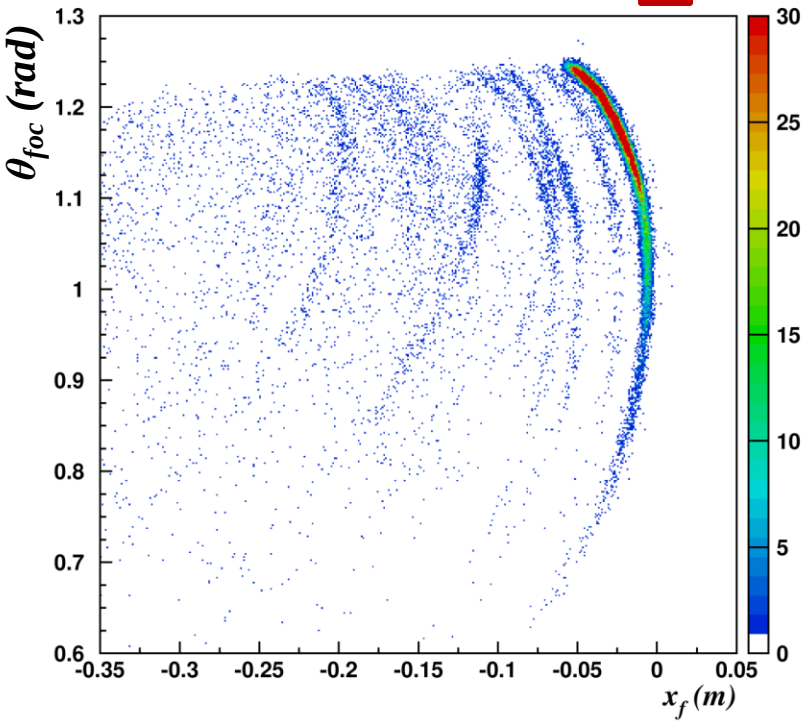

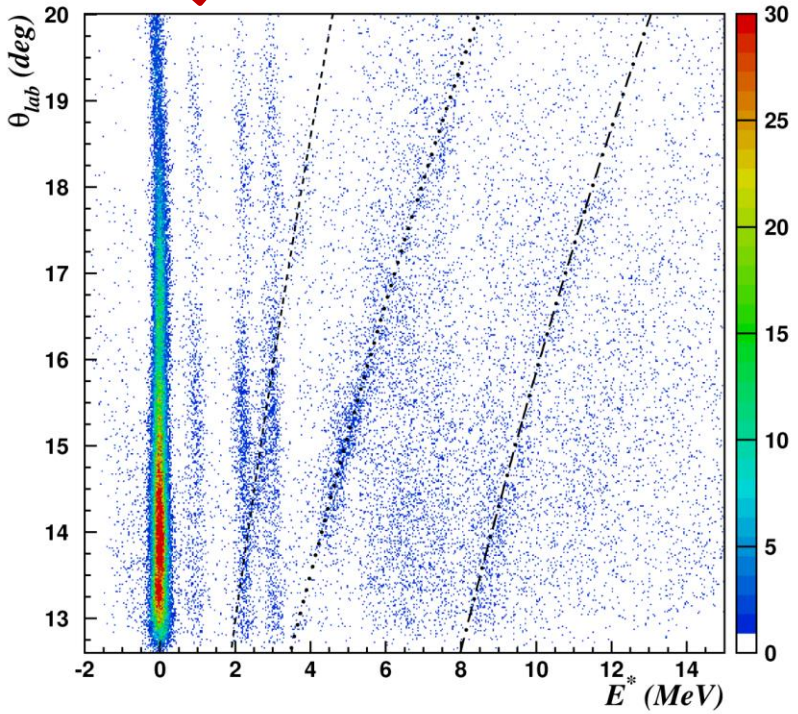

$$E^* = Q - K\left(1 + \frac{M_{ejectile}}{M_{residual}}\right) + E_{beam}\left(1 - \frac{M_{beam}}{M_{residual}}\right) + 2\frac{\sqrt{M_{beam}M_{ejectile}}}{M_{residual}}\sqrt{E_{beam}K}\cos\theta_{lab}$$

M. Cavallaro et al., NIMA 648 (2011) 46-51

F. Cappuzzello et al., NIMA 638 (2011) 74-82

Typical angular distribution

$^{18}O + {}^{12}C_{g.s.}(0^+) \rightarrow {}^{18}O + {}^{14}C_{g.s.}(0^+)$ **$L = 0$**

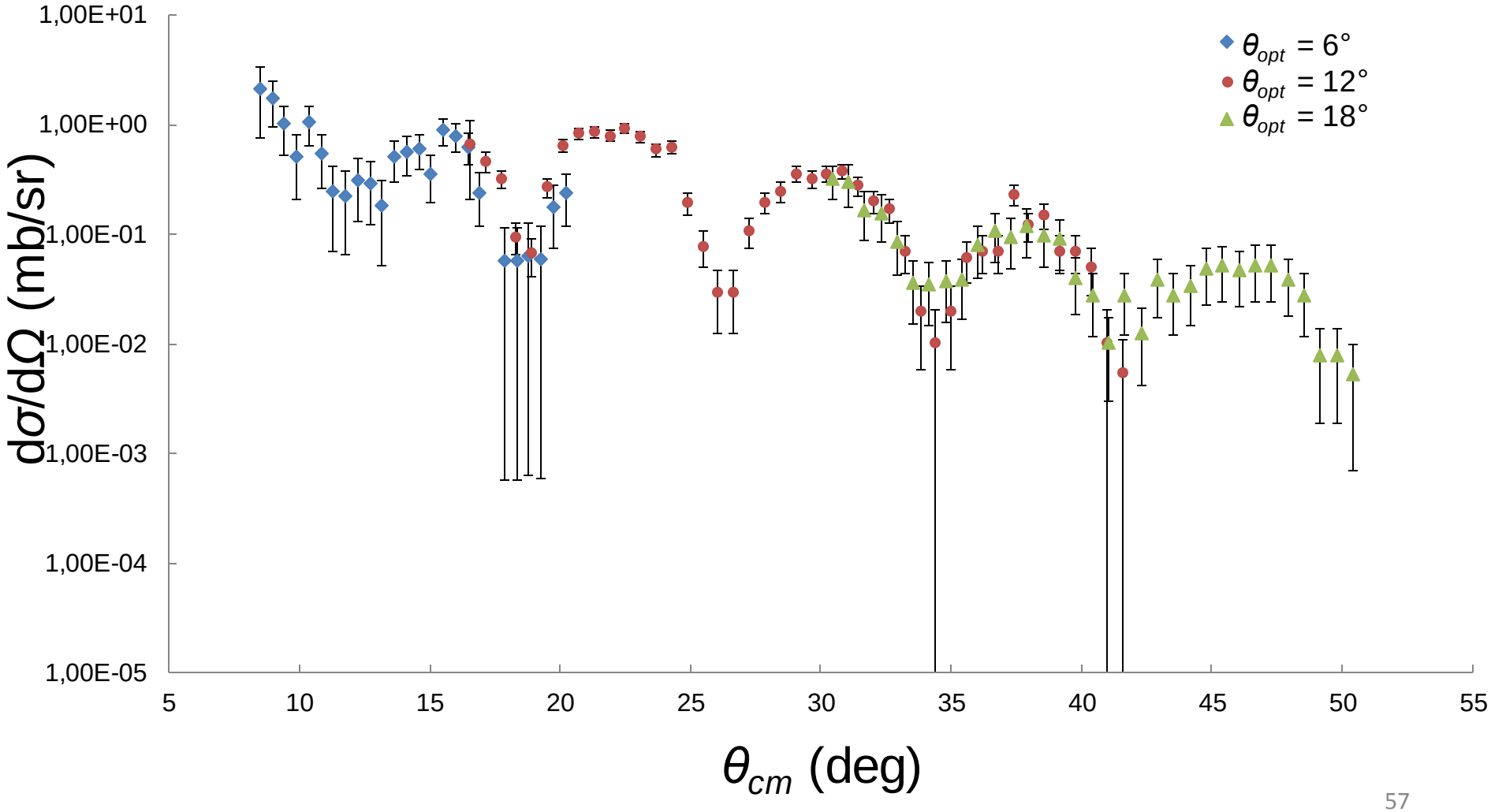

MAGNEX FPD characteristics

Horizontal and vertical position resolution (FWHM)	0.6 mm
Horizontal and vertical angular resolution (FWHM)	0.3°
Mass resolution[a]	0.6%
Explored ion mass range	from $A = 1$ to $A = 48$
Energy loss resolution[b]	6.3%
Maximum incident ion rate (uniform distribution)	5 kHz
Maximum incident ion rate (localized in ~ 1 cm)	2 kHz

For O at 300 MeV
10^4 Hz/mm^2

The NUMEN experiment

Manuela Cavallaro

INFN – Laboratori Nazionali del Sud

(Italy)

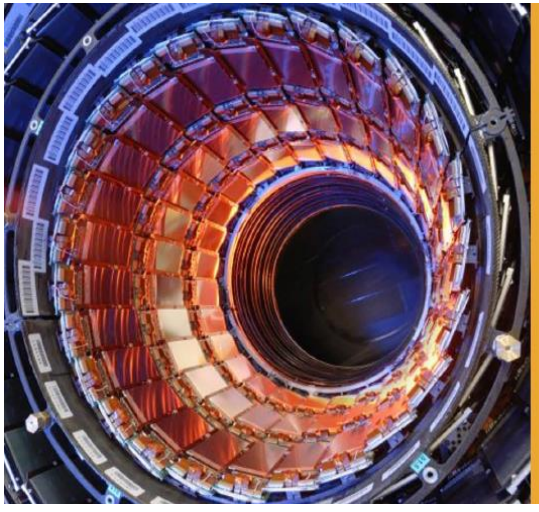

XXVI GIORNATE DI STUDIO SUI RIVELATORI

Scuola F. Bonaudi

Cogne, 13 – 17 February 2017

Advantages of magnetic spectrometry

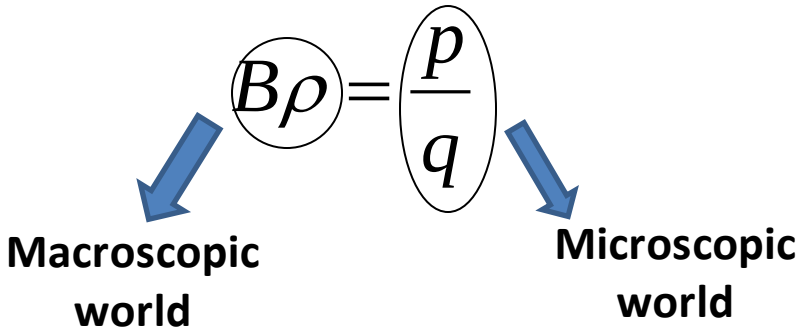

- Good selection of reaction products
- Possibility to measure near 0°
- High momentum and mass resolution

MAGNEX: a large acceptance QD spectrometer

- **The Quadrupole**: vertically focusing
  (Aperture radius 20 cm, effective length 58 cm. Maximum field strength 5 T/m)

- **The Dipole**: momentum dispersion (and horizontal focus)
  (Mean bend angle 55°, radius 1.60 m. Maximum field ~ 1.15 T)

- **The surface coils**, located between the dipole pole faces and the inner high vacuum chamber, giving tunable quadrupolar and sextupolar corrections

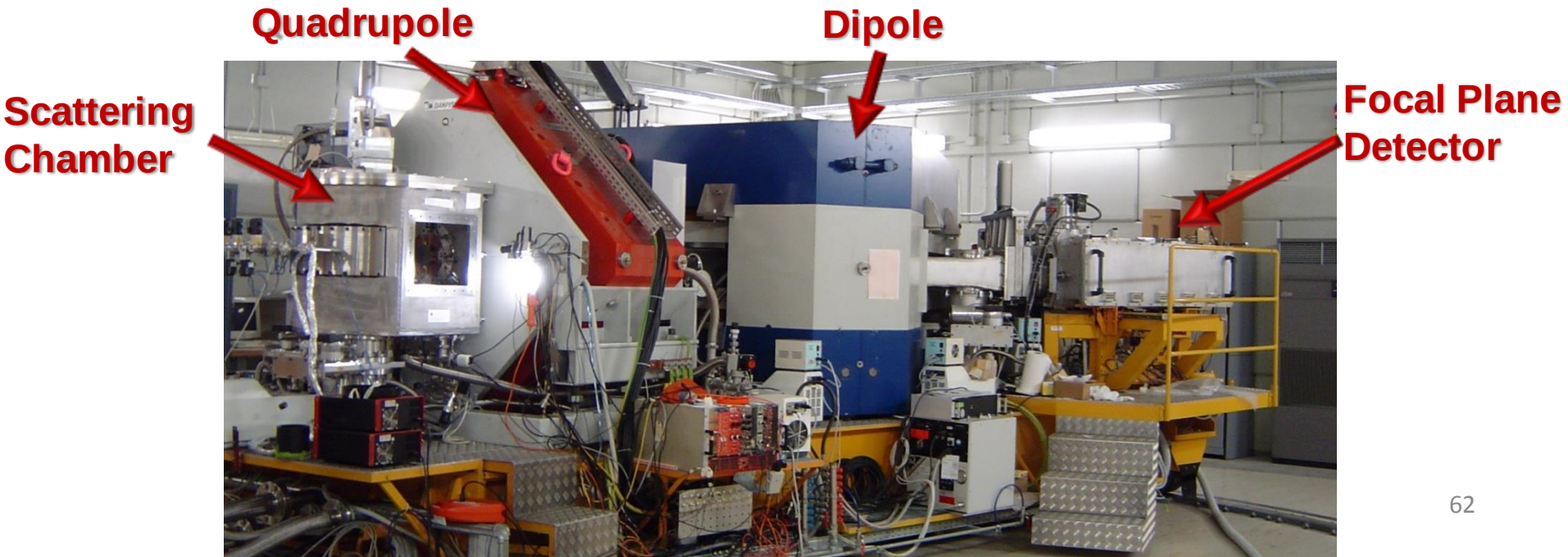

The large acceptance problem

$$F: \vec{X}_i \rightarrow \vec{X}_f$$

F transport matrix

Large acceptance

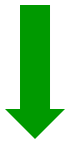

Aberrations

$$x_i(f) = \sum_j R_{ij}\, x_j(i) + \sum_{j,k} T_{ijk}\, x_j(i)\, x_k(i) + \ldots..$$

Up to 10° order

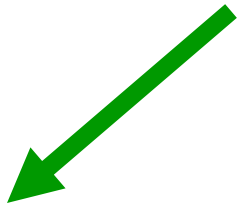

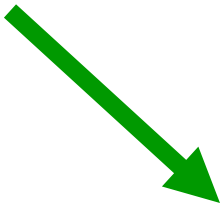

Careful hardware design
(to minimize the aberrations)

Software ray-reconstruction
(to know the aberrations)

3) Algorithm to transport and invert

ALGEBRIC
RAY-RECONSTRUCTION
(*Differential Algebras*)
COSY-INFINITY

Solution of the equation of motion for each detected particle

$$F : \vec{X}_i \rightarrow \vec{X}_f$$

Direct transport map

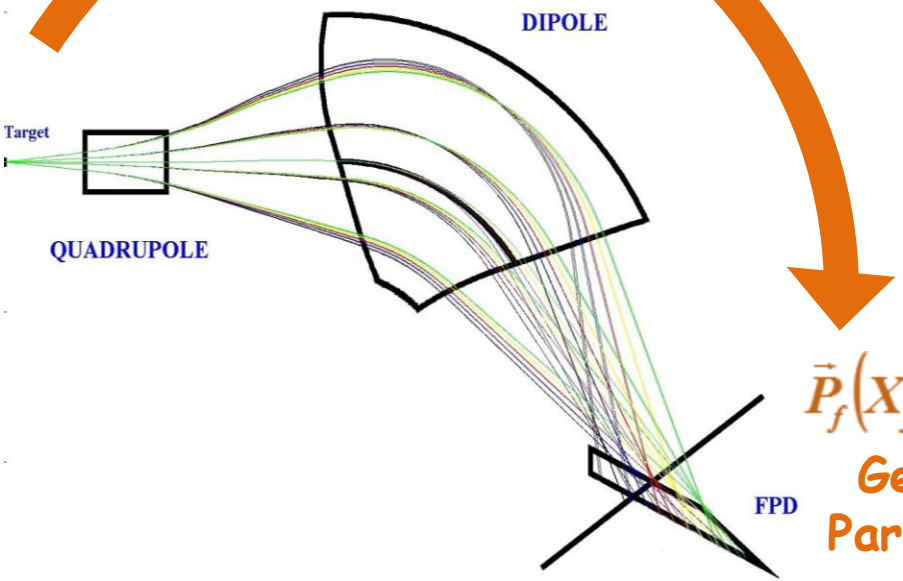

$\vec{P}_i(E^*, \theta_{lab})$
Physical Parameters at the target

$\vec{P}_f(X_{foc}, Y_{foc}, \theta_{foc}, \varphi_{foc})$
Geometrical Parameters at the FPD

F. Cappuzzello, et al., NIM A 638, (2011) 74

3) Algorithm to transport and invert

ALGEBRIC RAY-RECONSTRUCTION
(*Differential Algebras*)
COSY-INFINITY

Solution of the equation of motion for each detected particle

$$F^{-1} : \vec{X}_f \rightarrow \vec{X}_i$$

Inverted transport map

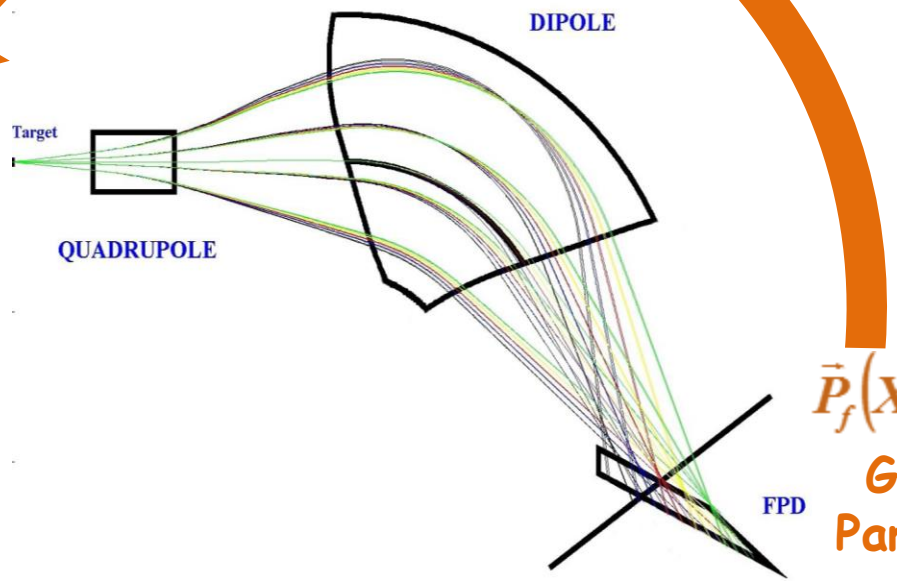

$\vec{P}_i(E^*, \theta_{lab})$
Physical Parameters at the target

$\vec{P}_f(X_{foc}, Y_{foc}, \theta_{foc}, \varphi_{foc})$
Geometrical Parameters at the FPD

F. Cappuzzello, et al., NIM A 638, (2011) 74

3) Algorithm to transport and invert

$^{27}Al(^{16}O,^{16}O)^{27}Al$ at 100 MeV

$13° < \theta_{lab} < 20°$

F^{-1}

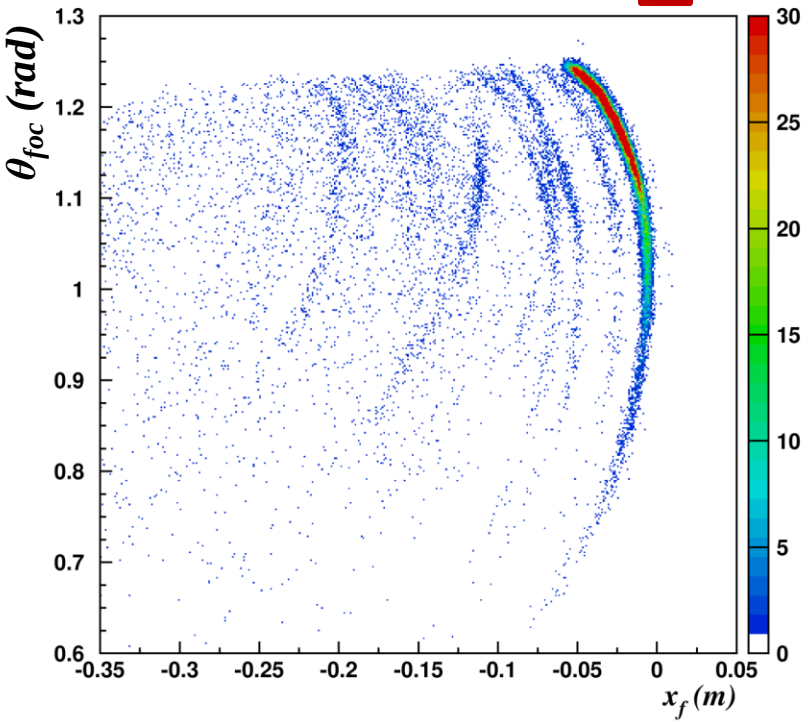

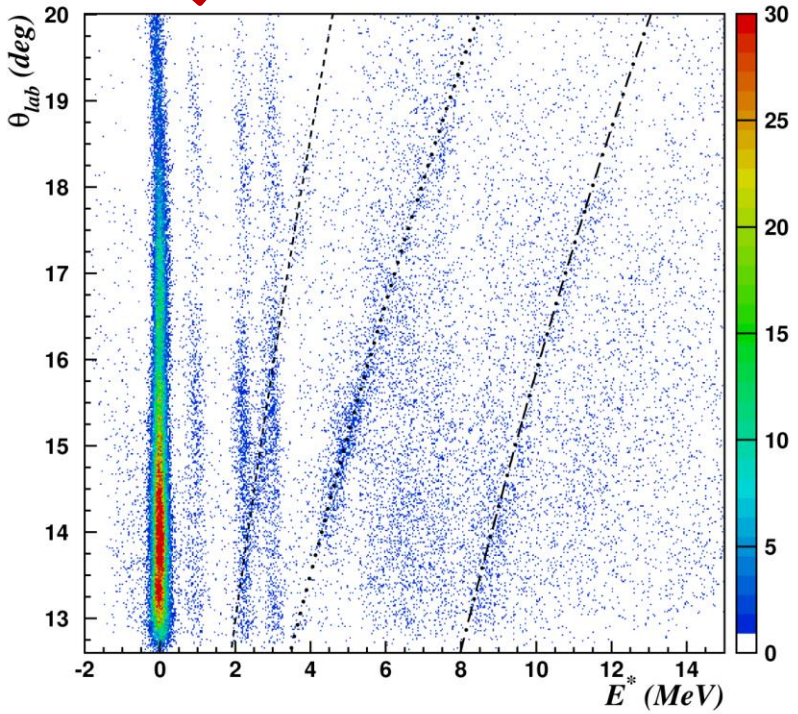

$$E^* = Q - K\left(1 + \frac{M_{ejectile}}{M_{residual}}\right) + E_{beam}\left(1 - \frac{M_{beam}}{M_{residual}}\right) + 2\frac{\sqrt{M_{beam}M_{ejectile}}}{M_{residual}}\sqrt{E_{beam}K}\cos\theta_{lab}$$

M. Cavallaro et al., NIMA 648 (2011) 46-51

F. Cappuzzello et al., NIMA 638 (2011) 74-82

Typical energy spectra

$^{12}C(^{18}O,^{16}O)^{14}C$

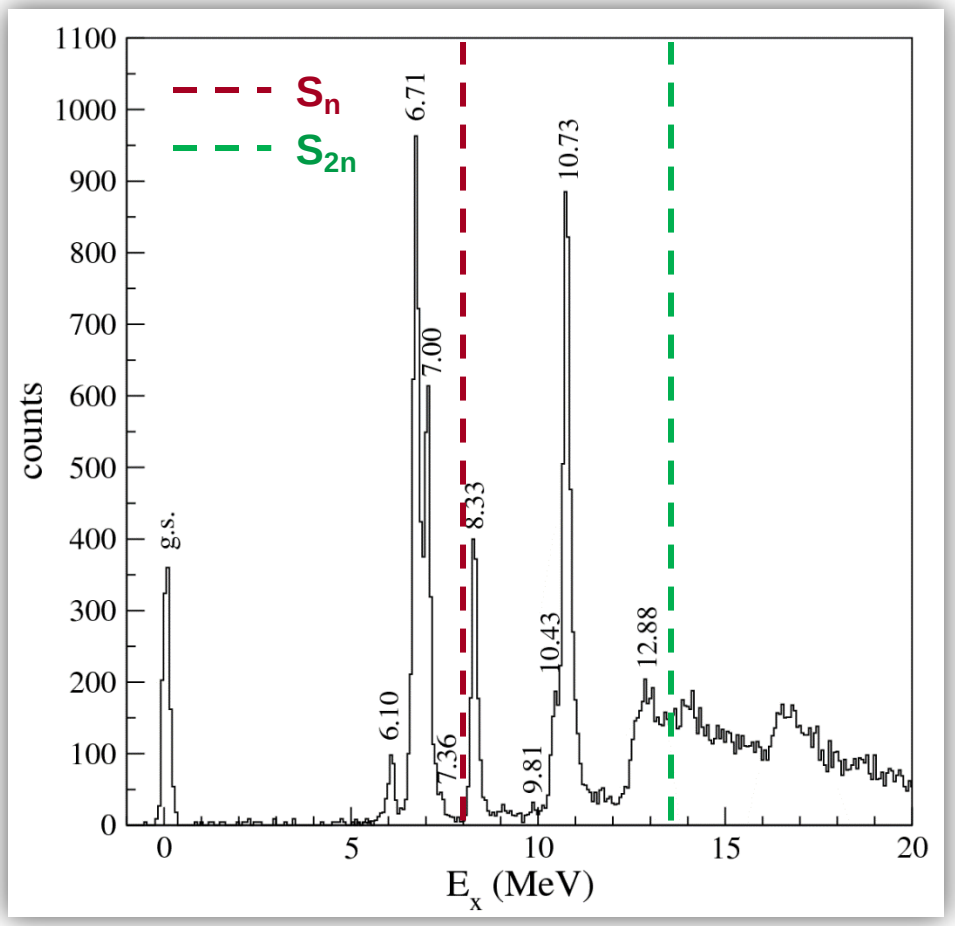

$^{13}C(^{18}O,^{16}O)^{15}C$

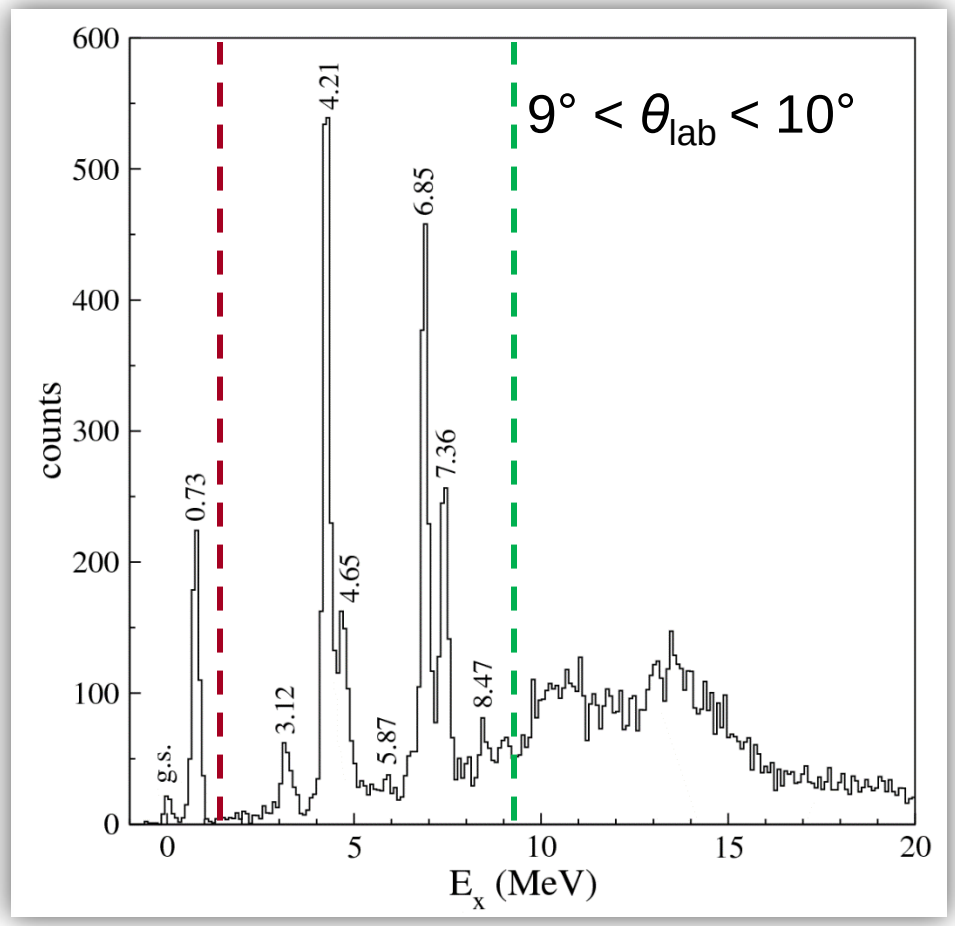

3) Algorithm to transport and invert

$^{27}Al(^{16}O,^{16}O)^{27}Al$ at 100 MeV

$13° < \theta_{lab} < 20°$

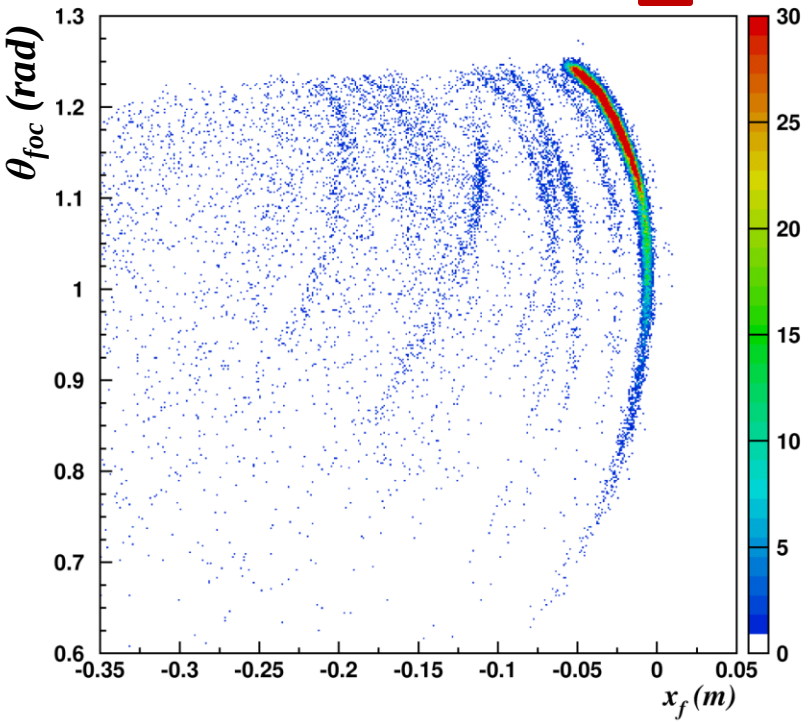

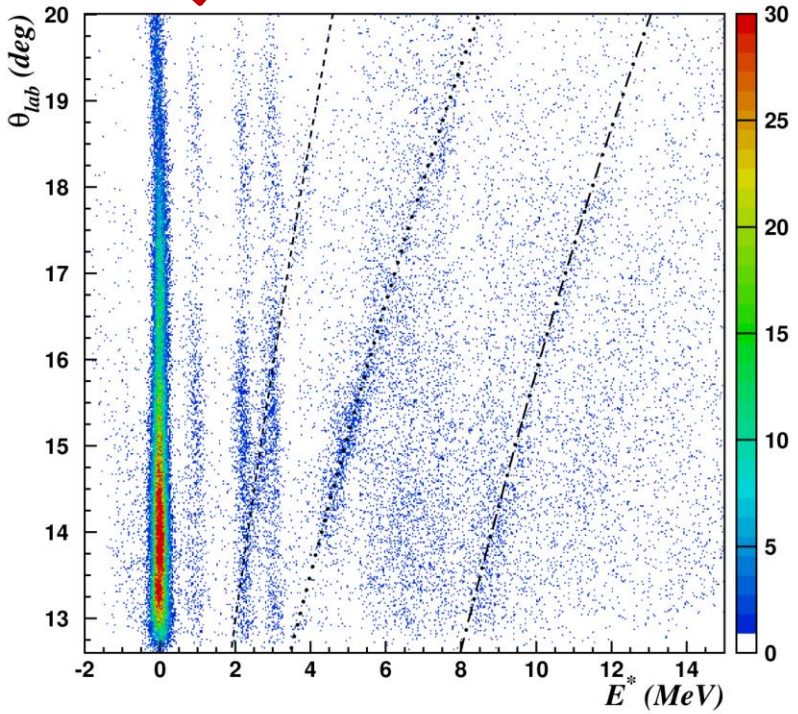

$$E^* = Q - K\left(1 + \frac{M_{ejectile}}{M_{residual}}\right) + E_{beam}\left(1 - \frac{M_{beam}}{M_{residual}}\right) + 2\frac{\sqrt{M_{beam}M_{ejectile}}}{M_{residual}}\sqrt{E_{beam}K}\cos\theta_{lab}$$

M. Cavallaro et al., NIMA 648 (2011) 46-51

F. Cappuzzello et al., NIMA 638 (2011) 74-82

Typical angular distribution

$^{18}O + {}^{12}C_{g.s.}(0^+) \rightarrow {}^{18}O + {}^{14}C_{g.s.}(0^+)$ **$L = 0$**

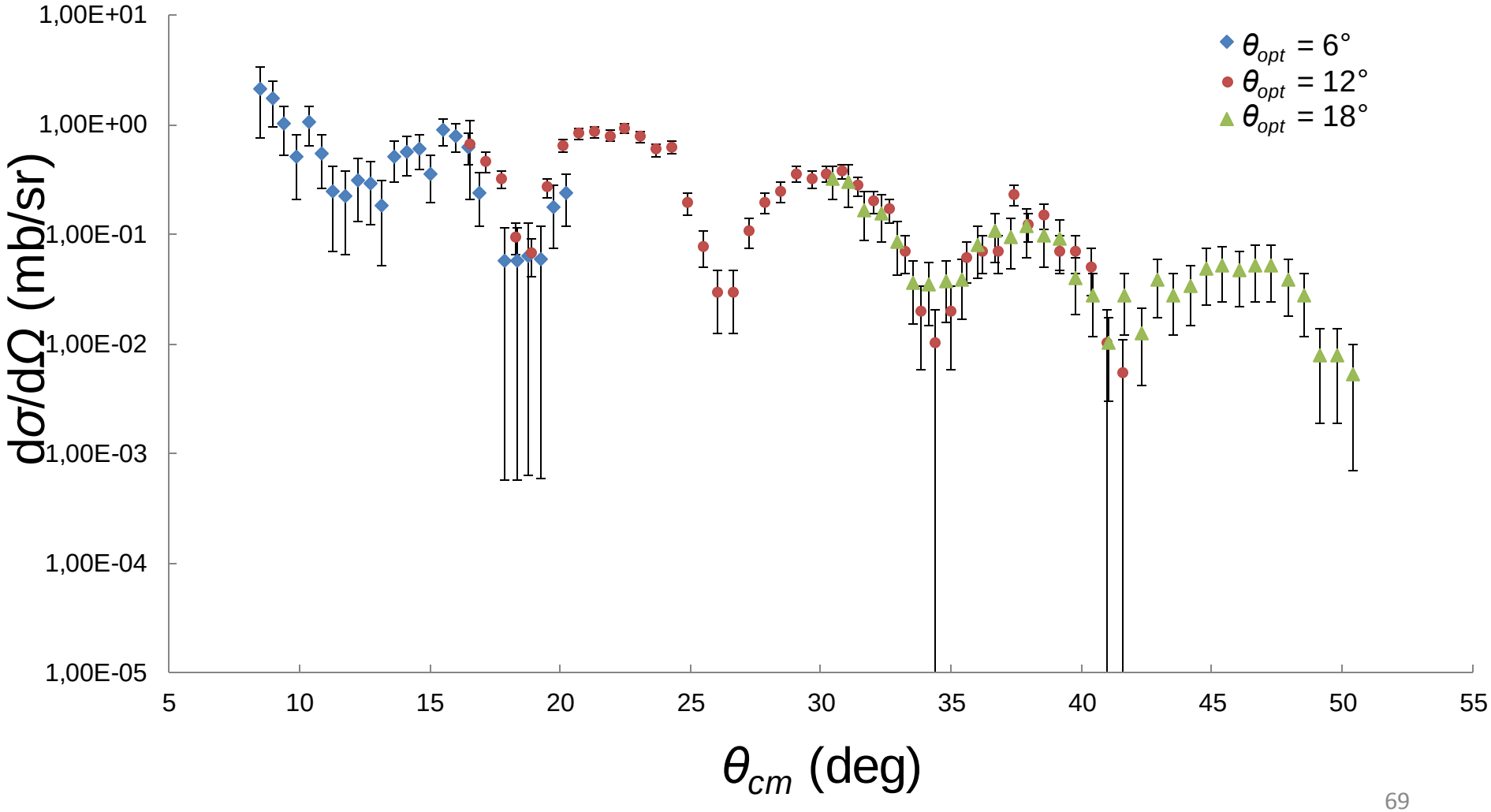

Nuclear Reactions for Neutrinoless Double Beta Decay

0νββ decay

Open problem in modern physics:

Neutrino absolute mass scale

Neutrino nature

0νββ is considered the **most promising approach**

Still not observed

$$^{A}_{Z}X_{N} \rightarrow {}^{A}_{Z+2}Y_{N-2} + 2e^{-} + (2\bar{\nu})$$

Beyond standard model

^{76}Br	^{77}Br	^{78}Br	^{79}Br	^{80}Br
^{75}Se	^{76}Se	^{77}Se	^{78}Se	^{79}Se
^{74}As	^{75}As	^{76}As	^{77}As	^{78}As
^{73}Ge	^{74}Ge	^{75}Ge	^{76}Ge	^{77}Ge
^{72}Ga	^{73}Ga	^{74}Ga	^{75}Ga	^{76}Ga

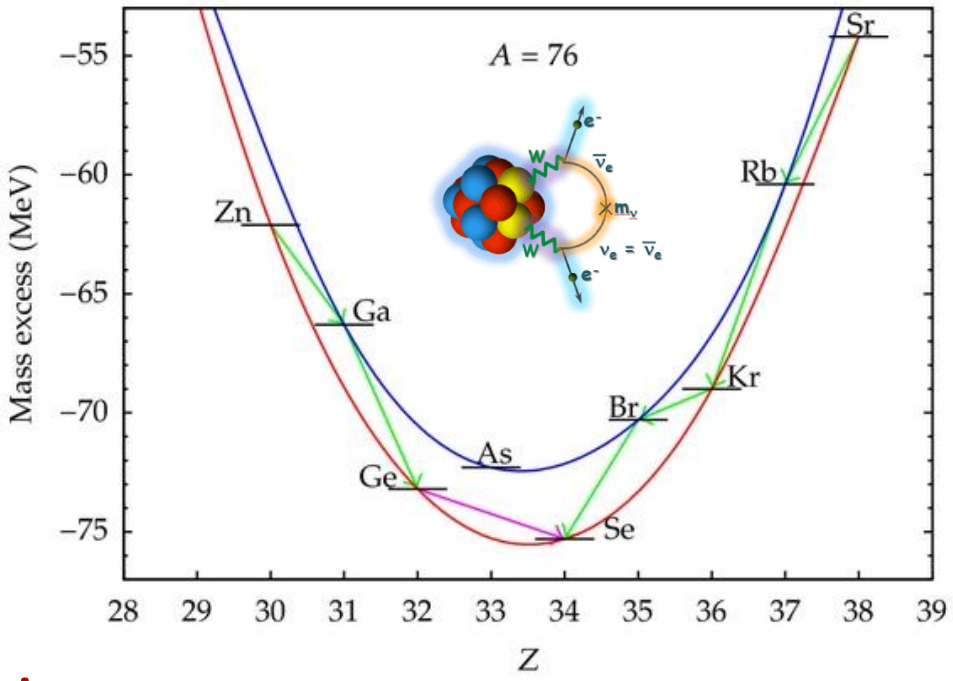

- ✓ Process mediated by the **weak interaction**
- ✓ Occurring in even-even nuclei where the **single β-decay** is energetically **forbidden**

Search for 0νββ decay. A worldwide race

Experiment	Isotope	Lab	Status
GERDA	^{76}Ge	LNGS [Italy]	Operational
CUORE	^{130}Te	LNGS [Italy]	Construction
Majorana	^{76}Ge	SURF [USA]	Construction
KamLAND-Zen	^{136}Xe	Kamioka [Japan]	Operational
EXO/nEXO	^{136}Xe	WIPP [USA]	Operational
SNO+	^{130}Te	Sudbury [Canada]	Construction
SuperNEMO	^{82}Se (or others)	LSM [France]	R&D
CANDLES	^{48}Ca	Kamioka [Japan]	R&D
COBRA	^{116}Cd	LNGS [Italy]	R&D
Lucifer	^{82}Se	LNGS [Italy]	R&D
DCBA	many	[Japan]	R&D
AMoRe	^{100}Mo	[Korea]	R&D
MOON	^{100}Mo	[Japan]	R&D

List not complete…

Nuclear Matrix Elements

0νββ decay **half-life**

Phase space factor

contains the average neutrino **mass**

$$\left(T_{1/2}^{0\nu\beta\beta}(0^+ \rightarrow 0^+)\right)^{-1} = G_{0\nu\beta\beta}\left|M^{0\nu\beta\beta}\right|^2 \left|f(m_i, U_{ei})\right|^2$$

Nuclear Matrix Element (NME)

$$\left|M_{\varepsilon}^{0\nu\beta\beta}\right|^2 = \left|\left\langle \Psi_f \left| \hat{O}_{\varepsilon}^{0\nu\beta\beta} \right| \Psi_i \right\rangle\right|^2$$

Transition probability of a **nuclear** process

Nuclear physics plays a key role!

Nuclear Matrix Elements

Nuclear Matrix Element (NME)

$$\left|M_{\varepsilon}^{0\nu\beta\beta}\right|^2 = \left|\left\langle \Psi_f \left| \hat{O}_{\varepsilon}^{0\nu\beta\beta} \right| \Psi_i \right\rangle\right|^2$$

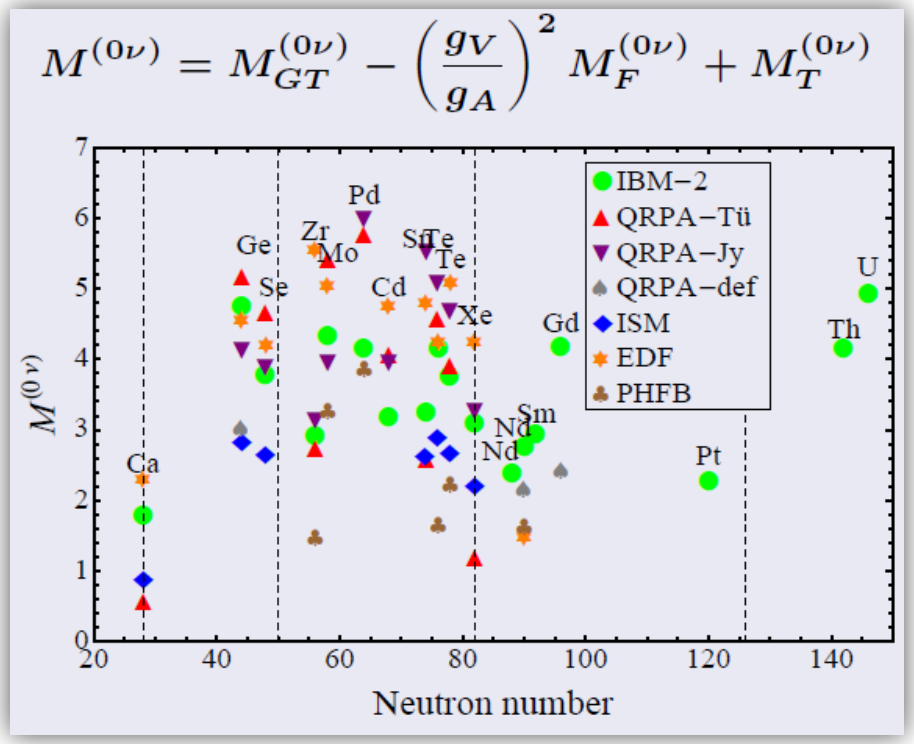

Calculations (still sizeable uncertainties):
QRPA, Large scale shell model, IBM, EDF …

E. Caurier, et al., PRL 100 (2008) 052503
N. L. Vaquero, et al., PRL 111 (2013) 142501
J. Barea, PRC 87 (2013) 014315
T. R. Rodriguez, PLB 719 (2013) 174
F.Simkovic, PRC 77 (2008) 045503.
…

Warning: Many body WaveFunctions!

The idea

Is there an **experimental way** to access the NME?

The ERC project NURE:

Nuclear reactions
Double Charge Exchange reactions (DCE)
to stimulate in the laboratory the same nuclear transition occurring in 0νββ

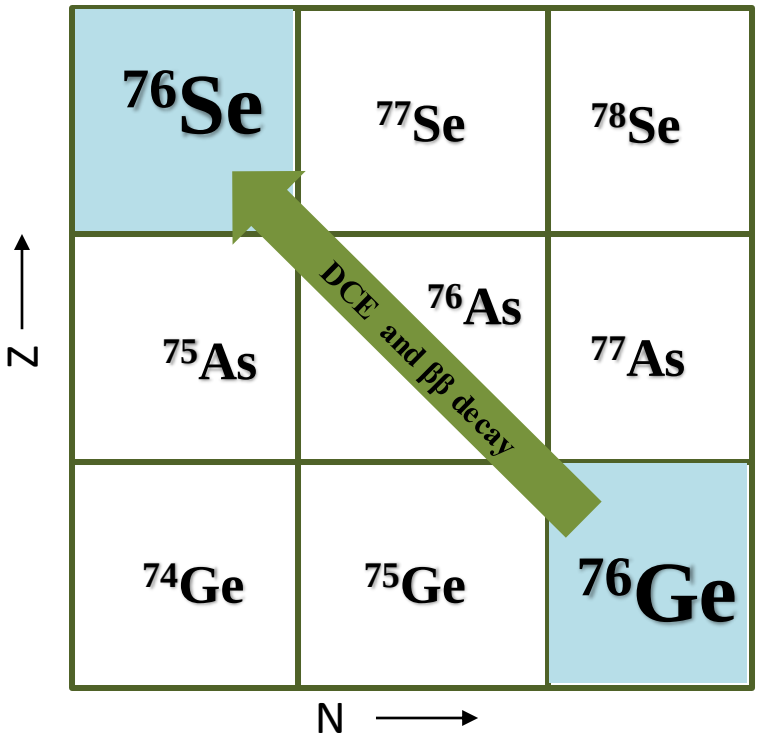

0νββ vs HI-DCE

Differences

- DCE mediated by **strong interaction**, 0νββ by **weak interaction**
- DCE includes **sequential** transfer **mechanism**

Similarities

- **Same initial and final states:** Parent/daughter states of the $0\nu\beta\beta$ decay are the same as those of the target/residual nuclei in the DCE
- **Similar operator:** Short-range Fermi, Gamow-Teller and rank-2 tensor components are present in both the transition operators, with tunable weight in DCE
- **Large linear momentum** (~100 MeV/c) available in the virtual intermediate channel
- **Non-local** processes: characterized by two vertices localized in a pair of valence nucleons
- **Same nuclear medium**: Constraint on the theoretical determination of quenching phenomena on $0\nu\beta\beta$
- **Off-shell propagation** through virtual intermediate channels

The project

NURE plans to measure the **absolute cross section** of **HI-DCE** reactions on **nuclei** candidates for 0νββ and to **extract «data-driven» NME**

the measured quantity is the **cross section**

details of the reaction

$$\frac{d\sigma}{d\Omega}(q,\omega) = \hat{f}(NME)$$

The extraction of nuclear structure information from measured cross sections is **not trivial** but **feasible (result of decades of nuclear physics)**

e.g. for single charge-exchange: NME extracted within 2-5% accuracy by proportionality relation

$$\frac{d\sigma}{d\Omega}(q,\omega) = \hat{\sigma}(E_p, A) F(q,\omega) NME(\alpha)$$

- E_p incident energy
- q momentum transfer
- ω excitation energy

The project

- **Only two transitions of interest for 0νββ:**
  ^{76}Ge↔^{76}Se and **^{116}Cd↔^{116}Sn**
  GERDA, MAJORANA, COBRA

- **Two directions**:
  ββ^{+} via (^{18}O,^{18}Ne) and ββ^{-} via (^{20}Ne,^{20}O)

- **Complete net** of reactions which can contribute to the DCE cross-section:
  1p-, 2p-, 1n-, 2n-transfer, single cex, DCE

- **Two (or more) incident energies**
  to study the reaction mechanism

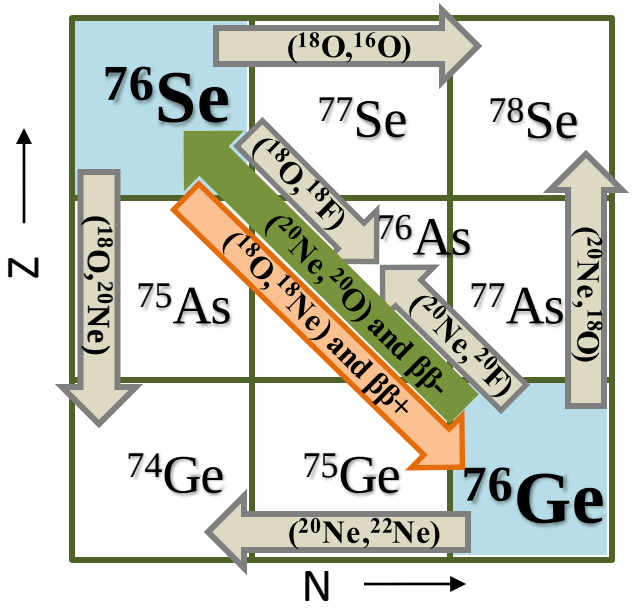

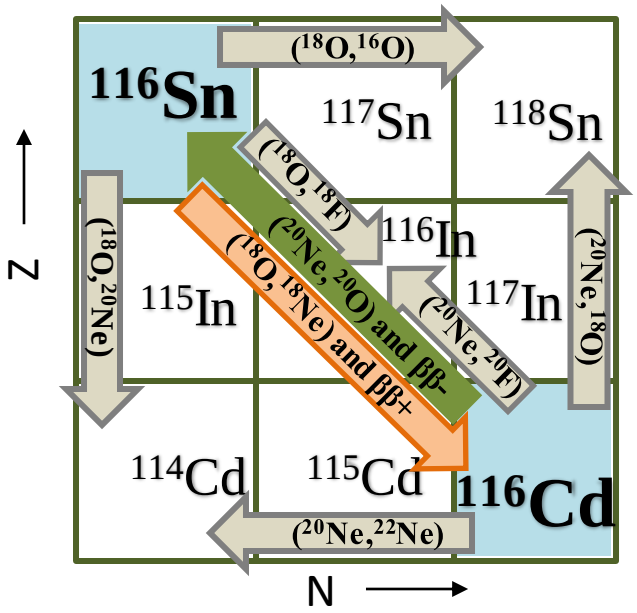

The context

Single charge-exchange reactions
induced by light ions (^{3}He,t), (d,^{2}He), …

Interesting for β-decay and 2νββ!

Weak interaction probes
β, 2νββ,
μ-capture,
ν-nucleus scattering, …

Other researches
to extract information on NME from experimental data and/or constrain the theory

Transfer reactions
for constraining Ψ_i, Ψ_f

Double charge-exchange
induced by **pions** ($\pi^{\pm}$, $\pi^{\mp}$)
abandoned in the 80's due to the large differences in the momentum transfer and lack of direct GT component in the operators

Heavy-ion induced **double charge-exchange**
limited in the past due to low cross-sections

Renewed interest (RIKEN, Osaka) but low resolution (~1.5 MeV)

The pilot experiment

$^{40}Ca(^{18}O,^{18}Ne)^{40}Ar$ @ 270 MeV

Catania

- $^{18}O^{7+}$ beam from Cyclotron at **270 MeV** (10 pnA, 3300 μC in 10 days)
- **^{40}Ca** target 300 μg/cm^2
- Ejectiles detected by the MAGNEX spectrometer $0° < \vartheta_{lab} < 10°$
  corresponding to a momentum transfer ranging **from 0.17 fm^{-1} to 2.2 fm^{-1}**

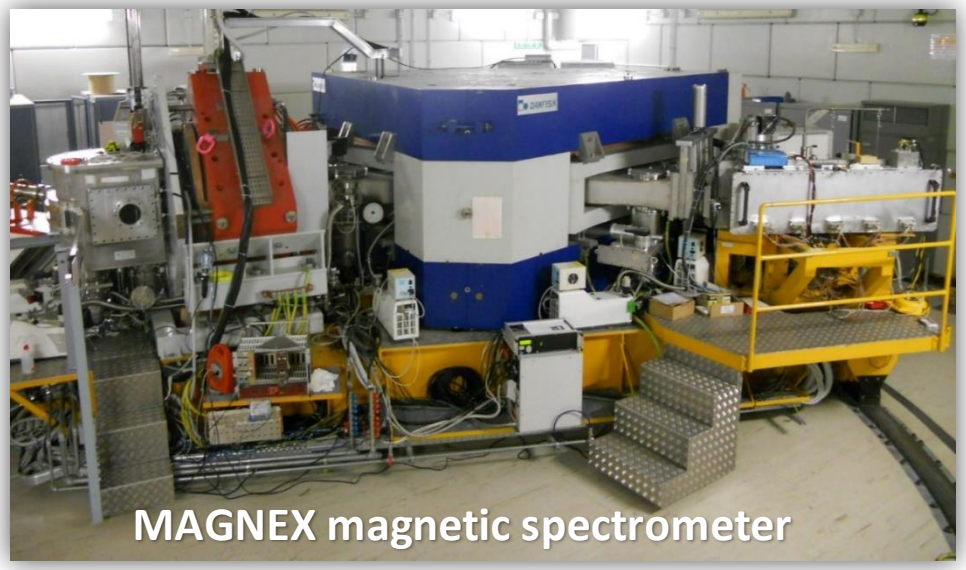

Zero-degree measurement

$\Theta_{MAGNEX} = +4°$
$-1° < \theta_{lab} < +10°$

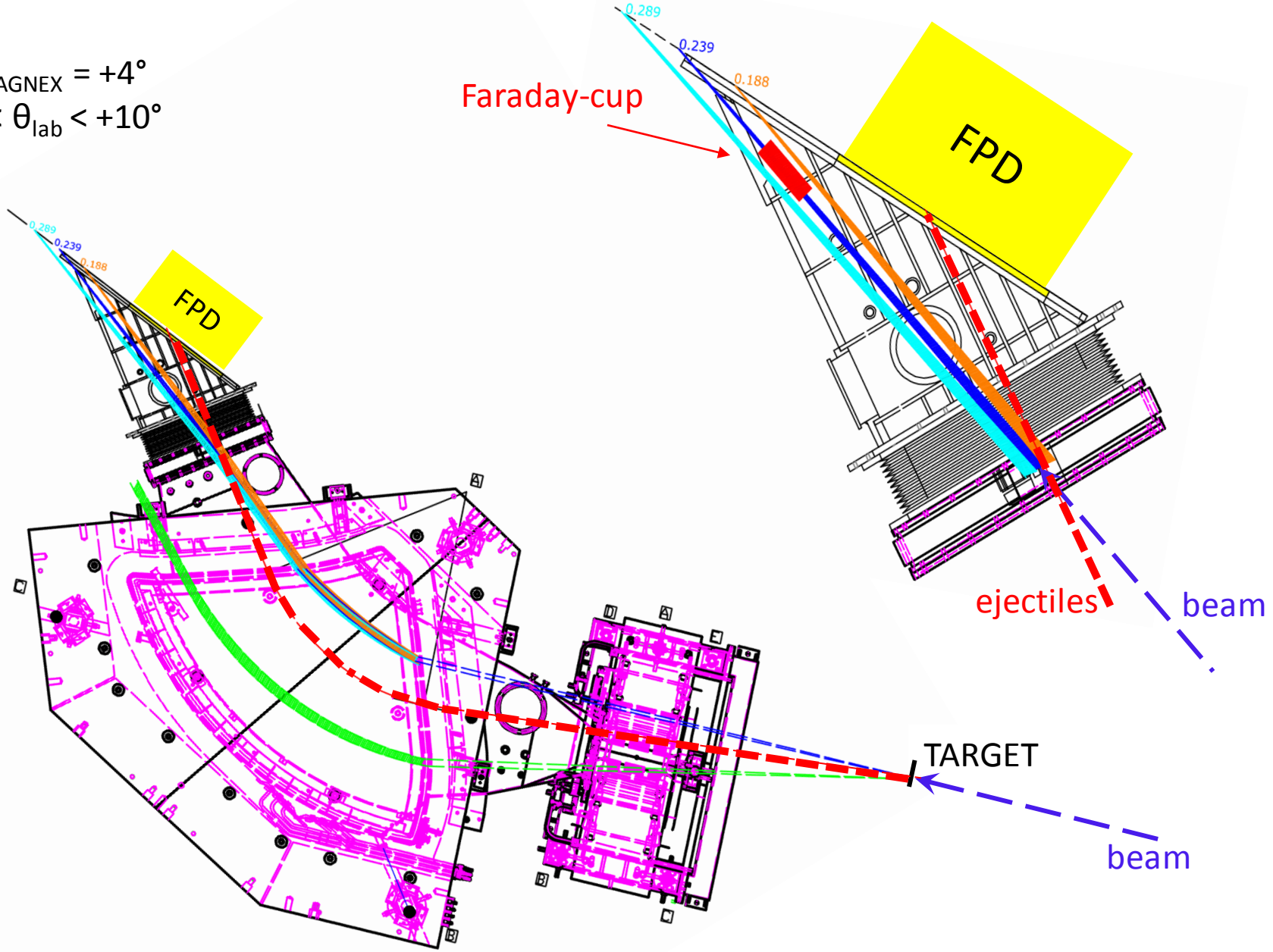

The pilot experiment

$^{18}O + {}^{40}Ca$ at 270 MeV

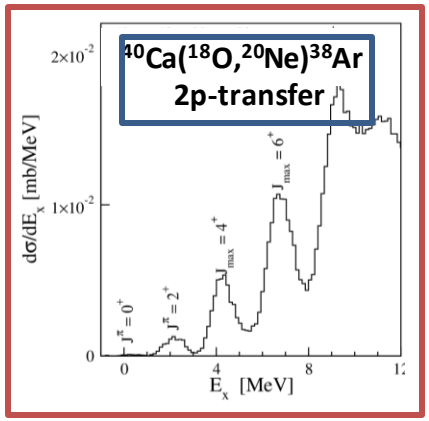

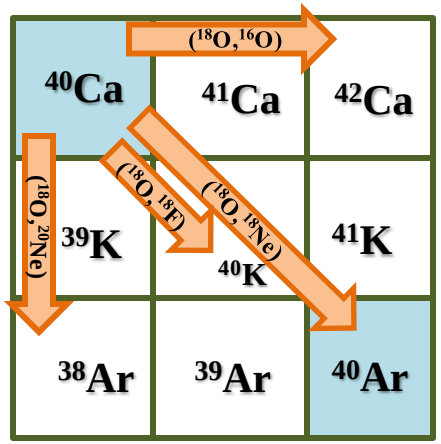

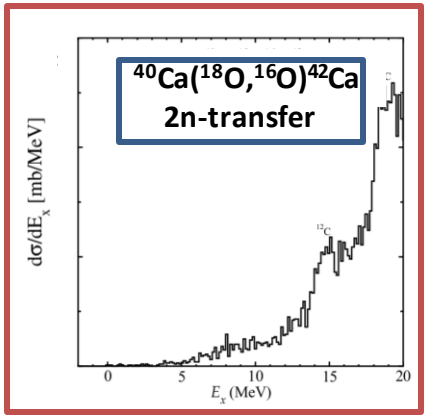

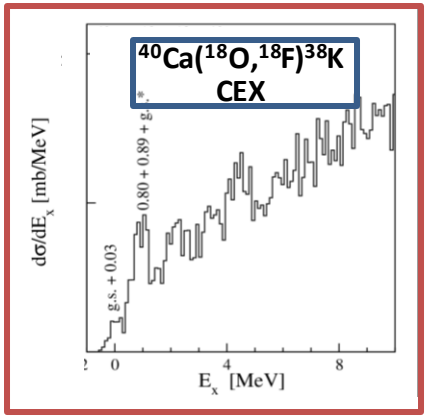

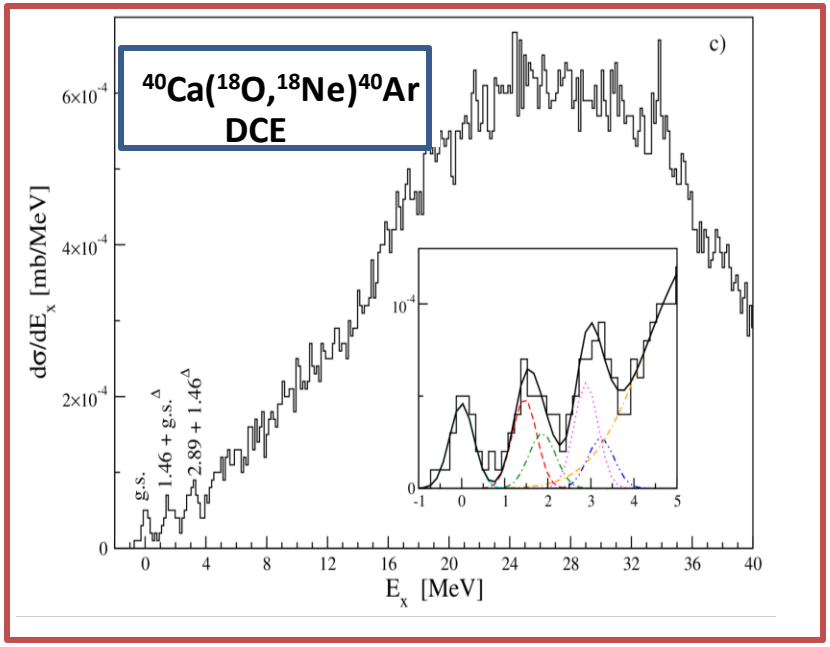

- **Experimental feasibility:** zero-deg, resolution (500 keV), low cross-section (μb/sr)
  Limitations of the past HI-DCE experiments are overcome!

- **Data analysis feasibility**: the analysis of the DCE cross-section has lead to NME compatible with the existing calculations

F. Cappuzzello, et al., Eur. Phys. J. A (2015) 51:145

Preliminary NME extraction

In the lack of «real» theory…

Under the hypothesis of validity of the factorization

$$\frac{d\sigma}{d\Omega_{DCE}}(q,\omega) = \hat{\sigma}_{\alpha}^{DCE}(E_p, A) F_{\alpha}^{DCE}(q,\omega) B_T^{DCE}(\alpha) B_P^{DCE}(\alpha)$$

$$\left|M\left(^{40}Ca\right)\right|^2 = 0.37 \pm 0.18$$

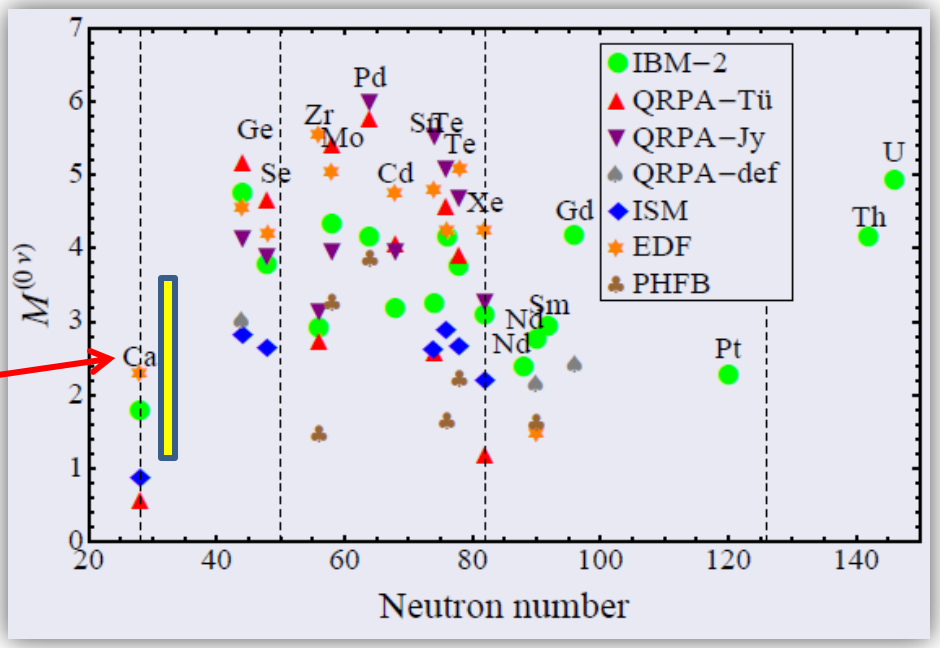

Just to speculate:
removing Pauli blocking one can roughly estimate

$$\left|M^{0\nu\beta\beta}\left(^{48}Ca\right)\right|^2 = 2.6 \pm 1.3$$

Pauli blocking about 0.14 for F and GT

F. Cappuzzello, et al., Eur. Phys. J. A (2015) 51:145

A broader view

Limitations of NURE:

- Only two systems can be studied in 5 years (due to the **low cross-sections**)
- A more accurate job on the **theory** is needed

The NUMEN program

A broader view

The **NUMEN** project

NUclear **M**atrix **E**lements for **N**eutrinoless double beta decay

TeBe

Theory

NUMEN_gr3
(R&D and experiments)
INFN CSN-III

NUMEN

NURE

erc

CS-upgrade

SiCILIA INFN call

Operating in a wider context, in a wider time scale (10-15 yr), in close synergy with NURE

A broader view

The **NUMEN** project

NUclear **M**atrix **E**lements for **N**eutrinoless double beta decay

The collaboration

Spokespersons: F. Cappuzzello and C. Agodi

E. Aciksoz, L. Acosta, C. Agodi, X. Aslanouglou, N. Auerbach, J. Bellone, R. Bijker, S. Bianco, D. Bonanno, D. Bongiovanni, T. Borello, I. Boztosun, V. Branchina, M.P. Bussa, L. Busso, S. Calabrese, L. Calabretta, A. Calanna, D. Calvo, F. Cappuzzello, D. Carbone, M. Cavallaro, E.R. Chávez Lomelí, M. Colonna, G. D'Agostino, N. Deshmuk, P.N. de Faria, C. Ferraresi, J.L. Ferreira, P. Finocchiaro, A. Foti, G. Gallo, U. Garcia, G. Giraudo, V. Greco, A. Hacisalihoglu, J. Kotila, F. Iazzi, R. Introzzi, G. Lanzalone, A. Lavagno, F. La Via, J.A. Lay, H. Lenske, R. Linares, G. Litrico, F. Longhitano, D. Lo Presti, J. Lubian, N. Medina, D. R. Mendes, A. Muoio, J. R. B. Oliveira, A. Pakou, L. Pandola, H. Petrascu, F. Pinna, F. Pirri, S. Reito, D. Rifuggiato, M.R.D. Rodrigues, A. Russo, G. Russo, G. Santagati, E. Santopinto, O. Sgouros, S.O. Solakcı, G. Souliotis, V. Soukeras, S. Tudisco, R.I.M. Vsevolodovna, R. Wheadon, V. Zagatto

Italy, Brazil, Greece, México, Germany, Turkey, Israel, Romania, Spain

73 members, 9 countries

The Goals of the Research Program

Main goal (Holy Graal):

Extraction from measured cross-sections of *"data-driven"* information on NME for all the systems candidate for 0νββ

Secondary goals:

- Constraints to the existing theories of NMEs
- Model-independent comparative information on the sensitivity of half-life experiments
- Complete study of the reaction mechanism

BY-PRODUCTS

A broader view

The **NUMEN** project

NUclear **M**atrix **E**lements for **N**eutrinoless double beta decay

- **Phase1**: The experimental **feasibility** (completed)
- **Phase2**: **Experimental exploration** of few cases (NURE) and **work on theory** (running until 2021)
- **Phase3**: **Facility upgrade** (Cyclotron, MAGNEX, beam line, …) to work with two orders of magnitude more intense beam
- **Phase4**: **Systematic experimental campaign** on all the systems with the upgraded facility

Upgrade of LNS facilities: The CS accelerator

- **CS** accelerator current (from 100 W to 5-10 kW);

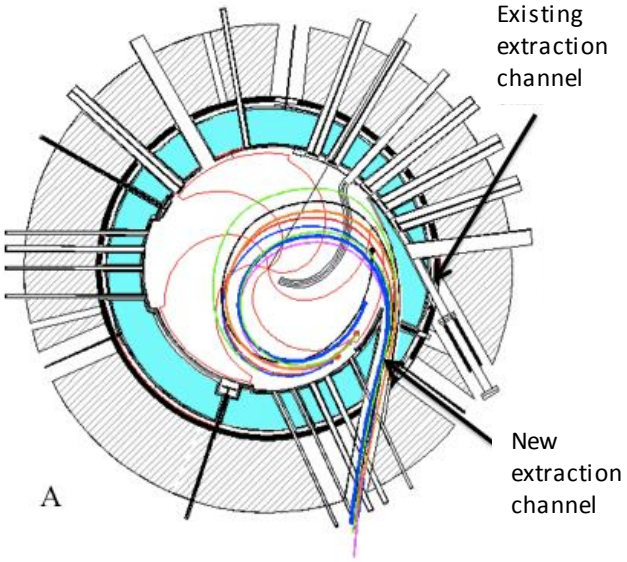

From electrostatic extraction (low efficiency 50%) to extraction by stripping (>99%)

- **beam transport line**

transmission efficiency to nearly 100%

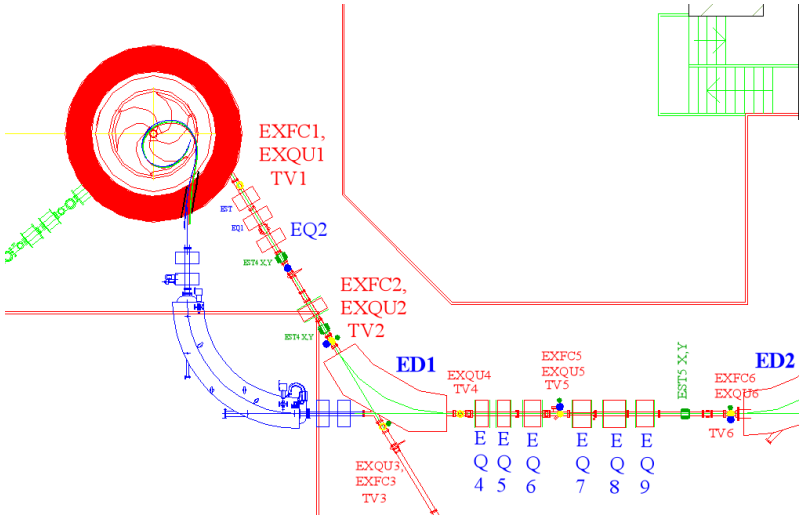

From D. Rifuggiato

Beam dump inside the MAGNEX hall

Present MAGNEX hall

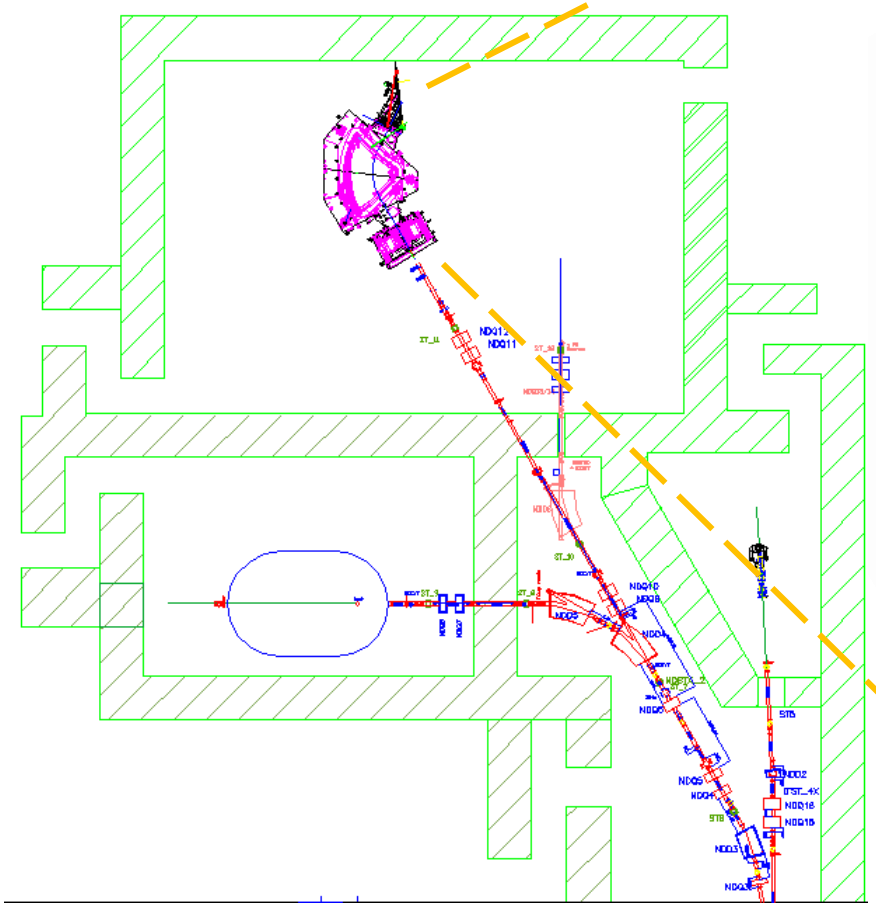

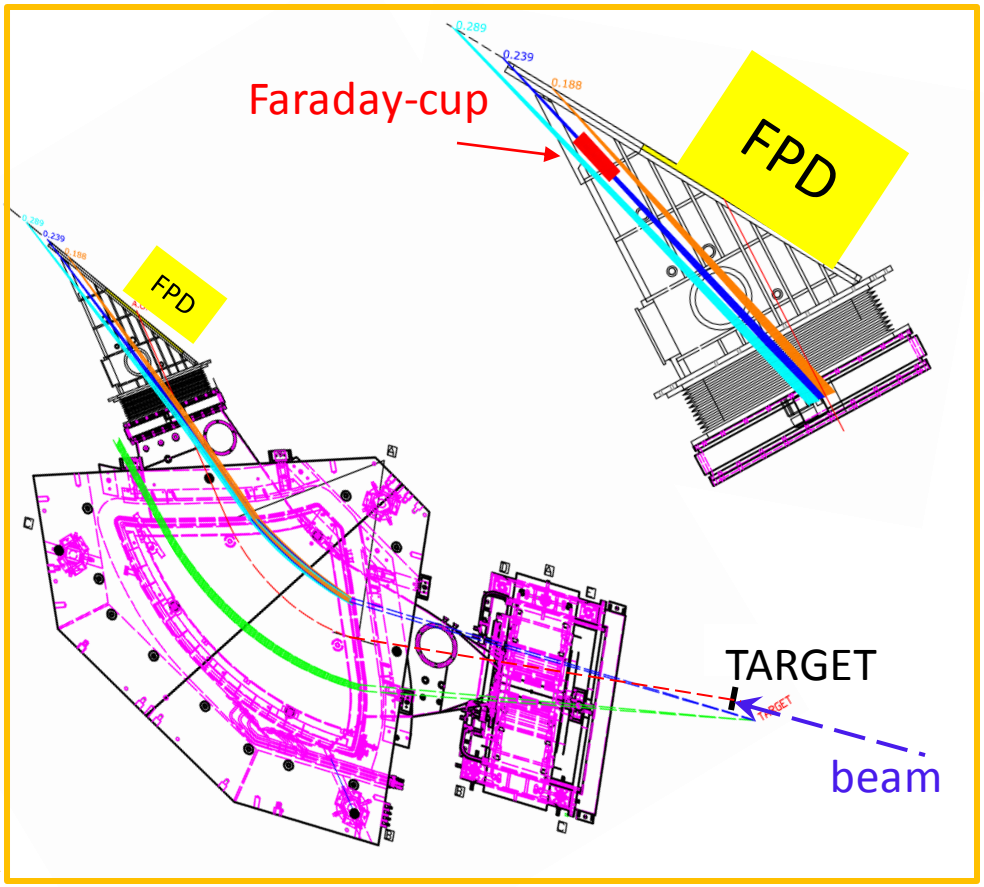

Beam dump inside the MAGNEX hall

Present MAGNEX hall

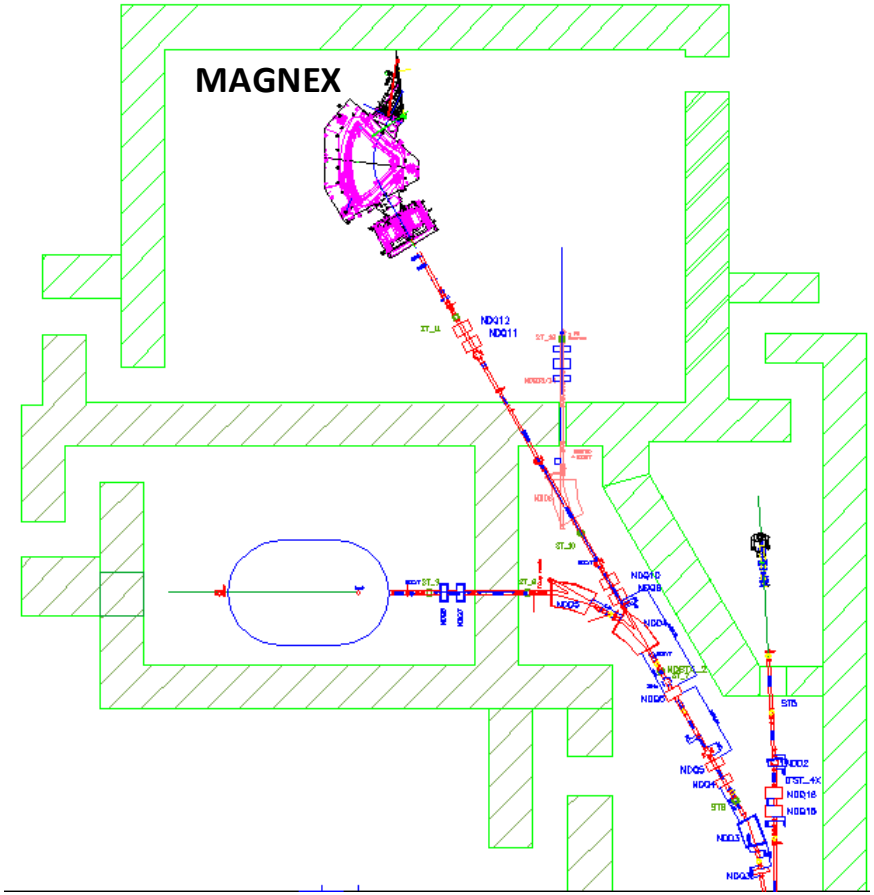

Future MAGNEX hall

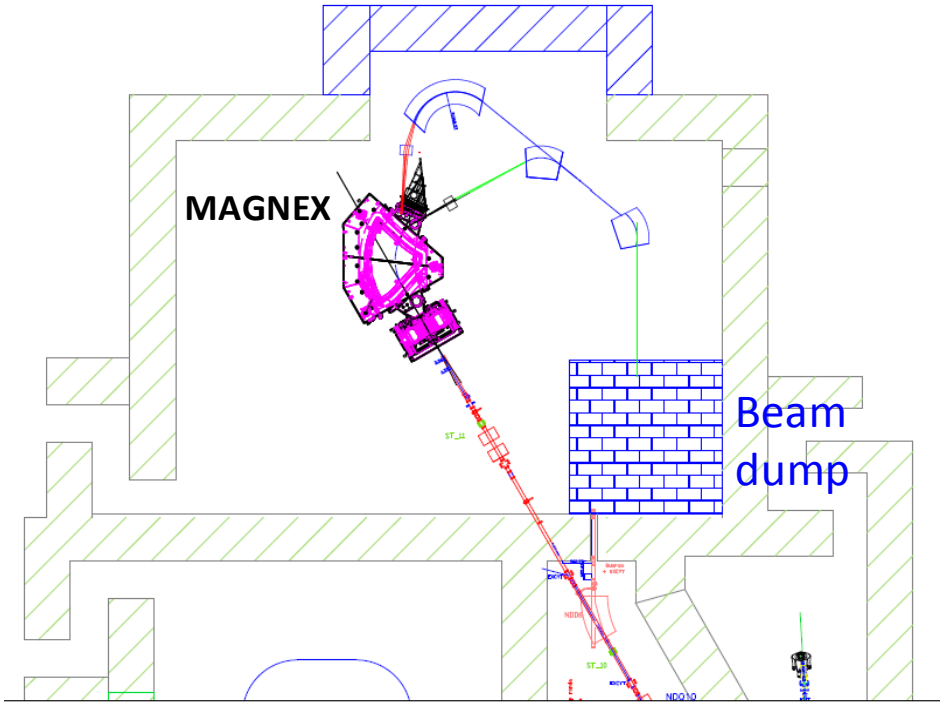

Beam dump inside the MAGNEX hall

85 μA beam of ^{18}O on Ag

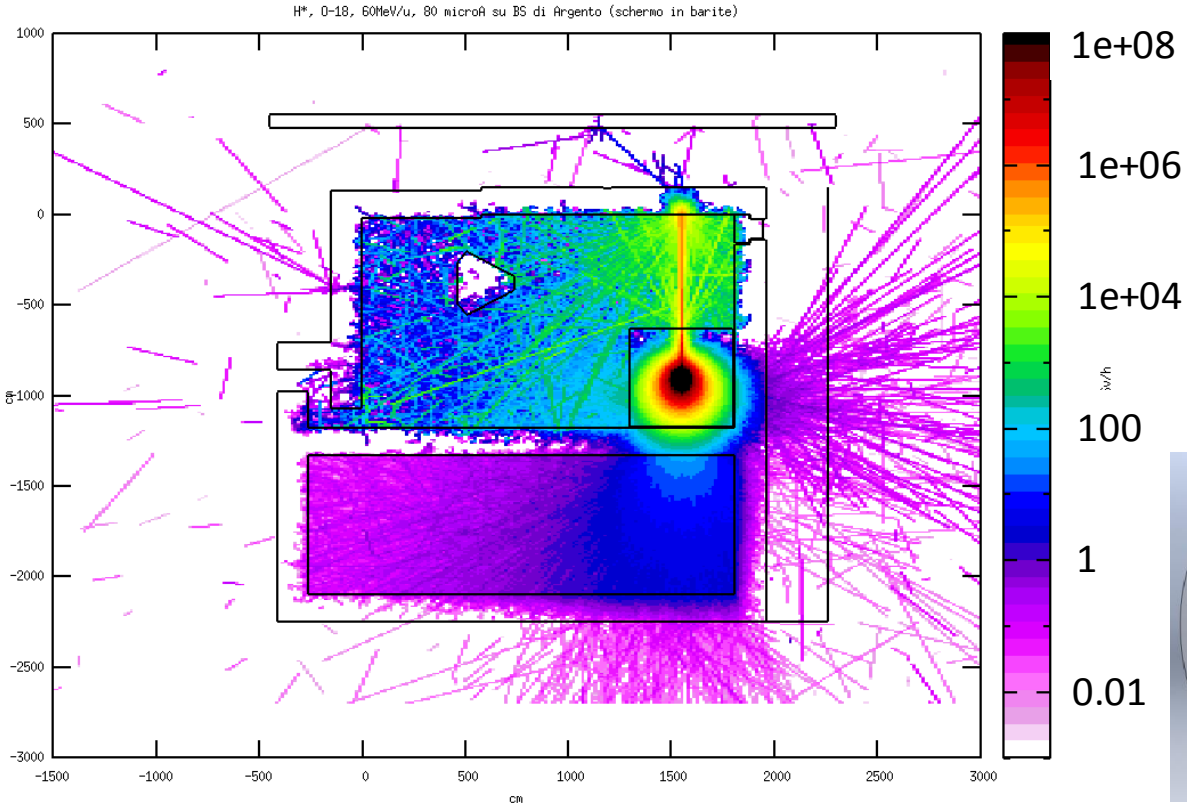

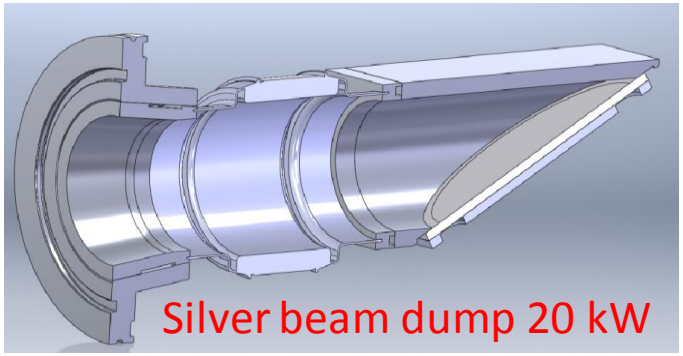

From S. Russo (LNS radioprotection service)

Upgrade of the MAGNEX Focal Plane Detector

Large volume: 1360mm X 200mm X 96mm

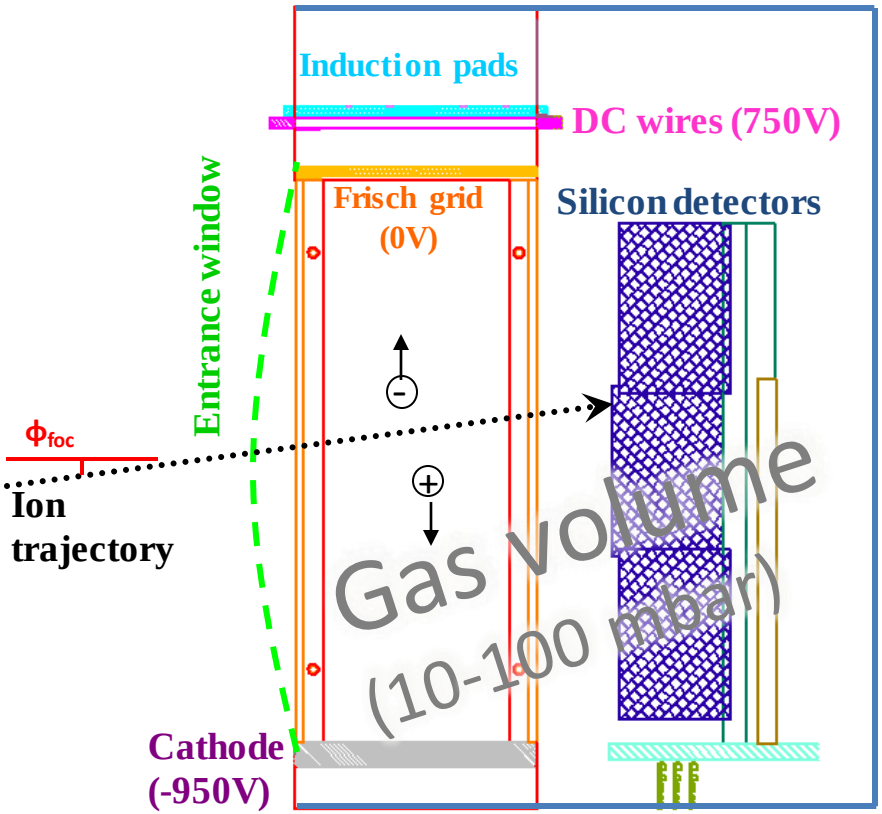

Section view

Wall of 60 stopping 7 X 5 cm^2 Silicon detectors
Covered area 100 X 20 cm^2
Thickness 500 – 1000 µm

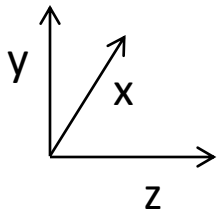

Hybrid detector:
Gas section: proportional wires and drift chambers
+
Stopping wall of silicon detectors

Upgrade of the MAGNEX FPD: Gas Tracker

Present:
wire-based gas tracker
Low pressure (10-100 mbar)
Rate limit **few KHz**

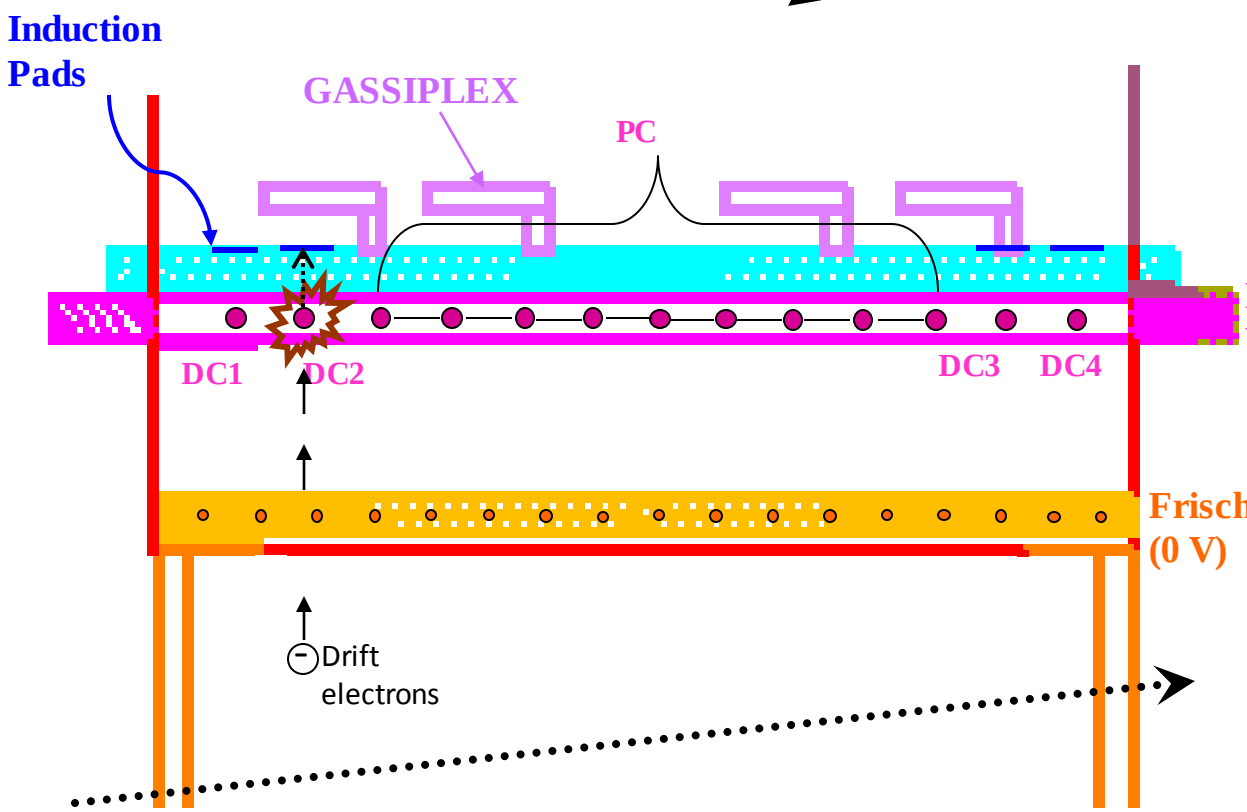

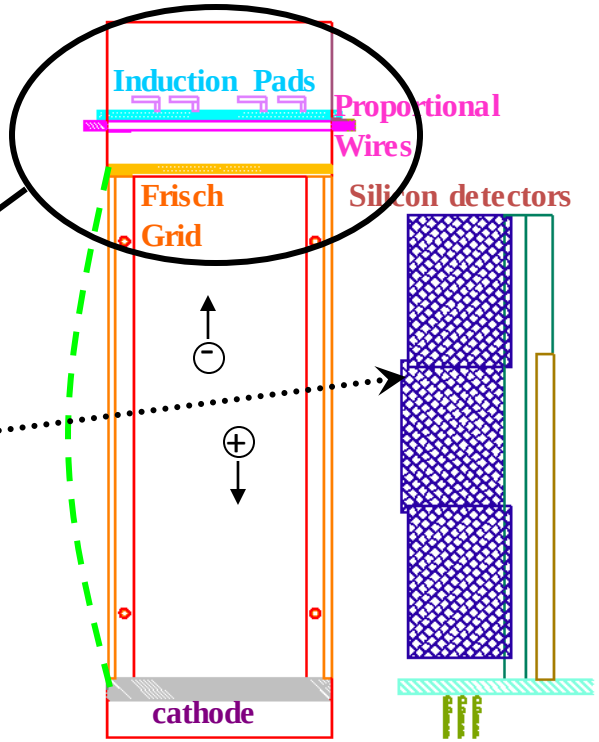

Rate from **few kHz to MHz**
Preserving low pressure operations

Gaseous detectors

MWPC 1968
G. Charpak
Nobel Prize in 1992

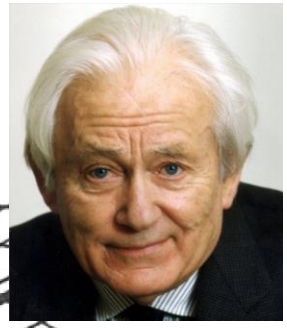

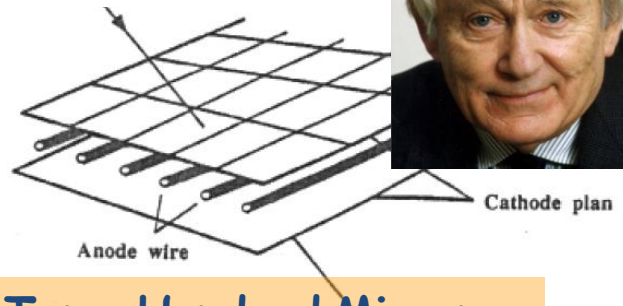

Tens-Hundred Microns

Multi-Wire Proportional Chamber -MWPC

Gaseous detectors: why?

- good stability, robustness and aging compared to solid/liquid detectors
- good space and moderate energy resolution
- three dimensional readout/flexible geometry
- cheap
- still today the only choice whenever large-area coverage with low material budget is required

From M. Cortesi

Limits of wire-based detectors

Wire-Based Detector:

Secondary effects ➔ Gain limits

Space charge ➔ Counting-rate limits (10^4 Hz/mm^2)

Aging ➔ Damage after long-term operation

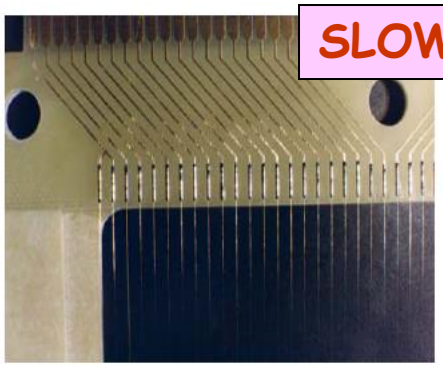

Wire spacing ➔ 1-2 mm

New Idea:

Move down in size & add cathodes very close to anodes to evacuate ions produced during the avalanche process

Micro-Pattern Gaseous Detector

MICRO-GROOVE CHAMBER

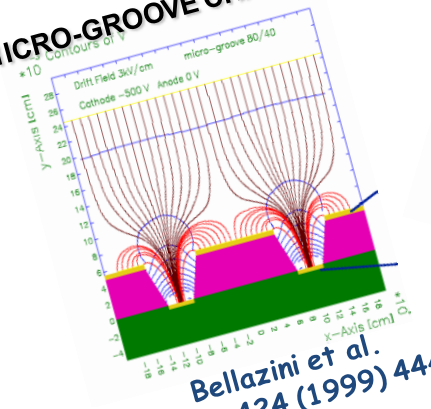

Bellazini et al.
NIMA 424 (1999) 444

MICROWIRE CHAMBER

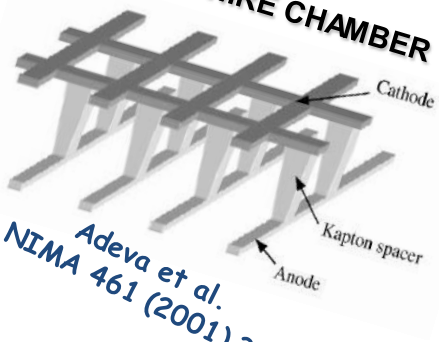

Adeva et al.
NIMA 461 (2001) 33

MICRO-PIXEL CHAMBER

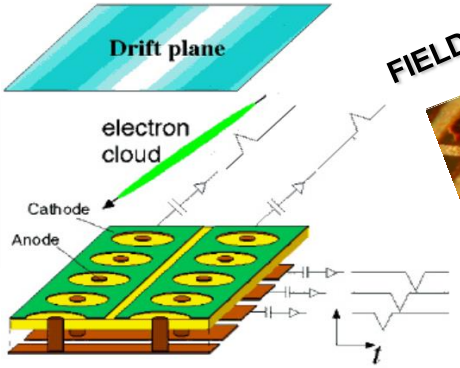

Ochi et al.
NIMA 471 (2001) 264

FIELD GRADIENT LATTICE DETECTOR

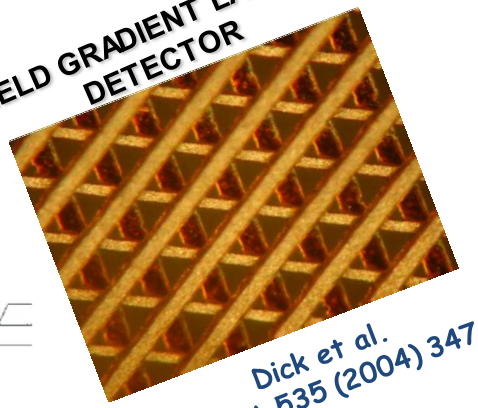

Dick et al.
NIMA 535 (2004) 347

MICROMEGAS

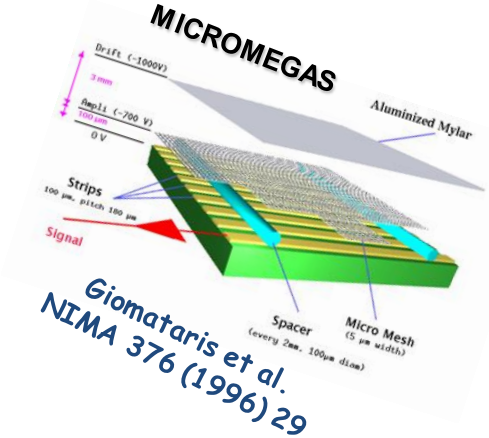

Giomataris et al.
NIMA 376 (1996) 29

GAS ELECTRON MULTIPLIER

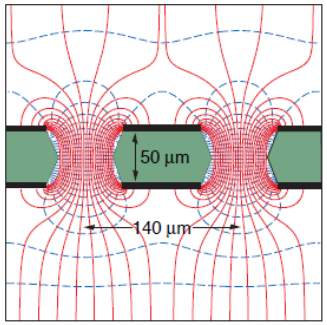

Sauli
NIMA 386 (1997) 531

MICRO-HOLE & STRIP PLATE

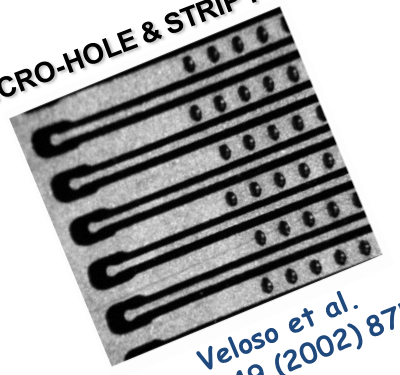

Veloso et al.
TNS 49 (2002) 875

MICRO-PIN ARRAY

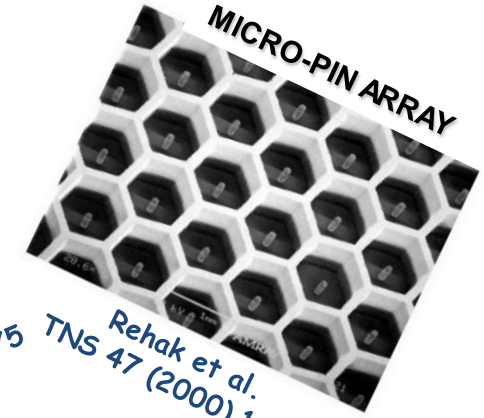

Rehak et al.
TNS 47 (2000) 1426

…. and many others

From M. Cortesi

Micro-strip gas chamber (MSGC)

FAST *A. Oed, NIMA 263 (1988) 351*

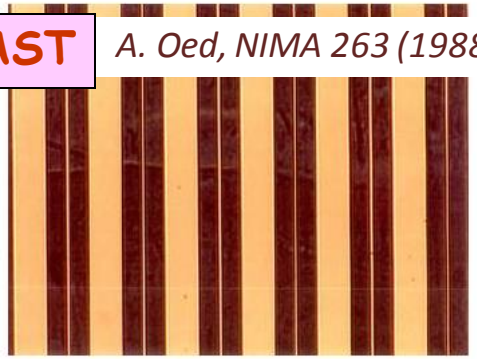

Anode spacing ➔ 200 μm

Micrometric structures of electrodes (photolithography techniques): Pattern of thin anode and cathode strips on high-resistivity substrate

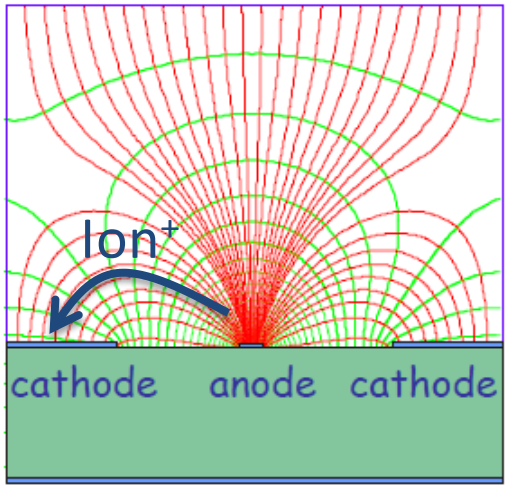

Rate Capability Limits due to space charge overcome by increasing the amplifying cell granularity

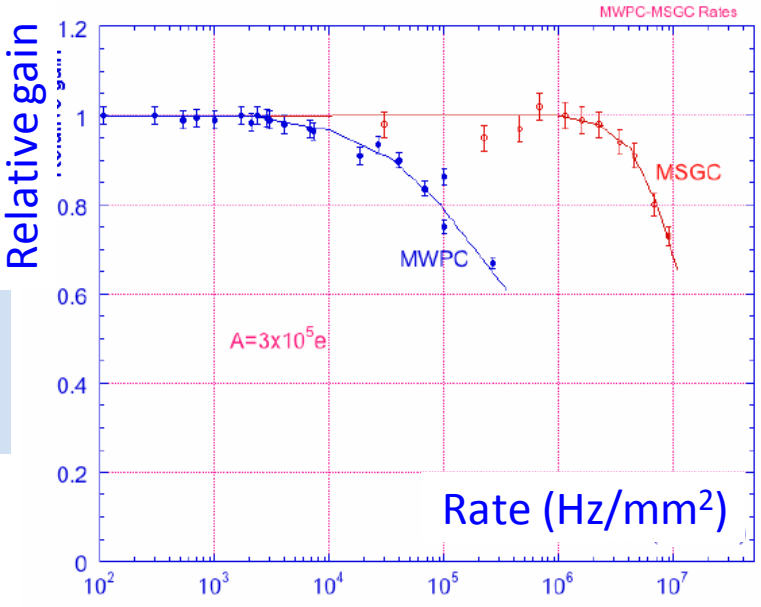

Limitations:

- High E-values at the edge between insulator and strips ➔ **discharges**
- Charge accumulation at the insulator ➔ **gain evolution vs time**

Gas Electron Multiplier (GEM)

Thin metal-coated polymer (Kapton) foil chemically pierced by a high density of holes

Sauli, NIMA 386 (1997) 531

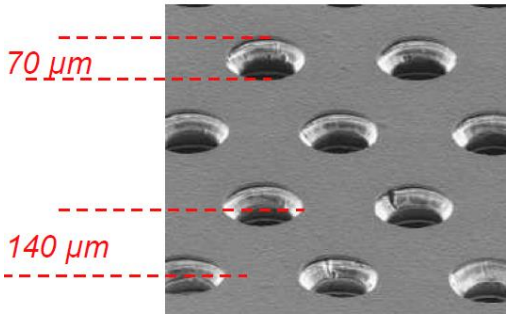

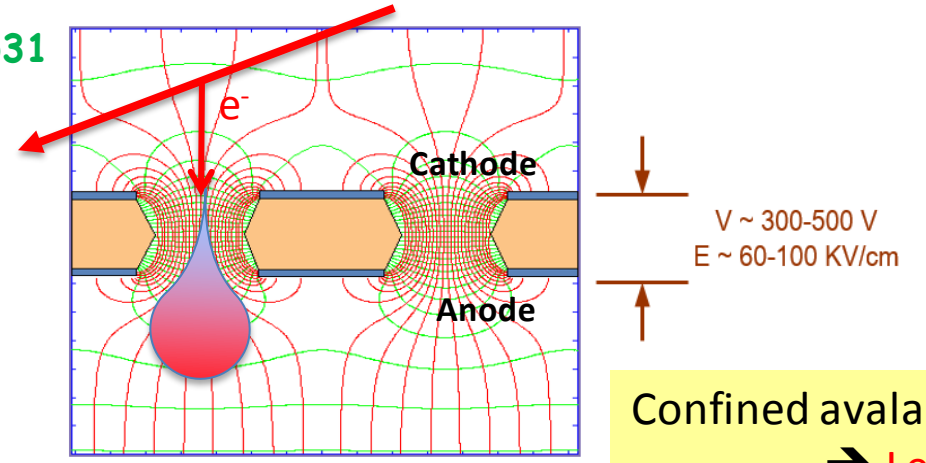

Confined avalanche within holes
➔ Lesser photon-mediated secondary effects

Multi-stage

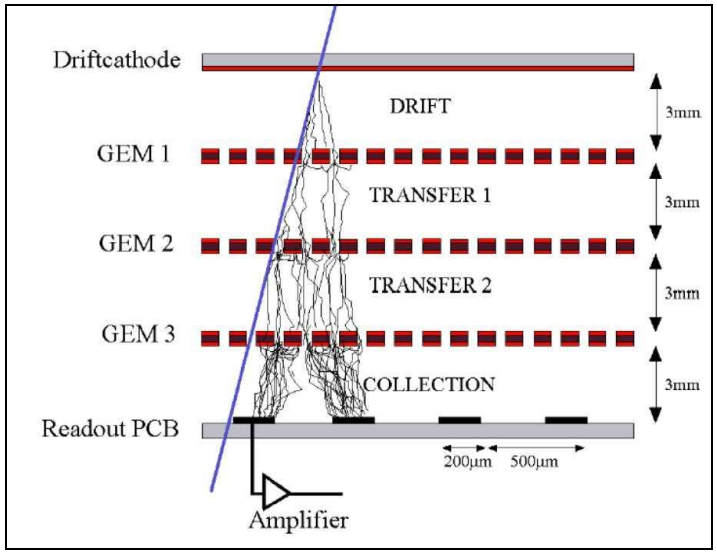

Properties:

- Large area
- High rate (up to 1 MHz/mm^2)
- High Spatial Resolution (≈40 μm)
- High gas gain (~ 10^3-10^4 single-stage, 10^6-10^7 multi-stage)
- 15-20% energy resolution (5.9 keV X-rays)
- Flexible detector shape and readout patterns

From M. Cortesi

Thick-Gas Electron Multiplier (THGEM)

Manufactured by standard PCB techniques of precise drilling in G-10/FR-4 (and other materials) and Cu etching → **Simple & Robust**

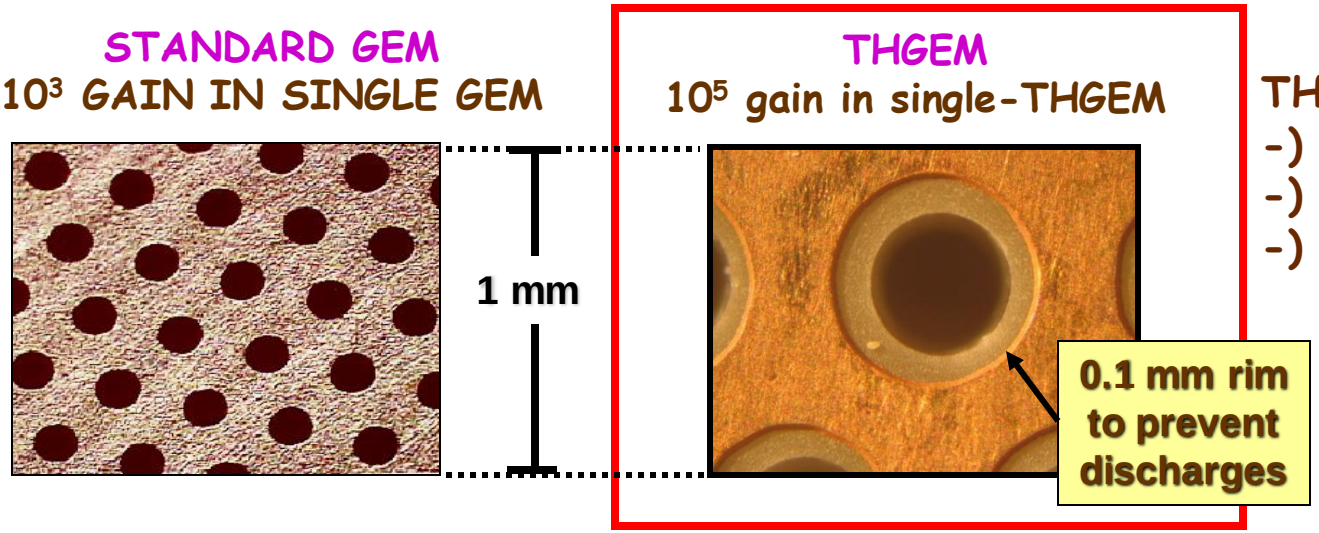

- **Effective single-electron detection**
- **High gas gain ~10^5 (>10^6) @ single (double) THGEM**
- **Few-ns RMS time resolution**
- **Sub-mm position resolution**
- **MHz/mm² rate capability**
- **Cryogenic operation: OK**
- **Gas: molecular and noble gases**
- **Pressure: 1mbar - few bar**

L. Periale et al., NIM A478 (2002) 377
P. Jeanneret, PhD thesis, Neuchatel U., 2001
P.S. Barbeau et al, IEEE NS50 (2003) 1285
R. Chechik et al., NIMA 535 (2004) 303

From M. Cortesi

Operation of THGEM in low-pressure, "pure" Noble Gas

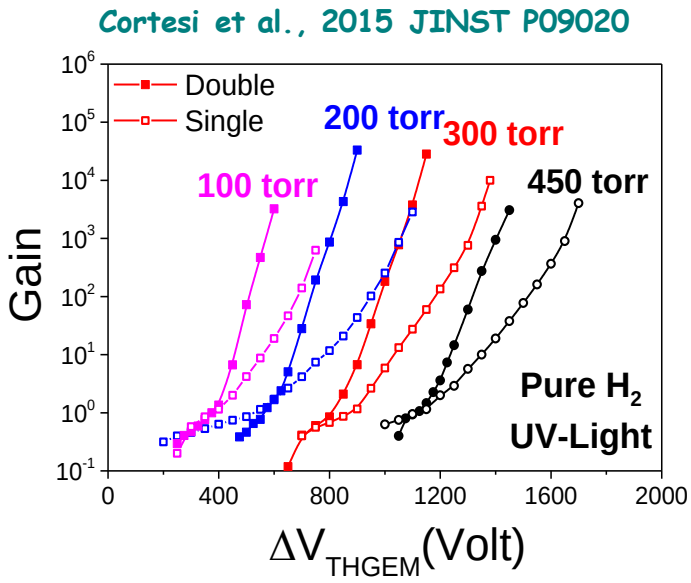

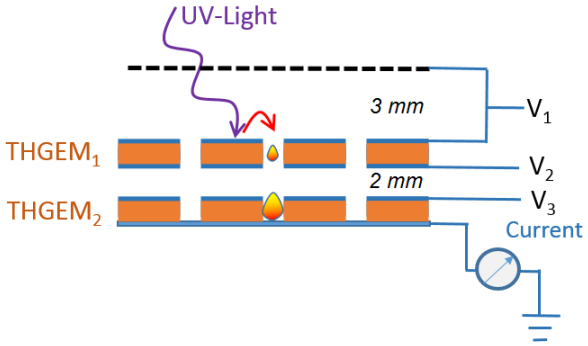

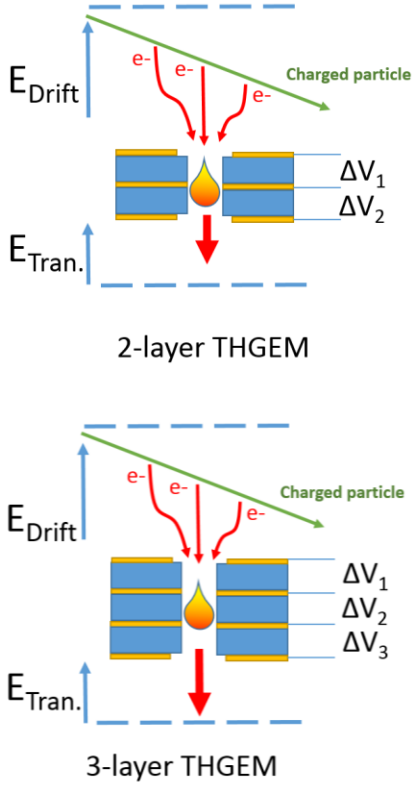

Large maximum achievable gain at low pressure due to:

1) Extended avalanche volume (larger than the e^- mean free path)
   ➔ high e^- multiplication
2) Avalanche confinement within the hole
   ➔ Lesser photon-mediated secondary effects

From M. Cortesi

Upgrade of the MAGNEX FPD: The Particle Identification

A radiation tolerant stopping wall for particle identification

Radiation hardness → expected 10^{14} ions in ten years activity
(silicon detector dead at 10^9 implanted ions/cm^2 (heavy ions not MIP!!))

From wal
detectors

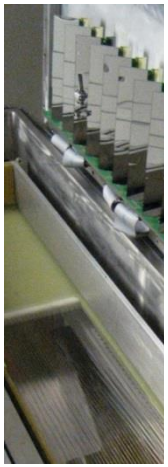

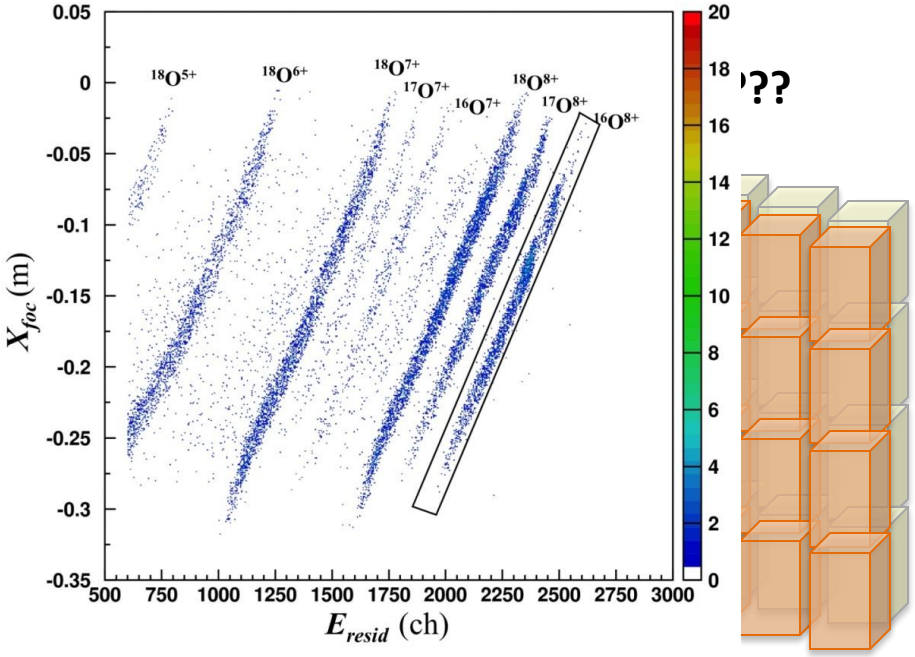

??

What is the right material??

- Radiation hard
- Heavy ions
- Working in gas environment
- Large area
- High energy resolution (1%)
- Timing resolution (few ns)

A big challenge!

Silicon Carbide (SiC)

Tetrahedron of Carbon and Silicon atoms with strong bonds in the crystal lattice. Very hard and strong material!

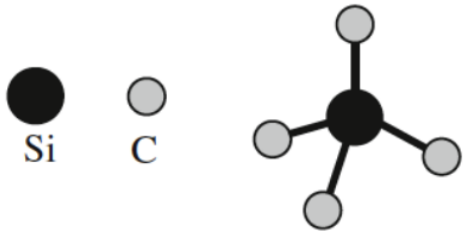

strong bonds !

General Properties of SiC

- high thermal conductivity
- low thermal expansion
- high strength (hardness)
- chemical inertness

→ Exceptional thermal shock resistant qualities

Applications on ELECTRONIS DEVICES

- High power
- High frequency
- High temperature
- Radiation detectors

SiC for radiation detectors

Property	Diamond	GaN	4H SiC	Si
E_g [eV]	5.5	3.39	3.28	1.12
$E_{breakdown}$ [V/cm]	10^7	$4 \cdot 10^6$	$3\text{-}4 \cdot 10^6$	$3 \cdot 10^5$
μ_e [cm^2/Vs]	1800	1000	800	1450
μ_h [cm^2/Vs]	1200	30	115	450
v_{sat} [cm/s]	$2.2 \cdot 10^7$	-	$2 \cdot 10^7$	$0.8 \cdot 10^7$
Z	6	31/7	14/6	14
ε_r	5.7	9.6	9.7	11.9
e-h energy [eV]	13	8.9	7.6-8.4	3.6
Density [g/cm3]	3.515	6.15	3.22	2.33
Displacem. [eV]	43	≥15	30-40	13-15

- Wide band-gap (3.3eV)

⇒ Visible blind

⇒ Lower Leakage current

- Signal

⇒ Less charge than Si, SiC≈Si/2

- Higher displaceme threshold

⇒ Radiation harder t

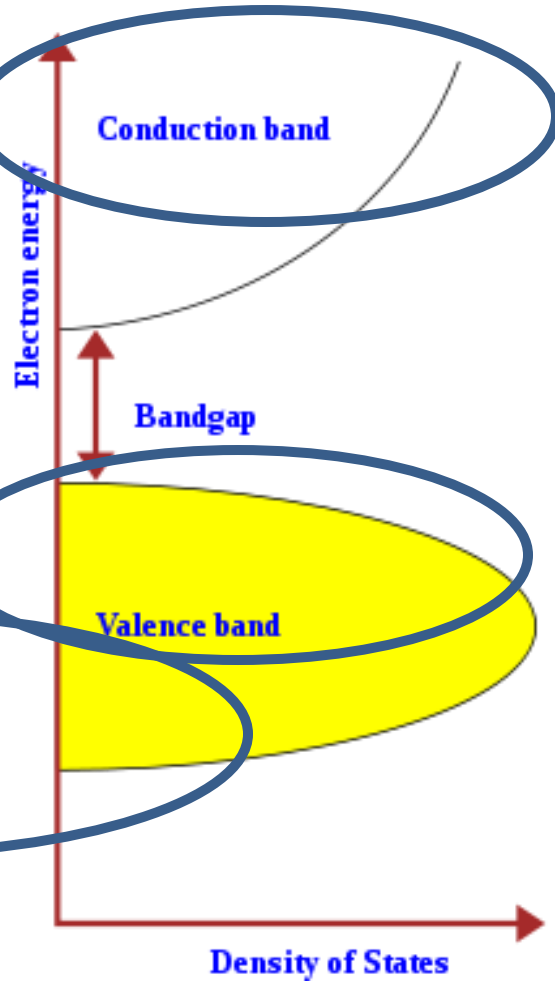

From S. Tudisco

Silicon Carbide (SiC)

Silicon Carbide technology offers then an ideal response to the challenges of NUMEN,
since it gives the opportunity to couple the **excellent properties of silicon detectors** (resolution, efficiency, linearity, compactness) with a **much bigger radiation hardness** (up to five orders of magnitude for heavy ions), thermal stability and insensitivity to visible light.

However…

Defects in SiC

Challenges in the growth of bulk SiC: to grow large single crystals in large quantities is a problem

Macroscopic defects
- polytype inclusions
- micropipes
- comets, carrots

Microscopic defects
- dislocations
- stacking faults
- interstitial, vacancies
- divacancies, antisites

Extended defects

Micro-pipe

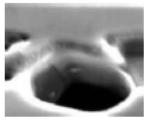

polytype inclusions

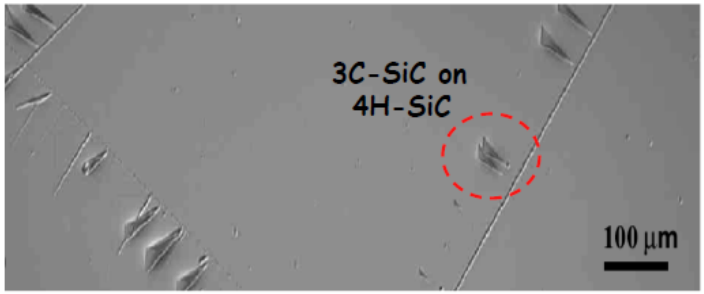

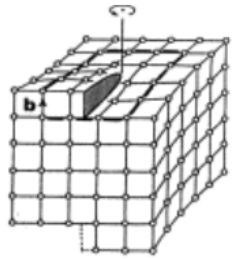

dislocations

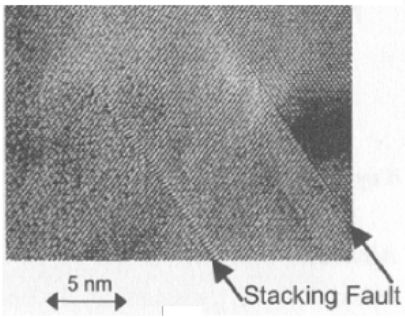

Point and Point-like defects

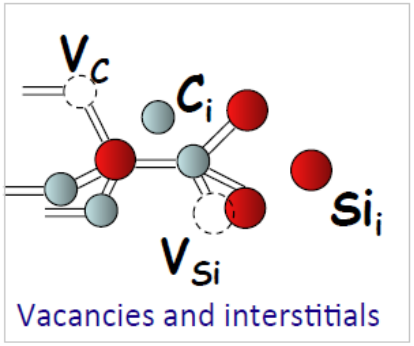

Vacancies and interstitials

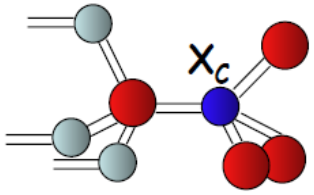

Substitional impurity

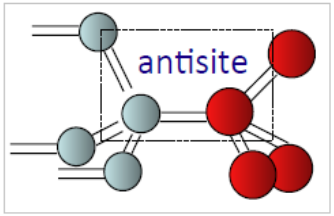

Donor & Acceptor Impurities

Deep levels in the gap =>

Defect-Levels

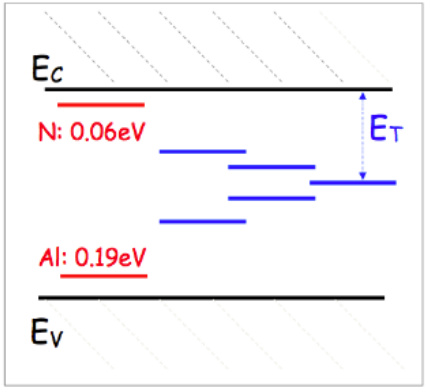

From S. Tudisco

Silicon Carbide Detectors for Intense Luminosity Investigations and Applications

P.I. S. Tudisco

SiC ΔE-E telescopes

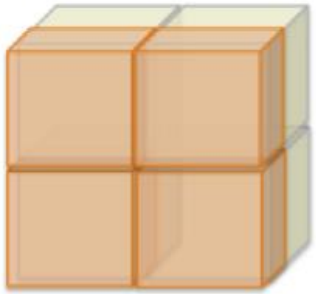

- ✓ Active area 1 cm^2
- ✓ ΔE stage thickness ≥ 100 μm
- ✓ E stage thickness 500 ÷ 1000 μm

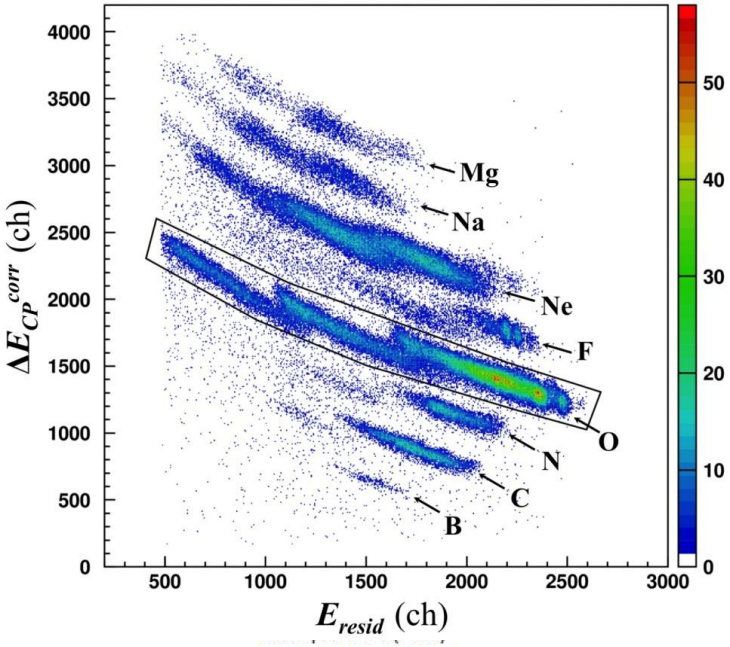

SiCILIA Strategy

Epitaxial growth SIC: beyond the state of the art (small number of defects)

New Tecnology

- Schottky junctions → FONDAZIONE BRUNO KESSLER
- p-n junctions → STMicroelectronics

From S. Tudisco

External institutions

CNR-IMM – Catania
CNR-INO – Pisa

Companies

Fondazione Bruno Kessler (**FBK**) – Trento
ST Microelectronics – Catania
LPE – Catania (**LPE**)

Participating INFN research units

*INFN Laboratori Nazionali del Sud di Catania (**LNS**)*

*INFN Sezione di Catania and "Gruppo collegato di Messina" (**CT-ME**)*

*INFN Sezione di Milano Bicocca (**MI-B**)*

*INFN Sezione di Milano (**MI**)*

*INFN Sezione di Firenze (**FI**)*

*INFN Sezione TIFPA (**TN**)*

*INFN Sezione Pisa (**PI**)*

Global Deliverables

- Tens of detectors: epitaxial grow SiC (50-150 µm thick) semi-insulating SiC (500-1000 µm thick)
- Study of the performance in the electrons and ions detection (radiation hardness, energetic resolution, timing, etc.)
- Study of the performance in the neutrons and X-ray detection
- Study of the ions identification through the pules shape analysis
- A wall of tens of SiC telescopes equipped with a VMM ASIC front-end as demonstrator
- Performance of demonstrator in operative conditions

Reaction targets

Target technology for intense heavy-ion beam (10pμA)

Isotopes candidate for 0νββ:
^{116}Sn, ^{116}Cd, ^{76}Ge, ^{76}Se, ^{130}Te, ^{48}Ca, …
Most of them have low melting temperature and low thermal conductivity

Idea:
Evaporation on a backing material with good properties (Graphen, Diamond, Graphite) and cooling

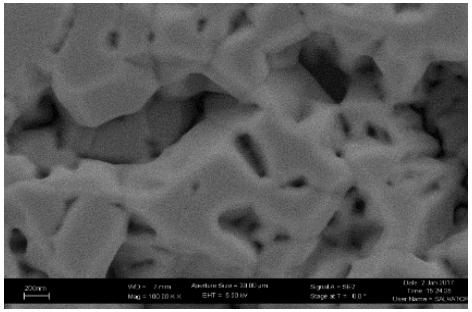

Politecnico Torino and INFN-Torino

The NUMEN challenges

Theory:
Formal development and calculation of reaction cross sections as a function of the NME

Accelerator and beam lines:
Upgrade of the Superconducting Cyclotron for high power

Detectors:
- Gas tracker for high rate heavy ions at low pressure (MPGD)
- PID wall covering a large area made of radiation hard and high resolution detectors (SiC)

Mechanics:
Beam dump for zero-degree beam downstream of the spectrometer

Targets:
For intense heavy-ion beams

Integration

Conclusions and Outlooks

- Many **experimental facilities** for $0\nu\beta\beta$ half-life, but not for the **NME**
- Pioneering experiments shown that **DCE cross sections can be suitably measured**
- First results for the (^{18}O,^{18}Ne) and (^{20}Ne,^{20}O) are encouraging, showing that **quantitative information on $0\nu\beta\beta$ NME** are not precluded
- **Experimental campaign** on nuclei candidates for $0\nu\beta\beta$ and work on the **theory** in the next 5 years
- The **upgrade** foreseen for the INFN-LNS cyclotron and the MAGNEX spectrometer will allow to build a **unique facility** for a systematic exploration of all the nuclei candidate for $0\nu\beta\beta$